# Nonlinear lower hybrid wave equations in collisional tokamak plasmas

OPEN ACCESS
IOP Publishing
Plasma Physics and Controlled Fusion
Plasma Phys. Control. Fusion **66** (2024) 095005 (45pp)
https://doi.org/10.1088/1361-6587/ad546c

# Nonlinear lower hybrid wave equations in collisional tokamak plasmas

**C Castaldo*** **and F Napoli**

Fusion and Nuclear Safety Department, ENEA, Via E. Fermi 45, 00044 Frascati (Roma), Italy

E-mail: carmine.castaldo@enea.it and francesco.napoli@enea.it

Received 25 September 2023, revised 24 May 2024
Accepted for publication 5 June 2024
Published 26 July 2024

**Abstract**

A new set of coupled integro-differential nonlinear lower hybrid (LH) wave equations is derived within the framework of a kinetic theory coupled to the Maxwell equations to study the parametric instabilities (PIs) produced by LH waves in collisional tokamak plasma. Previous models of nonlinear LH wave equations have been significantly improved. The wave equations derived overcome the limits and incorrectness of the standard theory of the PI in inhomogeneous plasma. They allow us to treat the full spectrum in the parallel and poloidal wavenumber of the coupled LH power wave, diffraction effects and possible cascade phenomena, which are elements of the nonlinear LH physics ignored in the standard PI theory. Numerical solutions of the new nonlinear LH wave equations are proposed. The relevant LH frequency spectra produced by PI are calculated, exhibiting characteristic features of PI observed in LH experiments. It is shown that the LH sideband amplification can be overestimated by orders of magnitude by the standard theory of PI. A benchmark of the new model is provided for spatially homogeneous plasmas. The role of the collisions for PI has been assessed. We demonstrate that previous analyses significantly overestimated their stabilization effect.

Keywords: heating, current drive, lower hybrid, nonlinear, collisional, tokamak

## 1. Introduction

In thermonuclear fusion research based on the tokamak concept, non-inductively-driven plasma current is a key to access improved stability and plasma confinement necessary for efficient fusion reactors [1]. The lower hybrid (LH) wave power coupling in tokamak plasmas has been theoretically suggested as a suitable method to drive plasma current [2, 3]. Many experiments have confirmed this theoretical prediction [4–6]. The LH current drive, in synergy with the bootstrap current [4], can provide full control of the steady-state profiles with a high fraction of the non-inductive plasma current driven in the outer half of the plasma column [7]. Unfortunately, the efficiency of the current drive was observed to decrease sharply above a critical plasma density, which is lower than the operating density envisaged for a fusion reactor [8–10]. However, the more recent experiments [11–13] indicate that the LH current drive might be efficient even at reactor-relevant plasma densities. In these experiments, suitable methods were used to reduce parasitic effects, such as LH parametric instabilities (PIs) and LH scattering off density fluctuations, which are believed to be responsible for the lack of LH current drive in high-density plasmas. In general, PI plays an important role in determining the physics of LH waves coupled to tokamak plasmas. These are nonlinear interaction phenomena, such that the power of the launched, large amplitude 'pump wave' is depleted to feed LH sideband waves in the frequency and wavenumber spectra. These sideband waves are coupled to the pump wave through low-frequency (LF) resonant waves or quasi-modes [14, 15]. PI prevented the LH power penetration in the plasma core in early LH experiments aimed at ion

* Author to whom any correspondence should be addressed.

heating, which were based on theoretical predictions [16, 17]. Strong depletion of the launched wave power and the excitation of sideband LH modes and cyclotron waves, absorbed at the plasma edge, were only observed in the experiments aimed at ion heating [18]. PI has also been invoked within the framework of LH current drive (LHCD) experiments as an important contribution to explain the density limit for significant LHCD [11] as well as to solve the so-called spectral gap problem [19–21].

Concerning the spectral gap problem, we note that the coupled LH spectrum versus the wave number parallel to the static magnetic field $k_{||}$ is accurately calculated by numerical codes for LH antennas based on phased waveguide arrays [22–26]. These codes have been validated by LH launched spectrum measurements provided by $CO_2$ laser scattering techniques [27] as well as by extensive experimental observations concerning the LH reflected power. A benchmark of the coupling code was performed by a comparison of the calculated reflection coefficients with the experimental measurements, which were found to be in quite general agreement [28]. We note that, even the first, pioneering coupling code developed by Brambilla [22] predicts the correct reflection coefficients. Therefore, it is used here, as discussed in section 4, to determine the coupled LH pump power wavenumber spectra for the numerical solutions of the nonlinear LH wave equations. Despite the accuracy of the coupling code, the LH power damping of the electrons and the current drive observed in LHCD experiments are orders of magnitude larger than calculated by the quasilinear theory on the basis of the coupled $k_{||}$ spectra. This inconsistency is known as the spectral gap problem. To solve this problem, geometrical effects in the wave propagation were invoked, producing significant $k_{||}$ upshift, as proposed in [29–34] based on ray-tracing codes within the eikonal theory [35]. This analysis also included possible effects of ray chaos [36–41] and ripple in the magnetic field [42–45]. Full-wave analysis suggested that diffraction effects could contribute to the enrichment of the LH spectra with slower waves [46, 47]. Scattering off density fluctuations might also affect the $k_{||}$ spectra, since they produce a rotation of the perpendicular wavenumber in the poloidal plane [48, 49]. Indeed, as a result of the LH propagation in the presence of magnetic shear, the poloidal components are produced by the scattering project in the parallel direction. However, the geometrical effects might be not be sufficient to bridge the spectral-gap problem [36, 50] and the experimental study performed in [21] suggested a leading role of PI in this context. Concerning the density limit in the LH current drive, the effects of ionization and resistive losses [51] as well as the LH scattering off density fluctuations have been invoked as a possible explanation [52–57]. However, the analysis performed in [58] demonstrated that the latter might not explain quantitatively the observed sharp decay of the LH current drive above a plasma density limit. In addition, the observed LH interaction with core plasma electrons at high density in FTU was obtained by experimental tools aimed at quenching PI, as documented by the frequency spectra detected [11]. We also mention the observation of the current profile modification in the edge region of the EAST tokamak, correlated with an increased level of PI during LHCD power injection [59]. The interpretation of LH experiments and the proper design of LH systems in future machines thus require an accurate modeling of the PI. For homogeneous plasmas, the relevant parametric dispersion equation (PDE) within the electrostatic approximation has been extensively studied in the archived literature, see e.g. [14, 15, 60, 61]. It is shown that two channels of PI are important for LH waves, namely LF ion-sound quasi-modes (ISQMs) and ion-cyclotron quasi-modes (ICQMs). A typical signature of the former is the broadening of the line frequency of the source, as detected by RF probes and RF spectrum analyzers. A typical signature of PI involving ICQM is the presence in the frequency spectra of sideband peaks at a distance from the line of the RF source roughly given by the cyclotron frequency of the main ion species and its harmonics. These experimental evidences are discussed, for example, in [19, 62, 63]. The effects of the collisions, in particular, with neutrals, were included in Miklos Porkolab's pioneering work on PI induced by LH waves near the LH resonance [14], and their importance was experimentally verified [64]. Full electromagnetic effects in PI have been considered more recently, showing that they might produce a non-negligible stabilizing effect in all PI channels [65]. The role of the collisions and some electromagnetic effects were also considered in [66], based on a kinetic equation with a particle conserving Bhatnagar, Gross and Krook (BGK) operator. However, the linear electron and ion LF responses were completely missing.

It is thus impossible to reproduce in the collisionless limit the correct PDE known in the archived literature, even within the model constraints introduced. Moreover, as shown in section 4, the stabilizing effect of the collisions is greatly overestimated. The standard modeling of PI in inhomogeneous plasma, as discussed in [15, 60, 67, 68], to evaluate the amplification of LH sidebands, the convective losses and the presence of a finite plasma region illuminated by the LH antenna have been considered within a plasma slab model and the WKB approximation. However, the latter is not justified in the plasma scrape-off layer (SOL) region near the LH launcher, mainly concerning the leading spectral components of the LH pump wave versus the parallel wavenumber and the LH sidebands at larger radial wavelengths. The characteristic lengths of radial variation of the plasma parameters in the peripheral plasma, e.g. the temperature and the density, are indeed in these cases of the same order as the LH wavelengths along the radial direction. Therefore, the eikonal hypothesis is not satisfied. An accurate modeling of the nonlinear LH physics in the SOL region thus requires a full-wave approach, as already performed concerning LHCD in the plasma core [69–72]. In addition, in the standard modeling of PI only four-wave interactions are considered, involving the LH pump wave, an upper and a lower LH sideband and an LF plasma quasi-mode, all of which are assumed to be monochromatic. The pump wave is thus described by a rough approximation with a single spectral component, neglecting the complex structure of the spectrum

in the parallel and poloidal wavenumber coupled by the LH launchers. This might result in overestimating the drive of the PI provided by the electric field of the pump wave, mainly in the presence of coupled LH pump spectral lobes with sufficiently large amplitude. Moreover, considering only four wave interactions, the treatment of cascade PI effects is prevented. Finally, the amplification of the LH sideband is calculated in the standard modeling, with the only exception being [67], considering the convective losses due to the mismatch of the wave coupling in inhomogeneous plasma and the finite area illuminated by the LH antenna but based only on the growth rate of PI as given at the antenna mouth, where the latter has the maximum value. As a result, the LH sideband amplification is overestimated. The objective of the present study is to overcome the above limits and incorrectness of the standard theory of the PI in inhomogeneous plasma and provide a correct assessment of the role of the collisions. To this end, we develop a novel full-wave modeling of the PI. Here, we improve on previous full-wave nonlinear LH modeling, proposed in [20, 73]. In the former, a fluid theory is considered to evaluate within a plasma slab model the time and space evolution of an LH wave with only two spectral components in the parallel wave number. This model is not suitable to study the nonlinear steady-state behavior of LH waves. Within a collisionless plasma slab model, the nonlinear LH physics is considered in the steady-state regime. However, a cold plasma model was used to derive the LH wave equation. The nonlinear LH behavior, resulting from the beating of LF density perturbation with LH waves, was treated considering only the parallel dynamics for both the electrons and ons, and only ISQM was allowed as a channel of PI. In the HF range, the nonlinear electron density perturbation is not properly evaluated, considering only the adiabatic limit. In the homogeneous plasma limit, it is thus impossible to reproduce the PDE known in the archived literature. In the present study, a new set of coupled integro-differential nonlinear LH wave equations is derived within the framework of a kinetic model for collisional plasmas coupled to the Maxwell equations, based on the spectral method and the weak turbulence theory up to the third order. In section 2, we derive the LH wave equations and discuss the hypothesis of the theory, summarized in suitable tables to show the model constraints and the relevant typical values of the plasma and RF parameters. In section 3, as a benchmark, both the linear and nonlinear wave equations are derived for homogeneous plasmas. It is shown that, within the limits of the assumptions made in the modeling, they coincide with the wave equations known in the archived literature for collisionless plasma.

Tiny differences emerge from the comparison of the relevant numerical solutions. Analytical expressions for the growth rates, correcting those indicated in [66], and the power threshold of PI, are derived for collisional plasma within the limit of parallel drive. In section 4, within this limit numerical solutions of the nonlinear wave equations are discussed. Frequency and parallel wavenumber spectra, emerging from a noisy background, are shown and the LH sideband amplification is compared with that calculated by the standard theory of PI. Section 5 is devoted to a summary of the results and a discussion of possible extensions of the model. Details are reported in appendices A–C. In particular, we show in appendix A that the collisional operator adopted reasonably captures the role of the collisions for PI. We have adopted the cgs units. A list of the main symbols used is proposed in table 1 below.

## 2. Nonlinear LH wave equations in collisional plasma

Here, we derive the nonlinear LH wave equation, based on a self-consistent system of Maxwell equations for the electromagnetic field (**E, B**) coupled to the following kinetic equation for the single-particle distributions $f_\alpha$ of each plasma species, with mass $m_\alpha$ and electric charge $q_\alpha$

$$\frac{\partial f_\alpha}{\partial t}+\mathbf{v}\cdot\frac{\partial f_\alpha}{\partial \mathbf{r}}+\frac{q_\alpha}{m_\alpha}\left[\mathbf{E}+\frac{\mathbf{v}}{c}\times\mathbf{B}\right]\cdot\frac{\partial f_\alpha}{\partial \mathbf{v}}=-\nu_\alpha\left[f_\alpha-f_{\alpha o}\frac{n_\alpha}{n_{\alpha o}}\right], \tag{2.1}$$

where $n_\alpha=\int d^3\mathbf{v}\, f_\alpha$ and $c$ is the speed of light in vacuum. The particle-conserving BGK collisional operator [74] is used as an approximate model of the collision integral. $f_{\alpha o}$ is the unperturbed equilibrium solution of the kinetic equation, $n_\alpha$ and $n_{\alpha o}$ are, respectively, the particle density and the equilibrium particle density, and $\nu_\alpha$ are characteristic relaxation rates. As discussed in appendix A, this simple collisional operator seems sufficient to capture the correct LH physics in the present context. A 1D slab geometry is adopted. The Cartesian axis $Z$ is aligned along the static magnetic field $\mathbf{B}_o=B_o\mathbf{z}$, which is assumed to be constant. A zero equilibrium electric field is assumed, i.e. $\mathbf{E}_o=0$. The axis $X$ is directed along the radial, inward direction and $x=0$ identifies the position of the LH antenna mouth, which is located in the $YZ$ plane. We note that poloidal and toroidal asymmetry might characterize realistic equilibrium density and temperature profiles in the plasma region in front of the LH launcher. Ponderomotive effects, induced by the injected LH wave power, might also modify the equilibrium profiles and contribute to the plasma asymmetry. We also note that in the presence of a static electric field, a temperature anisotropy in directions parallel and perpendicular to the magnetic field as well as the presence of a parallel current density (mainly carried by the plasma electrons) might occur in the plasma SOL region in front of the launcher. More realistic, 3D modeling can be considered for high-fidelity simulations, taking into account all these effects. However, we note that the analysis of the LH coupling characteristics performed in [28], considering a simple poloidally and toroidally symmetric 1D plasma slab, with static and constant plasma parameters in the $YZ$ plane and 1D antenna model in comparison to much more accurate antenna geometry and plasma models, suggests that more realistic approaches do not necessarily change significantly the predictions of the LH physics. Moreover, a 1D plasma

**Table 1.** List of the main symbols used. Hereinafter, the subscript $\alpha$ indicates the plasma species, both ions and electrons, the latter being identified by $\alpha = e$.

| $E$, $B$, $E_{\rm o}$, $B_{\rm o}$ | Electric and magnetic field and their equilibrium value |
|---|---|
| $q_\alpha, m_\alpha$ | Electric charge and mass of plasma species $\alpha$ |
| $n_\alpha, n_{\alpha o}$ | Particle densities and their equilibrium value |
| $T_\alpha, \mathrm{v}_{th,\alpha}$ | Temperatures and thermal velocities |
| $f_\alpha, f_{\alpha o}$ | Distribution functions and their equilibrium value |
| $\omega_{p\alpha}, \Omega_\alpha, \omega^*_\alpha, \lambda_{D,\alpha}, \rho_{th,\alpha}$ | Plasma and cyclotron angular frequencies, Debye lengths, thermal Larmor radii |
| $X, Y, Z$ | Cartesian axis: radial, poloidal and toroidal |
| $x, y, z$ | Cartesian coordinates: radial, poloidal and toroidal |
| $\boldsymbol{x}, \boldsymbol{y}, \boldsymbol{z}$ | Cartesian unit vectors: radial, poloidal, toroidal |
| $f, f_o, \omega_o$ | Wave frequency, LH pump frequency and LH pump angular frequency |
| $e, c$ | Elementary charge, speed of the light in vacuum |
| $\boldsymbol{r}, \mathbf{v}, \boldsymbol{t}$ | Position, velocity, time |
| $L_y, L_z$ | Poloidal and toroidal lengths of the slab geometry |
| $l_c$ | Connection lengths in the poloidal cross section |
| $L$ | Length of variation of the plasma parameters |
| $\mathrm{v}_\parallel, \mathrm{v}_\perp$ | Velocities parallel and perpendicular to $\mathbf{B_o}$ |
| $k_y, k_z = k_\parallel$ | Poloidal and toroidal wavenumbers |
| $N_y, N_z = N_\parallel$ | Poloidal and toroidal refractive index |
| $S_{\omega,k_y,k_z}(x)$ | Radial phase of the electromagnetic fields |
| $k_{x;\omega,k_y,k_z} = \mathrm{d}S_{\omega,k_y,k_z}/\mathrm{d}x$ | Generalized radial wave number |
| $k_\perp = \left(k_y^2 + k_x^2\right)^{1/2}$ | Generalized perpendicular wave number |
| $\rho_{\alpha;\omega,k_y,k_z}$, $\boldsymbol{J}_{\alpha;\omega,k_y,k_z}$ | Charge and current densities |
| $E_{i;\omega,k_y,k_z}$, $B_{i;\omega,k_y,k_z}$ | Electric and magnetic field components (stV cm$^{-1}$, G) $i = x, y, z$ |
| $\tilde{E}_{i;\omega,k_y,k_z}$ | Electric field components (units $A_o$), $i = x,\ y,\ z$ |
| $A_o$ | Squared root of the time average of the squared peak parallel electric field of the LH pump wave |
| $\eta = eA_o/\left(m_e \mathrm{v}_{th,e}\omega_o\right)$ | Expansion parameter of the weak turbulence theory |
| $A_{i;\omega,k_y,k_z}$ | Amplitude of the electric field components (stV cm$^{-1}$) $i = x,\ y,\ z$ |
| $r_{E_\perp/E_\parallel} = \max_{i\in\{x,y\}} \left\lvert \omega E_{i;\omega,k_y,k_z} / \left(\Omega_e E_{z;\omega,k_y,k_z}\right)\right\rvert$ | Weighted ratio of perpendicular and parallel electric fields |
| $\nu_e$ | Collisional frequency of the electrons |
| $\mathcal{H}_o, \mathcal{H}_o^{-1}$ | Collisionless kinetic operator and its inverse |
| $\mathcal{F}$ | Fourier transform operator in $y,\ z,\ t$ |
| $\mathcal{I}_\perp$ | Integral operator in the perpendicular velocity space |
| $S_\sigma(u) = \sigma Z(\sigma u)$, with $\sigma = sgn(k_z)$ | Generalized plasma dispersion function |
| $Z(\zeta)$ | Fried–Conte function |
| $\chi_\alpha, \varepsilon$ | Susceptibilities and dielectric function |
| $F_\perp(u,u')$, $F_\parallel(u,u')$ | Perpendicular and parallel nonlinear coupling functions |
| $\delta$ | Angle between the perpendicular electric fields of the LH sidebands and the LH pump wave |

slab model and Maxwellian equilibrium were adopted in previous analysis of PI induced by LH waves in inhomogeneous plasma [15, 21, 60, 67, 68]. Reasonable consistency of the previous analysis with experimental results suggests that the 1D plasma slab model and the Maxwellian equilibrium distribution functions adopted here might provide useful comparisons with LHCD experiments and a suitable guide for the design of LHCD systems for future machines. We assume that the equilibrium distribution functions $f_{\alpha o}$ of the plasma particles are approximated by local Maxwellian, with temperature $T_\alpha$ and density $n_{\alpha o}$, i.e. $f_{\alpha o} = n_{\alpha o}\exp(-\mathrm{v}^2/\mathrm{v}^2_{th,\alpha})/\left(\pi^{3/2}\mathrm{v}^3_{th,\alpha}\right)$, where $\mathrm{v}_{th,\alpha} = \sqrt{2T_\alpha/m_\alpha}$ is the thermal velocity and the temperature is measured in energy units.

We obtain steady-state solutions of the coupled set of the above kinetic equations with the Maxwell equation, based on the perturbation theory and the spectral method. In this regard, we define the Fourier transform $\mathcal{F}$

$$\psi_{\omega,k_y,k_z}(x;\xi) = \mathcal{F}[\psi(\boldsymbol{r},t;\xi)] = \frac{1}{(2\pi)^3}\int_{-T}^{+T}\mathrm{d}t\int_{-L_y}^{+L_y}\mathrm{dy}\int_{-L_z}^{+L_z}\mathrm{d}z\,\psi(\boldsymbol{r},t;\xi)\,e^{i(\omega t - k_y y - k_z z)}. \tag{2.2}$$

Here, $\boldsymbol{r} = (x,\ y,\ z)$ is the position vector, $t$ is the time and $\xi$ indicates additional variables, e.g. the particle velocities. The

quantity $\Psi$ represents any component of the electromagnetic field or the single particle distribution function of the plasma ions or electrons as well as their charge and current densities. The spectral method is justified assuming steady-state conditions and symmetry in the $YZ$ plane. The time interval $[-T,T]$ occurs during this steady-state phase, and we assume that $T$ is much larger than any period of the electromagnetic field. The space intervals $[-L_y,L_y]$ and $[-L_z,L_z]$ limit the finite plasma region, which is illuminated by the LH pump wave and by the LH sideband waves excited by the PI. Concerning the radial dependence of the spectrum of the Cartesian components of the electric field, we can write the following:

$$E_{j;\omega,k_y,k_z}(x) = A_{j;\omega,k_y,k_z} e^{iS_{\omega,k_y,k_z}(x)}, \tag{2.3}$$

where the amplitude $A_{\omega,k_y,k_z}$ is real and positive and the phase $S_{\omega,k_y,k_z}(x)$ is complex. No lack of generality occurs. The index $j$ can assume the values $x$, $y$ or $z$. We define a sort of generalized wavenumber by $k_{x;\omega,k_y,k_z} = \partial S_{\omega,k_y,k_z}/\partial x$, so that we have $\partial E_{j;\omega,k_y,k_z}/\partial x = i k_{x;\omega,k_y,k_z} E_{j;\omega,k_y,k_z}$. In general, $k_{x;\omega,k_y,k_z}$ is a complex quantity, describing the wave amplification or damping as well as the oscillations along the slab radial coordinate $x$. For inhomogeneous plasmas, the eikonal hypothesis requires the following conditions:

$$\left|k_{x;\omega,k_y,k_z}\right| L \gg 1, \quad \left|\frac{1}{k_{x;\omega,k_y,k_z}} \frac{\mathrm{d}k_{x;\omega,k_y,k_z}}{\mathrm{d}x}\right| L \gg 1, \tag{2.4}$$

where $L$ indicates the smaller characteristic length of variation of the plasma temperature and density. These conditions are not always justified in the plasma region where PI occurs, mainly concerning the LH pump wave and the LH sidebands with sufficiently small parallel wavenumber. As the main purpose of the present study, we derive here a set of coupled nonlinear full-wave LH equations to overcome the lack of validity of the eikonal hypothesis.

A key feature of the PI induced by LH is the presence of two time scales for the electromagnetic field and particle dynamics or, equivalently, two well-separated spectral ranges in the frequency domain. The LF range concerns two quasi-modes, which are excited by the beating of LH waves, namely the ISQM, with typical frequencies 0.5 MHz $\leqslant f \leqslant$ 50 MHz and the ICQM, with typical frequencies of 50 MHz $\leqslant f \leqslant$ 500 MHz. We do not consider here the drift waves in the LF range, which are quasi-electrostatic normal plasma modes that are observed in inhomogeneous plasmas. In appendix B, we show that they do not contribute to the PI in the LHCD experiments and, within the present model constraints, the effects of the diamagnetic drift frequency can be neglected to evaluate the LF linear electron and ion density perturbations. The HF range $f_o \pm f$ concerns the coupled LH wave power, i.e. the LH pump wave at the operating source frequency $f_o$, typically of the order of 5 GHz, and the LH sidebands emerging from the noise and amplified by PI. As usual in the theory of PI, it is assumed that the amplitude of the LH pump-wave electric field spectral components is much larger than the spectral components of both the LH sidebands and the LF quasi-mode electric field, namely we have the ordering:

$$A_{j;\omega_o,k_{yo},k_{zo}} \gg A_{j;\omega_s,k_{ys},k_{zs}}, A_{j;\omega_q,k_{yq},k_{zq}}, \tag{2.5}$$

where the indices $o$, $s$ and $q$ denote, respectively, the spectral components of the LH pump wave, the LH sidebands and the LF quasi-modes.

As the expansion parameter of the perturbation theory we adopt the parameter:

$$\eta = \frac{eA_o}{m_e \mathrm{v}_{th,e} \omega_o} \ll 1. \tag{2.6}$$

Here $A_o$ is the squared root of the time average of the squared peak parallel electric field of the LH pump wave, with angular frequency $\omega_o$, and $e$ is the elementary charge. As suggested by the standard PI theory [14, 15, 60, 61], we need to solve self-consistently the coupled system of the Maxwell equations and the kinetic equations up to the third order in the expansion parameter $\eta$. In the HF range, at the first order of the perturbation theory, we obtain the linear kinetic equation for the plasma electrons:

$$\frac{\partial f_e^{HF(1)}}{\partial t} + \mathbf{v} \cdot \frac{\partial f_e^{HF(1)}}{\partial \mathbf{r}} + \frac{q_e}{m_e} \boldsymbol{E}^{\mathrm{HF}} \cdot \frac{\partial f_{eo}}{\partial \mathbf{v}} = -\nu_e \left[ f_e^{HF(1)} - f_{eo} \frac{n_e^{HF(1)}}{n_{eo}} \right], \tag{2.7}$$

where $n_e^{HF(1)} = \int d^3\mathbf{v}\, f_e^{HF(1)}$. We express the electric field and $n_e^{HF(1)}$ in terms of their inverse Fourier transforms, e.g.

$$\mathbf{E}^{HF}(\boldsymbol{r},t) = \int \mathrm{d}k_y \mathrm{d}k_z \mathrm{d}\omega\; e^{-i(\omega t - k_y y - k_z z)} \mathbf{E}^{HF}_{\omega,k_y,k_z}. \tag{2.8}$$

The local dependence of $\mathbf{E}^{HF}_{\omega,k_y,k_z}$ on the coordinate $x$ along the unperturbed orbits of the electrons can be described by the factor $e^{ik_x x}$ where $k_x$ is, in general, complex and such that $k_x \mathbf{E}^{HF} = -i\partial_x \mathbf{E}^{HF}$. It is constant along the unperturbed trajectories of the electrons since their radial width is of the order of the thermal electron Larmor radius $\rho_{th,e} = \mathrm{v}_{th,e}/|\Omega_e|$ and we assume that $|k_x|\rho_{th,e} \ll 1$. We note that, in the peripheral plasma where PI driven by LHCD injection occurS, the ordering $\omega_{pe}^2 \ll \Omega_e^2/2$ is well justified for most LHCD scenarios. Here, $\omega_{pe} = \sqrt{4\pi n_{eo} e^2/m_e}$ and $\Omega_e = -eB_o/(m_e c)$ are, respectively, the angular plasma frequency and the electron cyclotron angular frequency. The above ordering implies that $\rho_{th,e} \ll \lambda_{D,e}$, where $\lambda_{D,e} = \sqrt{T_e/(4\pi n_{eo} e^2)}$ is the electron Debye radius. The kinetic equation used here as well as in the standard modeling of PI only concerns collective effects that occur on scale lengths much larger than the electron Debye length so that the condition $|k_x|\rho_{th,e} \ll 1$ that we assume here should be not considered, for most LHCD scenarios, as a limit of the present theory but a prerequisite of any modeling of PI based on the kinetic equation for the plasma electrons. In the same vein, we explicitly note that the plasma

parameters are constant along the unperturbed trajectories of the electrons, as we have assumed poloidal and toroidal symmetry and the characteristic length of variation of the plasma parameters along the radial direction is $L \gg \rho_{th,e}$. We define the perpendicular wave number as $k_\perp = \sqrt{k_x^2 + k_y^2}$, where the principal value is used to define the square root of the complex argument. We note that the particular determination of the square root as a complex function does not affect the final results. Moreover, we observe that all the identities involving the (ordinary or modified) Bessel functions of argument proportional to $k_\perp$ or to $k_\perp^2$, as reported in [75] and necessary to obtain the solutions of the kinetic equation, still hold for complex arguments. Following the method discussed in [75], the solutions of the kinetic equation (2) can be expressed as,

$$f_e^{HF(1)}(\mathbf{r},\mathbf{v},t) = \eta \int_{t-T^*,\mathcal{Q}}^{t} \mathrm{d}t' \int \mathrm{d}k_y \mathrm{d}k_z \mathrm{d}\omega\, e^{-i(\omega t' - \boldsymbol{k}\cdot\boldsymbol{r}')} e^{-\nu_e (t-t')} \times \tilde{\mathbf{E}}^{HF}_{\omega,k_y,k_z} \cdot \frac{\partial f_{eo}}{\partial \mathbf{v}'} \mathrm{v}_{th,e}\omega_o + \nu_e \frac{1}{n_{eo}} \int_{t-T^*,\mathcal{Q}}^{t} \mathrm{d}t' e^{-\nu_e (t-t')} \times \int \mathrm{d}k_y \mathrm{d}k_z \mathrm{d}\omega\, e^{-i(\omega t' - k\cdot r')} n^{HF(1)}_{e;\omega,k_y,k_z} f_{eo}(\mathbf{v}'). \tag{2.9}$$

The diacritic mark $\sim$ on the electric field components indicates hereinafter that they are measured in units of $A_o$. This time interval $[t - T^*, t]$ occurs during the steady-state phase of the LH wave coupled to the tokamak plasma.

Its duration is assumed to be much larger than any period of the HF electromagnetic field. We later discuss the meaning of the subscript $\mathcal{Q}$ in the integrals over the time $t'$. The latter has to be evaluated along an unperturbed zero-order trajectory $r'(t')$ so that $r'(t) = \mathbf{r}$. The relevant position and velocity within a Cartesian reference frame with the axis Z aligned in the local direction of the magnetic field are given by equation (36) of [75]. One obtains, for Maxwellian equilibrium distribution $f_{eo}$

$$f_e^{HF(1)}(\mathbf{r},\mathbf{v},t) = \eta \mathrm{v}_{th,e}\omega_o \int \mathrm{d}k_y \mathrm{d}k_z \mathrm{d}\omega e^{-i(\omega t - \boldsymbol{k}\cdot\boldsymbol{r})} \times \int_{0,\mathcal{Q}}^{T^*} \mathrm{d}\tau e^{i\beta} \left[ \tilde{E}^{HF}_{x;\omega,k_y,k_z} \frac{\partial f_{eo}}{\partial \mathrm{v}_\perp} \cos(\phi + \Omega_e\tau) + \tilde{E}^{HF}_{y;\omega,k_y,k_z} \frac{\partial f_{eo}}{\partial \mathrm{v}_\perp} \sin(\phi + \Omega_e\tau) + \tilde{E}^{HF}_{z;\omega,k_y,k_z} \frac{\partial f_{eo}}{\partial \mathrm{v}_\parallel} \right] + \frac{\nu_e}{n_{eo}} \int \mathrm{d}k_y \mathrm{d}k_z \mathrm{d}\omega e^{-i(\omega t - \boldsymbol{k}\cdot\boldsymbol{r})} n^{HF(1)}_{e;\omega,k_y,k_z} \times \int_{0,\mathcal{Q}}^{T^*} \mathrm{d}\tau e^{i\beta} f_{eo}(\mathrm{v}). \tag{2.10}$$

Here,

$$\tau = t - t',\ \beta = -\frac{\mathrm{k}_\perp \mathrm{v}_\perp}{\Omega_e}\left[\sin(\phi - \theta + \Omega_e\tau) - \sin(\phi - \theta)\right] + (\omega + i\nu_e - \mathrm{k}_\parallel \mathrm{v}_\parallel)\tau,$$

$$\mathrm{v}_x = \mathrm{v}_\perp \cos\phi,\ \mathrm{v}_y = \mathrm{v}_\perp \sin\phi$$

$$\mathrm{k}_x = \mathrm{k}_\perp \cos\theta,\ \mathrm{k}_y = \mathrm{k}_\perp \sin\theta.$$

Note that we often use for $\mathrm{k}_z$ and the parallel refractive index $\mathrm{N}_z$ equivalent notations, respectively $\mathrm{k}_\parallel$ and $\mathrm{N}_\parallel$ to allow a simpler comparison with results known in the archived literature, which are often expressed in terms of $\mathrm{k}_\parallel$ and $\mathrm{N}_\parallel$. The angle $\theta$ is complex and defined by $\theta = \cos^{-1}(\mathrm{k}_x/\mathrm{k}_\perp)$. The Fourier transform of equation (2.10) gives:

$$f^{HF(1)}_{e;\omega,k_y,k_z} = -2\eta\omega_o f_{eo} \int_{0,\mathcal{Q}}^{T^*} \mathrm{d}\tau e^{i\beta} \left[ \tilde{E}^{HF}_{x;\omega,k_y,k_z} \frac{\mathrm{v}_\perp}{\mathrm{v}_{th,e}} \cos(\phi + \Omega_e\tau) + \tilde{E}^{HF}_{y;\omega,k_y,k_z} \frac{\mathrm{v}_\perp}{\mathrm{v}_{th,e}} \sin(\phi + \Omega_e\tau) + \tilde{E}^{HF}_{z;\omega,k_y,k_z} \frac{\mathrm{v}_\parallel}{\mathrm{v}_{th,e}} \right] + \frac{\nu_e}{n_{eo}} n^{HF(1)}_{e;\omega,k_y,k_z} f_{eo} \int_{0,\mathcal{Q}}^{T^*} \mathrm{d}\tau e^{i\beta}. \tag{2.11}$$

Based on the identity (with $n$ integer),

$$e^{i\xi\sin\varphi} = \sum_{n=-\infty}^{+\infty} e^{in\varphi} J_n(\xi), \tag{2.12}$$

and defining $\xi = \mathrm{k}_\perp \mathrm{v}_\perp/\Omega_e$ we can rewrite equation (2.11) in the following form:

$$f^{HF(1)}_{e;\omega,k_y,k_z} = -2\eta\omega_o f_{eo} \sum_{n=-\infty}^{+\infty} J_n(\xi) \sum_{m=-\infty}^{+\infty} (\xi) \times \int_{0,\mathcal{Q}}^{T^*} \mathrm{d}\tau e^{-in(\phi-\theta+\Omega_e\tau)} e^{im(\phi-\theta)} e^{i(\omega + i\nu_e - \mathrm{k}_\parallel \mathrm{v}_\parallel)\tau} \times \left[ \tilde{E}^{HF}_{x;\omega,k_y,k_z} \frac{\mathrm{v}_\perp}{\mathrm{v}_{th,e}} \cos(\phi + \Omega_e\tau) + \tilde{E}^{HF}_{y;\omega,k_y,k_z} \frac{\mathrm{v}_\perp}{\mathrm{v}_{th,e}} \sin(\phi + \Omega_e\tau) + \tilde{E}^{HF}_{z;\omega,k_y,k_z} \frac{\mathrm{v}_\parallel}{\mathrm{v}_{th,e}} \right] + \frac{\nu_e}{n_{eo}} n^{HF(1)}_{e;\omega,k_y,k_z} f_{eo} \sum_{n=-\infty}^{+\infty} J_n(\xi) \sum_{m=-\infty}^{+\infty} J_m(\xi) \times \int_{0,\mathcal{Q}}^{T^*} \mathrm{d}\tau e^{-in(\phi-\theta+\Omega_e\tau)} e^{im(\phi-\theta)} e^{i(\omega + i\nu_e - \mathrm{k}_\parallel \mathrm{v}_\parallel)\tau}. \tag{2.13}$$

The calculation of $f^{HF(1)}_{e;\omega,k_y,k_z}$ should be performed by integrals over the time $\tau$ of the following kind:

$$\mathcal{J}_l(\omega, \mathrm{k}_\parallel) = \int_{0,\mathcal{Q}}^{T^*} \mathrm{d}\tau e^{i(\omega + i\nu_e - \mathrm{k}_\parallel \mathrm{v}_\parallel - l\Omega_e)\tau}. \tag{2.14}$$

In this regard, we note that there are fundamental differences between the solution discussed in [75] and that proposed here, though they are formally similar. In [75], homogeneous and infinite plasmas are considered and it is assumed

that the angular frequencies have an imaginary part, corresponding to the onset of the wave fields, in order to perform the above integration over the time $\tau$. As a result, the following is obtained:

$$\mathcal{J}_l\left(\omega,\mathrm{k}_\parallel\right)=\frac{i}{\omega+i\nu_e-\mathrm{k}_\parallel\mathrm{v}_\parallel-l\Omega_e}. \tag{2.15}$$

It is also discussed in [75] that the collisions might provide the same results. Here, we consider a steady-state condition with real $\omega$. Moreover, the plasma is confined in the vacuum vessel of a tokamak device and the unperturbed trajectories in the scrape-off region might hit the solid-state plasma-facing components (PFCs) during the time interval of integration. However, it should be considered that the interaction of the electrons with the HF electromagnetic field, due both to the LH pump wave and the LH sideband waves excited by PI, occurs on a limited plasma region of surface area $4L_yL_y$. We assume that there the relevant connection lengths $l_c$ are larger than $2L_y$ and $2L_z$. As a consequence, a cutoff of the interaction occurs at the time $T^*$ due to the quenching of the HF electromagnetic fields. Therefore, within these assumptions, the integrals $\mathcal{J}_l\left(\omega,\mathrm{k}_\parallel\right)$ are still given by equation (2.15) even for the case here considered. The electromagnetic field quenching effect is formally indicated by the subscript $\mathcal{Q}$ in the time integrals of equation (2.9). We have calculated the perturbed electron density $n^{HF(1)}_{e;\omega,k_y,k_z}$ and the perturbed current density $\boldsymbol{J}^{HF(1)}_{e;\omega,k_y,k_z}$ at the first order in $\eta$ by performing the relevant integrals in the velocity space, respectively:

$$\rho^{HF(1)}_{e;\omega,k_y,k_z}=-e\int_0^{2\pi}\mathrm{d}\varphi\int_0^{+\infty}\mathrm{d}\mathrm{v}_\perp\mathrm{v}_\perp\int_{-\infty,\mathcal{L}}^{+\infty}\mathrm{d}\mathrm{v}_\parallel f^{HF(1)}_{e;\omega,k_y,k_z}, \tag{2.16}$$

$$J^{HF(1)}_{e;\omega,k_y,k_z}=-e\int_0^{2\pi}\mathrm{d}\varphi\int_0^{+\infty}\mathrm{d}\mathrm{v}_\perp\mathrm{v}_\perp\int_{-\infty,\mathcal{L}}^{+\infty}\mathrm{d}\mathrm{v}_\parallel \mathbf{v} f^{HF(1)}_{e;\omega,k_y,k_z}. \tag{2.17}$$

To this end, we have used the identities listed in [75] as well as the recurrence relations for ordinary and modified Bessel function in [76]. The integrals over the parallel velocity have been performed following the Landau prescription to treat the poles, as indicated by the subscript $\mathcal{L}$. As a benchmark, we have verified that the susceptibility tensor in [75] is obtained in the limit of homogeneous plasma for $k_y=0$ and $\nu_e=0$. As discussed above, after equation (2.8), the condition $|k_\perp\mathrm{v}_{th,e}/\Omega_e|\ll 1$ is a prerequisite for any modeling of PI based on the kinetic equation for the plasma electrons, so that we consistently select only terms at the lowest order in $|k_\perp\mathrm{v}_{th,e}/\Omega_e|$. Moreover, since the LH frequency region is well away from where electron cyclotron damping can occur, we use the asymptotic expansion of the plasma dispersion function of argument $u_{\pm1}=\left(\omega+i\nu_e-\mathrm{k}_\parallel\mathrm{v}_\parallel\pm\Omega_e\right)/\left(k_z\mathrm{v}_{th,e}\right)$. As a result, we obtain:

$$\begin{aligned}\rho^{HF(1)}_{e;\omega,k_y,k_z}=&-\frac{in_{eo}e\eta\omega_o\mathrm{v}_{th,e}}{1+i\gamma_eS_\sigma\left(u_e\right)}\left\{\frac{-i\partial_x\tilde{E}^{HF}_{x;\omega,k_y,k_z}+k_y\tilde{E}^{HF}_{y;\omega,k_y,k_z}}{\Omega_e^2-\left(\omega+i\nu_e\right)^2}\right.\\&+i\frac{k_y\tilde{E}^{HF}_{x;\omega,k_y,k_z}+i\partial_x\tilde{E}^{HF}_{y;\omega,k_y,k_z}}{\mathrm{k}_\parallel\mathrm{v}_{th,e}\Omega_e}\\&\times\left[S_\sigma\left(u_e\right)+\frac{\left(\omega+i\nu_e\right)\mathrm{k}_\parallel\mathrm{v}_{th,e}}{\left(\omega+i\nu_e\right)^2-\Omega_e^2}\right]\\&\left.+2\frac{1+u_eS_\sigma\left(u_e\right)}{\mathrm{k}_\parallel\mathrm{v}_{th,e}^2}\tilde{E}^{HF}_{z;\omega,k_y,k_z}\right\},\end{aligned} \tag{2.18}$$

$$\begin{aligned}J^{HF(1)}_{e;x;\omega,k_y,k_z}=&\,n_{eo}\eta e\omega_o\mathrm{v}_{th,e}\frac{\Omega_e}{\Omega_e^2-\left(\omega+i\nu_e\right)^2}\\&\times\left(\tilde{E}^{HF}_{y;\omega,k_y,k_z}-i\frac{\omega+i\nu_e}{\Omega_e}\tilde{E}^{HF}_{x;\omega,k_y,k_z}\right)+\\&-\frac{n_{eo}\eta e\omega_o\mathrm{v}_{th,e}}{\Omega_e}\frac{\mathrm{k}_y}{\mathrm{k}_\parallel}\left[1+u_eS_\sigma\left(u_e\right)\right]\tilde{E}^{HF}_{z;\omega,k_y,k_z}\\&-\frac{\nu_e\rho^{HF(1)\prime}_{e;\omega,k_y,k_z}}{2\mathrm{k}_\parallel}S_\sigma\left(u_e\right)\frac{\mathrm{k}_y\mathrm{v}_{th,e}}{\Omega_e},\end{aligned} \tag{2.19}$$

$$\begin{aligned}J^{HF(1)}_{e;y;\omega,k_y,k_z}=&-n_{eo}\eta e\omega_o\mathrm{v}_{th,e}\frac{\Omega_e}{\Omega_e^2-\left(\omega+i\nu_e\right)^2}\\&\times\left(\tilde{E}^{HF}_{x;\omega,k_y,k_z}+i\frac{\omega+i\nu_e}{\Omega_e}\tilde{E}^{HF}_{y;\omega,k_y,k_z}\right)+\\&-i\frac{n_{eo}\eta e\omega_o\mathrm{v}_{th,e}}{\Omega_e}\left[1+u_eS_\sigma\left(u_e\right)\right]\frac{1}{\mathrm{k}_\parallel}\partial_x\tilde{E}^{HF}_{z;\omega,k_y,k_z}\\&+i\frac{\nu_e\partial_x\rho^{HF(1)\prime}_{e;\omega,k_y,k_z}}{2\mathrm{k}_\parallel}S_\sigma\left(u_e\right)\frac{\mathrm{v}_{th,e}}{\Omega_e},\end{aligned} \tag{2.20}$$

$$\begin{aligned}J^{HF(1)}_{e;z;\omega,k_y,k_z}=&\left\{\frac{n_{eo}\eta e\omega_o\mathrm{v}_{th,e}}{\mathrm{k}_\parallel}\left[\frac{k_y}{\Omega_e}\tilde{E}^{HF}_{x;\omega,k_y,k_z}+\frac{i}{\Omega_e}\partial_x\tilde{E}^{HF}_{y;\omega,k_y,k_z}\right.\right.\\&\left.\left.-2i\frac{u_e}{\mathrm{v}_{th,e}}\tilde{E}^{HF}_{z;\omega,k_y,k_z}\right]-\frac{i\nu_e}{\mathrm{k}_\parallel}\rho^{HF(1)}_{e;\omega,k_y,k_z}\right\}\left[1+u_eS_\sigma\left(u_e\right)\right].\end{aligned} \tag{2.21}$$

Here, we define $u_e=\left(\omega+i\nu_e\right)/\left(\mathrm{k}_\parallel\mathrm{v}_{th,e}\right)$, $\gamma_e=\nu_e/\left(\mathrm{k}_\parallel\mathrm{v}_{th,e}\right)$ and $S_\sigma\left(u_e\right)=\sigma Z(\sigma u_e)$, where $\sigma$ is the sign of $\mathrm{k}_\parallel$ and $Z$ is the Fried–Conte function [77], which is the generalized plasma dispersion function. The prime in $\rho^{HF(1)\prime}_{e;\omega,k_y,k_z}$ indicates the need to drop the first term in the curl parenthesis of equation (2.18) as it produces terms of higher order in $|k_\perp\mathrm{v}_{th,e}/\Omega_e|$. We note that the differential operator in $\partial_x\rho^{HF(1)\prime}_{e;\omega,k_y,k_z}$ acts only on the electric field components, due to the definition of $k_x$. Although the above charge and current densities have been derived by a solution method valid within the homogeneous plasma limit in the regime *I* of sufficiently large values of $|k_x|$ and sufficiently large characteristic lengths of variation of the plasma parameters, so that the eikonal hypothesis is well justified, and so this approach is valid and has reasonable accuracy. In the opposite regime *II* of relatively small values of $|k_x|$, so that the eikonal hypothesis is not well justified, the cold plasma approximation can be used

and, under suitable conditions discussed below, the parallel dynamics of the electrons is dominant and the perpendicular current densities can be neglected. In this case, as shown in appendix C, the charge density and the parallel current density given above coincide with those obtained by a different approach, which is valid for inhomogeneous plasmas. The following model hypotheses are required:

$$(i)\ |\omega/\Omega_e| \ll 1,\ (ii)\ \left|N_\parallel\right| > 1.5,$$
$$(iii)\ r_{E_\perp/E_\parallel} = \max_{i\in\{x,y\}} \left|\omega E_{i;\omega,k_y,k_z}/\left(\Omega_e E_{z;\omega,k_y,k_z}\right)\right| \ll 1.$$

It is straightforward to see that within this hypothesis one obtains the ordering $\left|J^{HF(1)}_{e;x;\omega,k_y,k_z}\right|, \left|J^{HF(1)}_{e;y;\omega,k_y,k_z}\right| \ll \left|J^{HF(1)}_{e;z;\omega,k_y,k_z}\right|$ in the regime *I*, so that the perpendicular dynamics of the electrons can be neglected. The first hypothesis is verified in any LHCD experiment. However, it can also be relaxed to the much less severe requirement $\mathcal{O}\left[1-\omega^2/\Omega_e^2\right]^{-1} = 1$. The hypothesis (*ii*), where $N_\parallel = k_\parallel c/\omega$ is the parallel (toroidal) refractive index, provides a rough criterion to avoid the mode conversion of the LH waves into whistler waves for typical peripheral plasma parameters in LHCD experiments. We stress that the hypothesis (*iii*) needs to be verified only in the plasma region where regime *II* occurs. As a simple criterion to identify the transition between regimes *II* and *I* we adopt the condition $|k_x|L = 10$, with regime *II* occurring for $|k_x|L < 10$. Any criterion to identify the above transition is somewhat arbitrary. More generally, the actual meaning of acceptability or unacceptability of using the eikonal representation supersedes the wave used here, while also taking into account the limits of 1D modeling. However, we think that the condition adopted is reasonable, though to be taken *cum grano salis*. We use the electrostatic approximation as an order of magnitude estimate to identify regime *II* by the ordering $\omega_{pe} < 10c/\left|N_\parallel L\right| < 20c/(3L)$. Typically, $L$ is of the order of 1 cm, so that regime *II* occurs in the peripheral plasma with electron particle density less than $\sim 10^{13}\mathrm{cm}^{-3}$. Since the eikonal hypothesis is satisfied for $|k_x|L = 10$, though only marginally, the two regimes almost overlap in typical LHCD experimental scenarios, so we are confident that the charge and current density of the electrons given by equations (2.18)–(2.21) are reasonably accurate.

Concerning the plasma ions, we assume as a model hypothesis the ordering $|\omega| \gg \omega_{pj}, \Omega_j$ where $\omega_{pj} = \left[4\pi n_{jo} q_j^2/m_j\right]^{1/2}$ and $\Omega_j = q_j B_o/(m_j c)$ are, respectively, the angular ion plasma frequency and the angular ion cyclotron frequency for plasma ions of the species $j$. Moreover, we adopt the approximation that they can be treated as a cold unmagnetized fluid. Although recent analysis suggests that finite ion Larmor radius effects might be important for LH waves in some range of plasma parameters [78], this is not the case for LH propagating in the peripheral region of tokamak plasmas. The current density of the plasma ions of species $j$ with charge $q_j$ and mass $m_j$ is given by:

$$\boldsymbol{J}^{HF(1)}_{j;\omega,k_y,k_z} = i\frac{m_e n_{jo}\eta e Z_j^2 \omega_o \mathrm{v}_{th,e}}{m_j\omega}\tilde{\boldsymbol{E}}^{HF}_{\omega,k_y,k_z}. \tag{2.22}$$

From the Maxwell equation, we obtain the following linear LH wave equations at the first order in the expansion parameter $\eta$

$$\left(\frac{\omega^2}{c^2} - k_y^2 - k_z^2\right)\tilde{E}^{HF}_{x;\omega,k_y,k_z} - i\partial_x\left(k_y\tilde{E}^{HF}_{y;\omega,k_y,k_z} + k_z\tilde{E}^{HF}_{z;\omega,k_y,k_z}\right) = -\frac{4\pi i\omega}{c^2}\left[J^{HF(1)}_{e;x;\omega,k_y,k_z} + \sum_j J^{HF(1)}_{j;x;\omega,k_y,k_z}\right], \tag{2.23}$$

$$\left(\partial_x^2 - k_z^2 + \frac{\omega^2}{c^2}\right)\tilde{E}^{HF}_{y;\omega,k_y,k_z} - k_y\left(i\partial_x\tilde{E}^{HF}_{x;\omega,k_y,k_z} - k_z\tilde{E}^{HF}_{z;\omega,k_y,k_z}\right) = -\frac{4\pi i\omega}{c^2}\left[J^{HF(1)}_{e;y;\omega,k_y,k_z} + \sum_j J^{HF(1)}_{j;y;\omega,k_y,k_z}\right], \tag{2.24}$$

$$\left(\partial_x^2 - k_y^2 + \frac{\omega^2}{c^2}\right)\tilde{E}^{HF}_{z;\omega,k_y,k_z} - k_z\left(i\partial_x\tilde{E}^{HF}_{x;\omega,k_y,k_z} - k_y\tilde{E}^{HF}_{y;\omega,k_y,k_z}\right) = -\frac{4\pi i\omega}{c^2}\left[J^{HF(1)}_{e;z;\omega,k_y,k_z} + \sum_j J^{HF(1)}_{j;z;\omega,k_y,k_z}\right] \tag{2.25}$$

To compare our results with previous analysis, we consider two limiting cases. The former is obtained keeping the condition (*iii*) also in regime *I*, and assuming that $\left|\omega/\left(k_\parallel \mathrm{v}_{th,e}\right)\right| \geqslant 1$. It would be sufficient to require 0.83. In this case, the parameter $\alpha = 1 + u_e S_\sigma(u_e)$, for $\nu_e = 0$, has absolute value $0.75 > |\alpha| \geqslant \left(k_\parallel \mathrm{v}_{th,e}\right)^2/\left(2|\omega|^2\right)$. This inequality also holds if we add or subtract a small imaginary part to $\omega/\left(k_\parallel \mathrm{v}_{th,e}\right)$, $\left|Im\left(\omega/\left(k_\parallel \mathrm{v}_{th,e}\right)\right)\right| \leqslant 10^{-2} Re\left(\omega/\left(k_\parallel \mathrm{v}_{th,e}\right)\right)$, as shown in figure 1. Within this hypothesis, the ordering $\left|J^{HF(1)}_{e;x;\omega,k_y,k_z}\right|, \left|J^{HF(1)}_{e;y;\omega,k_y,k_z}\right| \ll \left|J^{HF(1)}_{e;z;\omega,k_y,k_z}\right|$ holds, in both regimes *I* and *II*, leading to negligible perpendicular dynamics of the electrons. In addition, a fixed ion background is assumed. As shown in appendix C, the parallel electric field $\tilde{E}_z^{HF}$ thus satisfies the linear wave equation:

$$\frac{\mathrm{d}^2\tilde{E}^{HF}_{z;k_y,k_z,\omega}}{\mathrm{d}x^2} = \beta^L(x,k_y,k_z,\omega)\,\tilde{E}^{HF}_{z;k_y,k_z,\omega}. \tag{2.26}$$

Here,

$$\beta^L(x,k_y,k_z,\omega) = k_y^2 + k_z^2 - \frac{\omega^2}{c^2} + \left(1 - \frac{\omega^2}{k_z^2c^2}\right)\frac{1}{\lambda_{De}^2}\frac{1+u_eS(u_e)}{1+i\gamma_eS(u_e)}. \tag{2.27}$$

The other components of the HF electromagnetic field, omitting the spectral indices, are:

$$\tilde{B}_x^{HF} = -\frac{N_y\tilde{E}_z^{HF}}{N_z^2-1}, \tag{2.28}$$

$$\tilde{B}_y^{HF} = -\frac{i(c/\omega)}{N_z^2-1}\partial_x\tilde{E}_z^{HF}, \tag{2.29}$$

$$\tilde{B}_z^{HF} = 0, \tag{2.30}$$

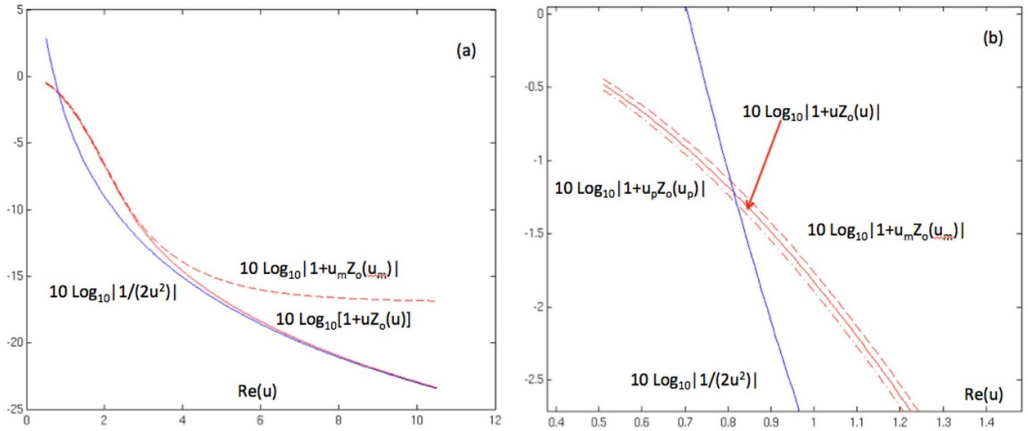


**Figure 1.** Plots of the function $1+uS_\sigma(u)$ with argument $u=\omega/(k_z v_{th,e})$, utilizing a logarithmic scale, are compared to the function $1/(2u^2)$. In (a), the lines relevant for functions of $u$ have pure real argument. Dashed line corresponds to a function of $u_m=u\ (1-0.01i)$. Dash-dotted line with $u_p=u\ (1+0.01i)$ is not distinguishable in (a) since it almost coincides with the line with pure real argument. It can be seen in the zoomed plot (b).

$$\tilde{E}_x^{HF}=-\frac{i(c/\omega)}{N_z^2-1}N_z\partial_x\tilde{E}_z^{HF}, \tag{2.31}$$

$$\tilde{E}_y^{HF}=\frac{N_yN_z\tilde{E}_z^{HF}}{N_z^2-1}. \tag{2.32}$$

We define the poloidal refractive index as $N_y=k_yc/\omega$.

The second limit in the case of the linear LH wave equation is obtained within the electrostatic approximation. In the next section, we report on it and the nonlinear electrostatic wave equation below to discuss a benchmark with the standard theory of PI [26], which is based on the electrostatic approximation. The electric field is expressed in terms of a potential, namely $\tilde{\boldsymbol{E}}^{HF}=-\nabla\tilde{\varphi}^{HF}$. The spectral analysis gives $\tilde{E}^{HF}_{x;\omega,k_y,k_z}=-\partial_x\tilde{\varphi}^{HF}_{\omega,k_y,k_z}$, $\tilde{E}^{HF}_{y;\omega,k_y,k_z}=-ik_y\tilde{\varphi}^{HF}_{\omega,k_y,k_z}$, $\tilde{E}^{HF}_{z;\omega,k_y,k_z}=-ik_z\tilde{\varphi}^{HF}_{\omega,k_y,k_z}$. The relevant wave equation is:

$$\left(1-\sum_j\frac{\omega_{pj}^2}{\omega^2}\right)\left(\partial_x^2-k_y^2-k_z^2\right)\tilde{\varphi}^{HF}_{\omega,k_y,k_z}$$
$$=\left[\frac{1}{1+i\gamma_eS(u_e)}\frac{\omega_{pe}^2}{\Omega_e^2}\frac{k_y^2-\partial_x^2}{1-\left(\frac{\omega+i\nu_e}{\Omega_e}\right)^2}+\frac{1}{\lambda_{De}^2}\frac{1+u_eS(u_e)}{1+i\gamma_eS(u_e)}\right]\tilde{\varphi}^{HF}_{\omega,k_y,k_z}. \tag{2.33}$$

The first-order distribution function relevant for the charge and current densities given by the equations (2.18)–(2.21) can be deduced from the general expression (2.13), considering Bessel functions of order $-1,\ 0,1$ only, excluding the product of the Bessel function of order $\pm1$ as well as resonant terms with second and higher harmonics of the cyclotron frequency, and using the power approximation of the Bessel functions up to the first order in their argument $\xi$.

We anticipate that these approximations will result in dropping of the nonlinear PI interaction due to the polarization drift, which requires the inclusion of Bessel functions of order $\pm2$. However, this interaction term is usually neglected in the archived literature concerning PI, as it gives negligible contribution to the solutions of the relevant parametric dispersion. We thus have:

$$\begin{aligned}f^{HF(1)}_{e;\omega,k_y,k_z}=&\left\{\eta\omega_af_{eo}\frac{1}{v_{th,e}}\left[\frac{k_xv_y-k_yv_x}{\Omega_e}-i\right]\right.\\&\times\left[\frac{v_x+iv_y}{\omega+i\nu_e-k_\parallel v_\parallel+\Omega_e}+\frac{v_x-iv_y}{\omega+i\nu_e-k_\parallel v_\parallel-\Omega_e}\right]\\&\left.+\eta\omega_af_{eo}\frac{v_\perp^2}{v_{th,e}}\frac{k_y}{\Omega_e}\frac{1}{\omega+i\nu_e-k_\parallel v_\parallel}\right\}\tilde{E}^{HF}_{x;\omega,k_y,k_z}\\&+\left\{-i\eta\omega_af_{eo}\frac{1}{v_{th,e}}\left[\frac{k_xv_y-k_yv_x}{\Omega_e}-i\right]\right.\\&\times\left[\frac{v_x+iv_y}{\omega+i\nu_e-k_\parallel v_\parallel+\Omega_e}-\frac{v_x-iv_y}{\omega+i\nu_e-k_\parallel v_\parallel-\Omega_e}\right]\\&\left.-\eta\omega_af_{eo}\frac{v_\perp^2}{v_{th,e}}\frac{k_x}{\Omega_e}\frac{1}{\omega+i\nu_e-k_\parallel v_\parallel}\right\}\tilde{E}^{HF}_{y;\omega,k_y,k_z}+\\&-i\eta\omega_af_{eo}\frac{v_\parallel}{v_{th,e}}\left\{\left[i\frac{k_xv_y-k_yv_x}{\Omega_e}+1\right]\right.\\&\left.\times\frac{2}{\omega+i\nu_e-k_\parallel v_\parallel}\right\}\tilde{E}^{HF}_{z;\omega,k_y,k_z}+i\frac{\nu_e}{n_{eo}}n^{HF(1)}_{e;\omega,k_y,k_z}f_{eo}\\&\times\left\{\left[i\frac{k_xv_y-k_yv_x}{\Omega_e}+1\right]\frac{1}{\omega+i\nu_e-k_\parallel v_\parallel}\right\}.\end{aligned} \tag{2.34}$$

As a benchmark, we have verified that the above expression for $f^{HF(1)}_{e;\omega,k_y,k_z}$ gives charge and current densities identical to equations (2.18)–(2.21). It is shown in appendix A that the effects of the collisions on the nonlinear second-order coupling terms are negligible. Therefore, the leading terms of the Cartesian components of the gradient of the distribution function, neglecting the collisions, are given by:

$$\left[\nabla_{\boldsymbol{v}}f^{HF(1)}_{e;\omega,k_y,k_z}\right]_x\cong-\frac{2\eta\omega_o}{v_{th,e}}\frac{v_\parallel}{\omega-k_\parallel v_\parallel}f_{eo}\frac{k_y}{\Omega_e}\tilde{E}^{HF}_{z;\omega,k_y,k_z}, \tag{2.35}$$

$$\left[\nabla_{\mathbf{v}} f^{HF(1)}_{e;\omega,k_y,k_z}\right]_y \cong \frac{2\eta\omega_o}{\mathrm{v}_{th,e}} \frac{\mathrm{v}_\parallel}{\omega - \mathrm{k}_\parallel \mathrm{v}_\parallel} f_{eo} \frac{k_x}{\Omega_e} \tilde{E}^{HF}_{z;\omega,k_y,k_z}, \tag{2.36}$$

$$\left[\nabla_{\mathbf{v}} f^{HF(1)}_{e;\omega,k_y,k_z}\right]_z \cong -\frac{2i\eta\omega_o}{\mathrm{v}_{th,e}} \frac{\partial}{\mathrm{v}_\parallel} \left[f_{eo} \frac{\mathrm{v}_\parallel}{\omega - \mathrm{k}_\parallel \mathrm{v}_\parallel}\right] \tilde{E}^{HF}_{z;\omega,k_y,k_z}. \tag{2.37}$$

In the LF range, as observed before, the beating of two LH waves is the driving of electrostatic quasi-modes, that are otherwise evanescent, namely the ISQM and the ICQM. Due to the ordering set by equation (2.5), the beating of an LH pump wave component with an LH sideband emerging from the noise produces the dominant non-linear term. Nonlinear terms due to the beating of LF fields are neglected, again due to the ordering set by equation (2.5). We observe that also in the LF range the components of the Fourier transform of the LF electric field $E^{LF}_{j;\omega,k_y,k_z}$ can be expressed in the form of equation (2.3) and we define $k_{x;\omega,k_y,k_z} = \partial S_{\omega,k_y,k_z}/\partial x$.

Measuring the fields in units of $A_o$, we obtain the kinetic equation for the plasma electrons in the LF range up to the second order in the expansion parameter $\eta$

$$\begin{aligned}&\frac{\partial f^{LF(2)}_e}{\partial t} + \mathbf{v}\cdot\frac{\partial f^{LF(2)}_e}{\partial \mathbf{r}} + \frac{q_e}{m_e}\frac{\mathbf{v}}{c}\times\mathbf{B}_o\cdot\frac{\partial f^{LF(2)}_e}{\partial \mathbf{v}} - \eta\tilde{\mathbf{E}}^{LF} \\ &\cdot\frac{\partial f_{eo}}{\partial \mathbf{v}}\mathrm{v}_{th,e}\omega_o - \eta\left[\tilde{\mathbf{E}}^{HF} + \frac{\mathbf{v}}{c}\times\tilde{\mathbf{B}}^{HF}\right] \\ &\cdot\frac{\partial f^{HF(1)}_e}{\partial \mathbf{v}}\mathrm{v}_{th,e}\omega_o = -\nu_e\left[f^{LF(2)}_e - f_{eo}\frac{n^{LF(2)}_e}{n_{eo}}\right].\end{aligned} \tag{2.38}$$

The solution of equation (2.38), which is linear in $f^{LF(2)}_e$, can be obtained as the sum of two distributions, namely $f^{LF(2)}_e = f^{LF(2),L}_e + f^{LF(2),NL}_e$.

The former solves the kinetic equation:

$$\begin{aligned}&\frac{\partial f^{LF(2),L}_e}{\partial t} + \mathbf{v}\cdot\frac{\partial f^{LF(2),L}_e}{\partial \mathbf{r}} + \frac{q_e}{m_e}\frac{\mathbf{v}}{c}\times\mathbf{B}_o\cdot\frac{\partial f^{LF(2),L}_e}{\partial \mathbf{v}} - \eta\tilde{\mathbf{E}}^{LF} \\ &\cdot\frac{\partial f_{eo}}{\partial \mathbf{v}}\mathrm{v}_{th,e}\omega_o \\ &= -\nu_e\left[f^{LF(2),L}_e - f_{eo}\frac{n^{LF(2),L}_e}{n_{eo}}\right],\end{aligned} \tag{2.39}$$

where $n^{LF(2),L}_e = \int d^3\mathbf{v} f^{LF(2),L}_e$.

The latter is the solution of the kinetic equation involving the beating of the HF fields:

$$\begin{aligned}&\frac{\partial f^{LF(2),NL}_e}{\partial t} + \mathbf{v}\cdot\frac{\partial f^{LF(2),NL}_e}{\partial \mathbf{r}} + \frac{q_e}{m_e}\frac{\mathbf{v}}{c}\times\mathbf{B}_o\cdot\frac{\partial f^{LF(2)}_e}{\partial \mathbf{v}} \\ &+ \nu_e\left[f^{LF(2),NL}_e - f_{eo}\frac{n^{LF(2),NL}_e}{n_{eo}}\right] \\ &= \eta\left[\tilde{\mathbf{E}}^{HF} + \frac{\mathbf{v}}{c}\times\tilde{\mathbf{B}}^{HF}\right]\cdot\frac{\partial f^{HF(1)}_e}{\partial \mathbf{v}}\mathrm{v}_{th,e}\omega_o,\end{aligned} \tag{2.40}$$

where $n^{LF(2),NL}_e = \int d^3\mathbf{v} f^{LF(2),NL}_e$.

We express the LF electric field and $n^{LF}_e$ in terms of their inverse Fourier transforms, e.g.

$$\tilde{\mathbf{E}}^{LF}(\boldsymbol{r},t) = \int \mathrm{d}k_y \mathrm{d}k_z \mathrm{d}\omega\; e^{-i(\omega t - k_y y - k_z z)} \tilde{\mathbf{E}}^{LF}_{\omega,k_y,k_z}. \tag{2.41}$$

The dependence on the coordinate $x$ is also described in the HF range. Following the same method used in the HF range, at the lowest order in $k_\perp\rho_e$, where $k_\perp = \sqrt{k_x^2 + k_y^2}$ (we use the principal value of the root, though the results are independent of the determination of the square root), taking into account the ordering $|\omega| \ll |\Omega_e|$, well justified in the LF range, we obtain the perturbed linear second-order charge density:

$$\begin{aligned}n^{LF(2),L}_{e;\omega,k_y,k_z} &= 2i\eta\frac{n_{eo}\omega_o}{k_\parallel \mathrm{v}_{th,e}}\frac{1 + u_e S(u_e)}{1 + i\gamma_e S(u_e)}\tilde{E}^{LF}_{z;\omega,k_y,k_z} \\ &= i\eta\frac{m_e\omega_o \mathrm{v}_{th,e} k^2}{4\pi e^2 k_\parallel}\chi_e \tilde{E}^{LF}_{z;\omega,k_y,k_z},\end{aligned} \tag{2.42}$$

where $k^2 = k_\parallel^2 + k_\perp^2$ and

$$\chi_e = \frac{1}{k^2\lambda^2_{De}}\frac{1 + u_e S(u_e)}{1 + i\gamma_e S(u_e)}. \tag{2.43}$$

Moreover, $u_e$ and $\gamma_e$ are defined as in the HF range (with LF angular frequency). The method used to calculate $f^{LF(2),L}_e$ is well justified only for large values of $|k_x|$, so that the limit of validity of the eikonal hypothesis is fulfilled. However, we observe that the perturbed linear density given by (2.42) can be calculated neglecting the perpendicular dynamics of the electrons. It is reasonable to assume that equation (2.42) is still valid for smaller values of $|k_x|$, so that the eikonal hypothesis is not justified and $|k_x|\rho_e$ is even smaller. Concerning equation (2.40), we first observe that the term proportional to the HF magnetic field is negligibly small. We can thus rewrite equation (2.40) in the following form:

$$\mathcal{H}_o f^{LF(2),NL}_e = \eta\mathbf{E}^{HF}\cdot\frac{\partial f^{HF(1)}_e}{\partial \mathbf{v}}\mathrm{v}_{th,e}\omega_o, \tag{2.44}$$

where $\mathcal{H}_o$ is the differential operator defined by:

$$\mathcal{H}_o = \frac{\partial}{\partial t} + \mathbf{v}\cdot\frac{\partial}{\partial \mathbf{r}} + \frac{q_e}{m_e}\frac{\mathbf{v}}{c}\times\mathbf{B}_o\cdot\frac{\partial}{\partial \mathbf{v}}.$$

It is shown in appendix A that the effect of the collisions is negligible in the nonlinear terms, so that the operator $\mathcal{H}_o$ is defined considering $\nu_e = 0$. The differential operator $\mathcal{H}_o$ has cylindrical symmetry in the velocity space around the direction of the magnetic field. The solution $f^{LF(2),NL}_e$ has the same symmetry since the gradient of $f^{HF(1)}_e$ and the boundary conditions in the velocity space do not break it. Due to the electrostatic character of the LF modes, we only need to evaluate the charge density of the electrons and ions. The Fourier transform of the nonlinear LF electron charge density is $\rho^{HF(3),NL}_{e;\omega,k_y,k_z} = -en^{HF(3),NL}_{e;\omega,k_y,k_z}$.

To calculate the perturbed nonlinear density $n^{HF(3),NL}_{e;\omega,k_y,k_z}$, we apply the operators $\mathcal{I}_\perp = \int \mathrm{d}\mathrm{v}_x \int \mathrm{d}\mathrm{v}_y$. and $\mathcal{F}$ to equation (2.44) and utilize the expression of the gradient in the velocity space

of the first-order distribution provided by equations (2.35)–(2.37). As a result, we obtain:

$$
\begin{aligned}
&g^{LF(2),NL}_{e;\omega,k_y,k_z} \\
&\quad = -2i\frac{n_{eo}\eta^2\omega_o^2}{\omega-\mathrm{k_z v_\parallel}}\frac{e^{-\mathrm{v}_\parallel^2/\mathrm{v}_{th,e}^2}}{\sqrt{\pi}\,\mathrm{v}_{th,e}}\int \mathrm{d}\omega'\int \mathrm{d}k_y' \\
&\qquad \times \int \mathrm{d}k_z'\,\tilde{E}^{HF}_{x,\omega-\omega',k_y-k_y',k_z-k_z'}\frac{\mathrm{v}_\parallel}{\omega'-k_z'\mathrm{v}_\parallel}\frac{k_y'}{\Omega_e}\tilde{E}^{HF}_{z;\omega',k_y',k_z'} \\
&\qquad + 2\frac{n_{eo}\eta^2\omega_o^2}{\omega-\mathrm{k_z v_\parallel}}\frac{e^{-\mathrm{v}_\parallel^2/\mathrm{v}_{th,e}^2}}{\sqrt{\pi}\,\mathrm{v}_{th,e}}\int \mathrm{d}\omega'\int \mathrm{d}k_y' \\
&\qquad \times \int \mathrm{d}k_z'\,\tilde{E}^{HF}_{y,\omega-\omega',k_y-k_y',k_z-k_z'}\frac{\mathrm{v}_\parallel}{\omega'-k_z'\mathrm{v}_\parallel}\frac{1}{\Omega_e}\partial_x\tilde{E}^{HF}_{z;\omega',k_y',k_z'} \\
&\qquad + 2\frac{n_{eo}\eta^2\omega_o^2}{\omega-\mathrm{k_z v_\parallel}}\int \mathrm{d}\omega'\int \mathrm{d}k_y'\int \mathrm{d}k_z'\,\tilde{E}^{HF}_{z,\omega-\omega',k_y-k_y',k_z-k_z'} \\
&\qquad \times \frac{\partial}{\partial \mathrm{v}_\parallel}\left[\frac{1}{\sqrt{\pi}}\frac{\mathrm{v}_\parallel}{\mathrm{v}_{th,e}}\frac{e^{-\mathrm{v}_\parallel^2/\mathrm{v}_{th,e}^2}}{\omega'-k_z'\mathrm{v}_\parallel}\right]\tilde{E}^{HF}_{z,\omega',k_y',k_z'},
\end{aligned}
\tag{2.45}
$$

where $g^{LF(2),NL}_{e;\omega,k_y,k_z} = \mathcal{I}_\perp \mathcal{F} f_e^{LF(2),NL}$.

The LF second-order density perturbation is now obtained by performing the integral of the above equation in the parallel velocity, following Landau's prescription to treat the relevant poles:

$$
\begin{aligned}
&n^{LF(2),NL}_{e;\omega,k_y,k_z} \\
&= \frac{2n_{eo}\eta^2\omega_o^2}{k_z\mathrm{v}_{th,e}^2}\left\{-i\int \mathrm{d}\omega'\int \mathrm{d}k_y'\int dk_z'\frac{1}{k_z'}\right. \\
&\quad \times \left[\tilde{E}^{HF}_{x,\omega-\omega',k_y-k_y',k_z-k_z'}\frac{k_y'\mathrm{v}_{th,e}}{\Omega_e}\tilde{E}^{HF}_{z,\omega',k_y',k_z'}\right]F_\perp(u,u') + \int \mathrm{d}\omega' \\
&\quad \times \int \mathrm{d}k_y'\int dk_z'\frac{1}{k_z'}\left[\tilde{E}^{HF}_{y,\omega-\omega',k_y-k_y',k_z-k_z'}\frac{\mathrm{v}_{th,e}}{\Omega_e}\partial_x\tilde{E}^{HF}_{z,\omega',k_y',k_z'}\right] \\
&\quad \times F_\perp(u,u') + \int \mathrm{d}\omega'\int \mathrm{d}k_y'\int dk_z' \\
&\quad \left.\times \frac{1}{k_z'}\tilde{E}^{HF}_{z,\omega-\omega',k_y-k_y',k_z-k_z'}\tilde{E}^{HF}_{z,\omega',k_y',k_z'}F_\parallel(u,u')\right\}.
\end{aligned}
\tag{2.46}
$$

Here, we define the coupling functions:

$$
\begin{aligned}
&F_\perp(u,u') = S(u) + u'\frac{S(u')-S(u)}{u'-u} \\
&F_\parallel(u,u') = 2u\frac{1+uS(u)}{u'-u} + u'\frac{S(u')-S(u)}{(u'-u)^2},\ u = \frac{\omega}{k_z\mathrm{v}_{th,e}}, \\
&u' = \frac{\omega'}{k_z'\mathrm{v}_{th,e}}.
\end{aligned}
\tag{2.47}
$$

We note that the quantities denoted above by a prime belong to the HF range. In addition, we omit the subscript $\sigma$ and $\sigma'$ to the functions $S(u)$ and $S(u')$ as well as in the coupling functions, but we recall that they also depend on the signs of $k_z$ and $k_z'$, respectively $\sigma$ and $\sigma'$.

Concerning the plasma ions in the LF range, the relevant kinetic equation at the second order in $\eta$ is given by:

$$
\begin{aligned}
&\frac{\partial f_i^{LF(2)}}{\partial t} + \mathbf{v}\cdot\frac{\partial f_i^{LF(2)}}{\partial \mathbf{r}} + \frac{q_i}{m_i}\frac{\mathbf{v}}{c}\times\mathbf{B}_o\cdot\frac{\partial f_i^{LF(2)}}{\partial \mathbf{v}} \\
&\quad + \frac{q_i}{m_i}\mathbf{E}^{LF}\cdot\frac{\partial f_{io}}{\partial \mathbf{v}} = 0.
\end{aligned}
\tag{2.48}
$$

This equation does not contain the nonlinear term due to the beating of the HF components since they are of a higher order in $\eta$. The expansion parameter of the weak turbulence theory concerning the kinetic equation for plasma ions is indeed a factor $Z_i(m_e/m_i)^{1/2}$ smaller than $\eta$, where $Z_i = q_i/e$ is the charge number of the ions species $i$. Nonlinear terms due to the beating of LF fields are also neglected, due to the ordering set by equation (2.5). In addition, the collisional operator is missing since the characteristic collisional frequency for plasma ions is orders of magnitude smaller than the typical frequencies in the LF range. If the eikonal hypothesis is fulfilled, the ion response can be calculated by the standard linear theory in terms of the ion susceptibility:

$$
\chi_i = \frac{1}{k^2\lambda_{D,i}^2}\left[1 + \frac{\omega}{k_z\mathrm{v}_{th,i}}\sum_{n=-\infty}^{+\infty} S\left(\frac{\omega-n\Omega_i}{k_z\mathrm{v}_{th,i}}\right)I_n(\lambda_i)\,e^{-\lambda_i}\right].
\tag{2.49}
$$

Here, $I_n$ is the modified Bessel function of integer order $n$ and, $\lambda_{D,i} = \left[k_B T_i/\left(4\pi n_{io} q_i^2\right)\right]^{1/2}$ and $\rho_{th,i} = \mathrm{v}_{th,i}/\Omega_i$ are, respectively, the Debye length and the thermal Larmor radius of the ion species $i$ and $\lambda_i = (1/2)\,k_\perp^2\rho_{th,i}^2$. The Fourier transform of the perturbed ion density at the second order in $\eta$ is thus:

$$
n^{LF(2)}_{i;\omega,k_y,k_z} = -i\eta\frac{m_e\omega_o\mathrm{v}_{th,e}}{e}\frac{1}{k_z}\frac{k^2}{4\pi\,q_i}\chi_i\tilde{E}^{LF}_{z;\omega,k_y,k_z}.
\tag{2.50}
$$

For $|\lambda_i| \ll 1$ the ion susceptibility is given by:

$$
\chi_i = \frac{1}{k^2\lambda_{D,i}^2}\left[1 + \frac{\omega}{k_z\mathrm{v}_{th,i}}S\left(\frac{\omega}{k_z\mathrm{v}_{th,i}}\right)\right].
\tag{2.51}
$$

In this case, the ion density perturbation can be thus calculated neglecting the ion dynamics perpendicular to the magnetic field. We recall that we have assumed as a reasonable, simplified condition for the validity of the eikonal hypothesis the ordering $|k_x|L > 10$. Moreover, we assume as a model hypothesis $L^2 \gg 50\rho_{th,i}^2$ and $|k_y| < |k_x|$. In this regard, we note that, within the framework of the electrostatic and eikonal approximations, which are reasonably valid for sufficiently large parallel wavenumbers, the angle $\delta$ between the perpendicular electric fields of the LH sidebands $E_\perp = E_x\hat{x} + E_y\hat{y}$ and the LH pump wave $E_{\perp o} \cong E_{xo}\hat{\boldsymbol{x}}$ should be much less than one (in rad units) to achieve significant amplification of the LH sidebands. This is shown in [68], where the value $\delta \cong 0.14$ was indicated to minimize the convective losses so that we achieve the largest amplification of the LH sidebands. Here, $\hat{x}$ and $\hat{y}$ are unit vectors, along the Cartesian axis, respectively $X$ and $Y$. In standard LHCD experiments, the injected LH power wave is characterized by a dominant radial electric field with respect to the poloidal component. This maximizes the radial LH power flow and is obtained by setting close to zero

the relative phase of the waveguides along the poloidal direction in the LH launchers. Within the framework mentioned above, the condition $\delta \ll 1$ thus implies $|E_y| \cong \delta |E_x|$ and the ordering $|k_y| \ll |k_x|$. If the eikonal hypothesis is not fulfilled we have:

$$\frac{1}{2}\left(|k_x|\,\rho_{th,i}\right)^2 \leqslant \frac{50\rho_{th,i}^2}{L^2} \ll 1. \tag{2.52}$$

Therefore, since it is assumed that $|k_y| < |k_x|$, we obtain $|\lambda_i| \ll 1$. This ordering suggests that $n^{LF(2)}_{i;\omega,k_y,k_z}$ can be calculated with a reasonable approximation neglecting the ion dynamics perpendicular to the magnetic field. In practice, to avoid jumps in the LH wave equations, we use equation (2.50) with the ion susceptibility given by equation (2.49). If the eikonal hypothesis is not well justified, the latter smoothly converges to the expression valid in this case, given by equation (2.51). In the LF range, the Fourier transform of the parallel component of the electric field, measured in units of $A_o$, fulfills the steady-state equation for electrostatic waves:

$$\begin{aligned}&\frac{d^2\tilde{E}^{LF}_{z;\omega,k_y,k_z}}{dx^2} - \left(k_y^2 + k_z^2\right)\tilde{E}^{LF}_{z;\omega,k_y,k_z} \\ &\quad = \frac{4\pi i k_z}{A_o}\left[\sum_j q_j n^{LF(2)}_{j;\omega,k_y,k_z} - e\left(n^{LF(2),L}_{e;\omega,k_y,k_z} + n^{LF(2),NL}_{e;\omega,k_y,k_z}\right)\right].\end{aligned} \tag{2.53}$$

As a model hypothesis, to be verified by the numerical solutions, we assume that $\left|k_x^{-2}\mathrm{d}k_x/\mathrm{d}x\right| \ll 1$. We observe that ion-sound and ion-cyclotron modes, without the nonlinear term and considering only the relevant linear dispersion equation, are evanescent, i.e. quasi-modes, for the tokamak peripheral plasma parameters.

Near the antenna mouth, i.e. around $x = 0$, we consider the non-evanescent approximate solution of equation (2.53), obtained considering the above model hypothesis, to be valid, given by:

$$\begin{aligned}&\tilde{E}^{LF}_{z;\omega,k_y,k_z}(x) \\ &\quad \cong i\frac{\omega_o}{\mathrm{v}_{th,e}}\frac{\eta}{\lambda_{De}^2}\left\{-i\int \mathrm{d}\omega'\int \mathrm{d}k_y'\int \mathrm{d}k_z'\,\frac{1}{k_z' k^2\varepsilon}\right. \\ &\qquad \times\left[\tilde{E}^{HF}_{x,\omega-\omega',k_y-k_y',k_z-k_z'}\frac{k_y'\mathrm{v}_{th,e}}{\Omega_e}\tilde{E}^{HF}_{z,\omega',k_y',k_z'}\right]F_\perp(u,u') \\ &\qquad + \int \mathrm{d}\omega'\int \mathrm{d}k_y'\int \mathrm{d}k_z'\,\frac{1}{k_z' k^2\varepsilon} \\ &\qquad \times\left[\tilde{E}^{HF}_{x,\omega-\omega',k_y-k_y',k_z-k_z'}\frac{\mathrm{v}_{th,e}}{\Omega_e}\partial_x\tilde{E}^{HF}_{z,\omega',k_y',k_z'}\right]F_\perp(u,u') \\ &\qquad + \int \mathrm{d}\omega'\int \mathrm{d}k_y'\int \mathrm{d}k_z'\,\frac{1}{k_z' k^2\varepsilon}\tilde{E}^{HF}_{z,\omega-\omega',k_y-k_y',k_z-k_z'} \\ &\qquad \left.\times\,\tilde{E}^{HF}_{z,\omega',k_y',k_z'}F_\parallel(u,u')\right\}.\end{aligned} \tag{2.54}$$

Here, $\varepsilon(\omega,\boldsymbol{k},x) = 1 + \chi_e + \sum_i \chi_i$ is the LF dielectric function, $\boldsymbol{k} = \left(k_{x;\omega,k_y,k_z}(x), k_y, k_z\right)$ and we define,

$$k_{x;\omega,k_y,k_z} = \left[\frac{\partial S_{\omega-\omega',k_y-k_y',k_z-k_z'}}{\partial x}\right] + \left[\frac{\partial S_{\omega',k_y',k_z'}}{\partial x}\right]. \tag{2.55}$$

We observe that $S_{\omega-\omega',k_y-k_y',k_z-k_z'}$ and $S_{\omega',k_y',k_z'}$ are, respectively, the phase of $\boldsymbol{E}^{HF}_{\omega-\omega',k_y-k_y',k_z-k_z'}$ and $\boldsymbol{E}^{HF}_{\omega',k_y',k_z'}$ as defined in equation (2.3). Equation (2.55) is the matching condition for the radial component of the wavenumber and is assumed to be valid at $x = 0$. We thus use equation (2.54) only to evaluate $E^{LF}_{z;\omega,k_y,k_z}$ and its first derivative with respect to $x$ at $x = 0$, namely $E^{LF}_{z;\omega,k_y,k_z}(0)$ and $\partial_x E^{LF}_{z;\omega,k_y,k_z}(0) = ik_{x;\omega,k_y,k_z}(0)\,E^{LF}_{z;\omega,k_y,k_z}(0)$, i.e. the initial conditions for the solutions of equation (2.53). It is important to note that we consider here LH sideband waves originated by the RF source and coupled by the LH antenna. As we will discuss in a future work in more detail and shown in [67], LH sideband waves originated by the plasma thermal noise might not produce significant PI. As an alternative approach, the LF initial conditions can be obtained from the LF noise, which might be important as suggested by the fluctuation-dissipation theorem [79]. In this case, the corresponding HF initial conditions are obtained by approximate solutions of the relevant wave equations, in analogy with equation (2.54) based on matching conditions analogous to equation (2.55). However, we will showin a future work that the approach here considered does provide the dominant PI effect for typical RF source noise and sufficiently low temperature at the LH antenna.

A suitable method to solve the LF wave equation (2.53) is obtained adopting the expression of the electric field $\tilde{E}^{LF}_{z;\omega,k_y,k_z} = \tilde{E}^{LF}_{z;\omega,k_y,k_z}(0)\exp\left[iS_{\omega,k_y,k_z}(x)\right]$ with complex phase $S(x)$. The second-order differential equation (2.53) is equivalent to the following couple of first-order differential equations:

$$\frac{\mathrm{d}S_{\omega,k_y,k_z}}{\mathrm{d}x} = k_{x;\omega,k_y,k_z}, \tag{2.56}$$

$$\frac{\mathrm{d}k_{x;\omega,k_y,k_z}}{\mathrm{d}x} = -ik^2\varepsilon - \frac{e^{-iS}}{\tilde{E}^{LF}_{z;\omega,k_y,k_z}(0)}\frac{\eta\omega_o}{\mathrm{v}_{th,e}\lambda_{De}^2}\mathrm{K}_{\omega,k_y,k_z}(x), \tag{2.57}$$

where,

$$\begin{aligned}&\mathrm{K}_{\omega,k_y,k_z}(x) \\ &\quad = \left\{-i\int \mathrm{d}\omega'\int \mathrm{d}k_y'\int \mathrm{d}k_z'\,\frac{1}{k_z'}\right. \\ &\qquad \times\left[\tilde{E}^{HF}_{x,\omega-\omega',k_y-k_y',k_z-k_z'}\frac{k_y'\mathrm{v}_{th,e}}{\Omega_e}\tilde{E}^{HF}_{z,\omega',k_y',k_z'}\right]F_\perp(u,u') \\ &\qquad + \int \mathrm{d}\omega'\int \mathrm{d}k_y'\int \mathrm{d}k_z'\,\frac{1}{k_z'} \\ &\qquad \times\left[\tilde{E}^{HF}_{x,\omega-\omega',k_y-k_y',k_z-k_z'}\frac{\mathrm{v}_{th,e}}{\Omega_e}\partial_x\tilde{E}^{HF}_{z,\omega',k_y',k_z'}\right]F_\perp(u,u') \\ &\qquad + \int \mathrm{d}\omega'\int \mathrm{d}k_y'\int dk_z'\,\frac{1}{k_z'}\tilde{E}^{HF}_{z,\omega-\omega',k_y-k_y',k_z-k_z'} \\ &\qquad \left.\times\tilde{E}^{HF}_{z,\omega',k_y',k_z'}F_\parallel(u,u')\right\}.\end{aligned} \tag{2.58}$$

The initial conditions of the system (2.56), (2.57) are $S_{\omega,k_y,k_z}(0) = 0$ and $k_{x;\omega,k_y,k_z}(0)$, as given by equation (2.55). For $x > 0$, the solution of the LF wave equation can still

approximated be expressed in a valid form around $x=0$, namely:

$$\begin{aligned}&\tilde{E}^{LF}_{z;\omega,k_y,k_z}(x)\\&\cong i\frac{\omega_o}{\mathrm{v}_{th,e}}\frac{\eta}{\lambda^2_{De}}\left\{-i\int \mathrm{d}\omega'\int \mathrm{d}k'_y\int dk'_z\,\frac{1}{k'_z k^2\varepsilon}\right.\\&\times\left[\tilde{E}^{HF}_{x,\omega-\omega',k_y-k'_y,k_z-k'_z}\frac{k'_y\mathrm{v}_{th,e}}{\Omega_e}\tilde{E}^{HF}_{z,\omega',k'_y,k'_z}\right]F_\perp(u,u')\\&+\int \mathrm{d}\omega'\int \mathrm{d}k'_y\int dk'_z\,\frac{1}{k'_z k^2\varepsilon}\\&\times\left[\tilde{E}^{HF}_{x,\omega-\omega',k_y-k'_y,k_z-k'_z}\frac{\mathrm{v}_{th,e}}{\Omega_e}\partial_x\tilde{E}^{HF}_{z,\omega',k'_y,k'_z}\right]\\&\times F_\perp(u,u')+\int \mathrm{d}\omega'\int \mathrm{d}k'_y\int dk'_z\,\frac{1}{k'_z k^2\varepsilon}\\&\left.\times\,\tilde{E}^{HF}_{z,\omega-\omega',k_y-k'_y,k_z-k'_z}\tilde{E}^{HF}_{z,\omega',k'_y,k'_z}F_\parallel(u,u')\right\}.\end{aligned}\tag{2.59}$$

Here, $\varepsilon(\omega,\boldsymbol{k},x)$ is again the LF dielectric function, but, as a fundamental difference with the solution (2.54), we now define $\boldsymbol{k}=\left(k_{x;\omega,k_y,k_z}(x),k_y,k_z\right)$ where $k_{x;\omega,k_y,k_z}(x)$ is determined from the solution of the coupled system of LF and HF integro-differential nonlinear wave equations. For inhomogeneous plasma, this introduces a mismatch in the phase coherence of the interacting waves, quenching the nonlinear interaction during the wave propagation in the radial direction. The LF linear electron density perturbation from equations (2.42) and (2.59) is thus approximated by:

$$\begin{aligned}&n^{LF(2),L}_{e;\omega,k_y,k_z}\cong-\frac{2\eta^2 n_{eo}\omega_o^2}{\mathrm{v}^2_{th,e}}\chi_e\\&\times\left\{-i\int \mathrm{d}\omega'\int \mathrm{d}k'_y\int dk'_z\,\frac{1}{k'_z k_z\varepsilon}\right.\\&\times\left[\tilde{E}^{HF}_{x,\omega-\omega',k_y-k'_y,k_z-k'_z}\frac{k'_y\mathrm{v}_{th,e}}{\Omega_e}\tilde{E}^{HF}_{z,\omega',k'_y,k'_z}\right]F_\perp(u,u')\\&+\int \mathrm{d}\omega'\int \mathrm{d}k'_y\int dk'_z\,\frac{1}{k'_z k_z\varepsilon}\\&\times\left[\tilde{E}^{HF}_{x,\omega-\omega',k_y-k'_y,k_z-k'_z}\frac{\mathrm{v}_{th,e}}{\Omega_e}\partial_x\tilde{E}^{HF}_{z,\omega',k'_y,k'_z}\right]F_\perp(u,u')\\&+\int \mathrm{d}\omega'\int \mathrm{d}k'_y\int dk'_z\,\frac{1}{k'_z k_z\varepsilon}\tilde{E}^{HF}_{z,\omega-\omega',k_y-k'_y,k_z-k'_z}\\&\left.\times\,\tilde{E}^{HF}_{z,\omega',k'_y,k'_z}F_\parallel(u,u')\right\}=-\frac{\chi_e}{\varepsilon}n^{LF(2),NL}_{e;\omega,k_y,k_z}.\end{aligned}\tag{2.60}$$

Therefore, we have:

$$n^{LF(2)}_{e;\omega,k_y,k_z}=n^{LF(2),L}_{e;\omega,k_y,k_z}+n^{LF(2),NL}_{e;\omega,k_y,k_z}\cong\frac{\chi_e-\varepsilon}{\chi_e}n^{LF(2),L}_{e;\omega,k_y,k_z}.\tag{2.61}$$

From the electrostatic equation (2.53), the model hypothesis $\left|k_x^{-2}\mathrm{d}k_x/\mathrm{d}x\right|\ll 1$, the linear ion response, given by equations (2.50) and (2.61) we can express the Fourier transform of the toroidal electric field measured in stV cm$^{-1}$ as,

$$E^{LF}_{z;\omega,k_y,k_z}=-4\pi ie\frac{k_z}{k^2}\frac{1}{\chi_e-\varepsilon}n^{LF(2)}_{e;\omega,k_y,k_z}=-4\pi ie\frac{k_z}{k^2}\frac{1}{\chi_e}n^{LF(2),L}_{e;\omega,k_y,k_z}.\tag{2.62}$$

The contribution to the total toroidal electric field in stV cm$^{-1}$ due to the linear electron density perturbation is thus given by the LF linear component of the toroidal electric field, namely:

$$E^{LF,L}_{z;\omega,k_y,k_z}=-4\pi ie\frac{k_z}{k^2}\frac{1}{\chi_e-\varepsilon}n^{LF(2),L}_{e;\omega,k_y,k_z}=\frac{\chi_e}{\chi_e-\varepsilon}E^{LF}_{z;\omega,k_y,k_z}.\tag{2.63}$$

The perturbed linear distribution function associated with the LF linear component of the toroidal electric fields is obtained by the method used to calculate $f^{HF(1)}_{e;\omega,k_y,k_z}$, formally expressed as,

$$f^{LF(2),LL}_{e;\omega,k_y,k_z}=\mathcal{F}\mathcal{H}_o^{-1}\eta\mathcal{F}^{-1}\mathcal{F}\left[\eta\mathbf{E}^{LF,L}\cdot\frac{\partial f_{eo}}{\partial\mathbf{v}}\mathrm{v}_{th,e}\omega_o\right]\mathrm{v}_{th,e}\omega_o.\tag{2.64}$$

In performing this calculation, we keep only the Bessel function of integer order $-1,\ 0,1$ and use the ordering $|\omega|\ll|\Omega_e|$. Thus, we neglect the terms containing the angular cyclotron frequency. The calculation of $f^{LF(2),NL}_{e;\omega,k_y,k_z}$ can be performed by the same method. As a result, an equation similar to equation (2.61) also holds between the total and the linear second-order distribution functions corresponding to the linear component of the LF electric fields, namely:

$$f^{LF(2)}_{e;\omega,k_y,k_z}=\frac{\chi_e-\varepsilon}{\chi_e}f^{LF(2),LL}_{e;\omega,k_y,k_z}.\tag{2.65}$$

To evaluate the current densities in the HF range at the third order in $\eta$ we need the gradient in the velocity space of the second-order distribution. The contribution due to $f^{LF(2),LL}_e$ is calculated as in the HF range, namely, we have:

$$\begin{aligned}\left[\nabla_{\mathbf{v}}f^{LF(2),LL}_{e;\omega,k_y,k_z}\right]_x&\cong-\frac{2\eta\omega_o}{\mathrm{v}_{th,e}}\frac{\mathrm{v}_\parallel}{\omega-\mathrm{k}_\parallel\mathrm{v}_\parallel}f_{eo}\frac{k_y}{\Omega_e}\tilde{E}^{LF,L}_{z;\omega,k_y,k_z}\\\left[\nabla_{\mathbf{v}}f^{LF(2),LL}_{e;\omega,k_y,k_z}\right]_y&\cong\frac{2\eta\omega_o}{\mathrm{v}_{th,e}}\frac{\mathrm{v}_\parallel}{\omega-\mathrm{k}_\parallel\mathrm{v}_\parallel}f_{eo}\frac{k_x}{\Omega_e}E^{LF,L}_{z;\omega,k_y,k_z}\\&=-\frac{2i\eta\omega_o}{\mathrm{v}_{th,e}}\frac{\mathrm{v}_\parallel}{\omega-\mathrm{k}_\parallel\mathrm{v}_\parallel}f_{eo}\frac{1}{\Omega_e}\partial_x\tilde{E}^{LF,L}_{z;\omega,k_y,k_z}\\\left[\nabla_{\mathbf{v}}f^{LF(2),LL}_{e;\omega,k_y,k_z}\right]_z&\cong-\frac{2i\eta\omega_o}{\mathrm{v}_{th,e}}\frac{\partial}{\partial\mathrm{v}_\parallel}\left[f_{eo}\frac{\mathrm{v}_\parallel}{\omega-\mathrm{k}_\parallel\mathrm{v}_\parallel}\right]\tilde{E}^{LF,L}_{z;\omega,k_y,k_z}.\end{aligned}\tag{2.66}$$

From equation (2.65) we obtain:

$$\nabla_{\mathbf{v}}f^{LF(2)}_{e;\omega,k_y,k_z}=\frac{\chi_e-\varepsilon}{\chi_e}\nabla_{\mathbf{v}}f^{LF(2),LL}_{e;\omega,k_y,k_z}.\tag{2.67}$$

As discussed in the next section, to compare our results with the standard theory in the limit of homogeneous plasma, we need to express both the gradient in the velocity space of the second-order distribution and the second-order toroidal electric field in terms of $E^{LF,L}_{z;\omega,k_y,k_z}$ by means of equations (2.67) and (2.63), respectively. Conversely, to derive the coupled set of nonlinear full-wave integro-differential equations, we need

the second-order field $\tilde{E}^{LF}_{z;\omega,k_y,k_z}$ and $\nabla_{\mathbf{v}} f^{LF(2)}_{e;\omega,k_y,k_z}$ expressed in terms of it, namely:

$$\left[\nabla_{\mathbf{v}} f^{LF(2)}_{e;\omega,k_y,k_z}\right]_x \cong -\frac{2\eta\omega_o}{\mathrm{v}_{th,e}} \frac{\mathrm{v}_\parallel}{\omega - \mathrm{k}_\parallel \mathrm{v}_\parallel} f_{eo} \frac{k_y}{\Omega_e} \tilde{E}^{LF}_{z;\omega,k_y,k_z}, \tag{2.68}$$

$$\left[\nabla_{\mathbf{v}} f^{LF(2)}_{e;\omega,k_y,k_z}\right]_y \cong -\frac{2i\eta\omega_o}{\mathrm{v}_{th,e}} \frac{\mathrm{v}_\parallel}{\omega - \mathrm{k}_\parallel \mathrm{v}_\parallel} f_{eo} \frac{1}{\Omega_e} \partial_x E^{LF}_{z;\omega,k_y,k_z}, \tag{2.69}$$

$$\left[\nabla_{\mathbf{v}} f^{LF(2)}_{e;\omega,k_y,k_z}\right]_z \cong -\frac{2i\eta\omega_o}{\mathrm{v}_{th,e}} \frac{\partial}{\partial \mathrm{v}_\parallel} \left[f_{eo} \frac{\mathrm{v}_\parallel}{\omega - \mathrm{k}_\parallel \mathrm{v}_\parallel}\right] E^{LF}_{z;\omega,k_y,k_z}. \tag{2.70}$$

We observe that $f^{LF(2)}_e$ and its gradient in the velocity space is calculated here as a self-consistent solution of the coupled system of the kinetic equations for electron and ion plasma species, the wave equation for LF electrostatic quasi-modes, namely ISQM and ICQM, driven by the beating of HF fields as well as the wave equation in the HF range that will be derived below. The ion dynamics affects the perturbed electron density in the LF range. This result corrects previous evaluations of the nonlinear electron density perturbation in the LF range in [66]. Finally, we consider the kinetic equation in the HF range up to the third order of the perturbation theory, including the nonlinear terms, namely:

$$\begin{aligned}&\frac{\partial f^{HF(3)}_e}{\partial t} + \mathbf{v}\cdot\frac{\partial f^{HF(3)}_e}{\partial \mathbf{r}} + \frac{q_e}{m_e}\mathbf{E}^{HF}\cdot\frac{\partial f_{eo}}{\partial \mathbf{v}} + \frac{\mathbf{v}}{c}\times\mathbf{B}_o\cdot\frac{\partial f^{HF(3)}_e}{\partial \mathbf{v}} \\ &+ \frac{q_e}{m_e}\mathbf{E}^{HF}\cdot\frac{\partial f^{LF(2)}_e}{\partial \mathbf{v}} + \frac{q_e}{m_e}\mathbf{E}^{LF}\cdot\frac{\partial f^{HF(1)}_e}{\partial \mathbf{v}} \\ &= -\nu_e\left[f^{HF(3)}_e - f_{eo}\frac{n^{HF(3)}_e}{n_{\alpha o}}\right].\end{aligned} \tag{2.71}$$

Here, $n^{HF(3)}_e = \int d^3\mathbf{v} f^{HF(3)}_e$.

Equation (2.71) is linear in $f^{HF(3)}_e$. Its solution can be expressed as the sum of two distributions, namely $f^{HF(3)}_e = f^{HF(3),L}_e + f^{HF(3),NL}_e$. The former is the solution of the following kinetic equation, which is linear in the HF electric field:

$$\begin{aligned}&\frac{\partial f^{HF(3),L}_e}{\partial t} + \mathbf{v}\cdot\frac{\partial f^{HF(3),L}_e}{\partial \mathbf{r}} + \frac{q_e}{m_e}\mathbf{E}^{HF}\cdot\frac{\partial f_{eo}}{\partial \mathbf{v}} + \frac{\mathbf{v}}{c}\times\mathbf{B}_o \\ &\cdot\frac{\partial f^{HF(3),L}_e}{\partial \mathbf{v}} = -\nu_e\left[f^{HF(3),L}_e - f_{eo}\frac{n^{HF(3),L}_e}{n_{\alpha o}}\right],\end{aligned} \tag{2.72}$$

where $n^{HF(3),L}_e = \int d^3\mathbf{v} f^{HF(3),L}_e$,

The latter is the solution of the kinetic equation involving nonlinear terms in the HF electric fields, where we drop the collisional operator, as in the appendix A we have shown that it provides negligible contribution to the nonlinear terms:

$$\begin{aligned}&\frac{\partial f^{HF(3),NL}_e}{\partial t} + \mathbf{v}\cdot\frac{\partial f^{HF(3),NL}_e}{\partial \mathbf{r}} + \frac{\mathbf{v}}{c}\times\mathbf{B}_o\cdot\frac{\partial f^{HF(3),NL}_e}{\partial \mathbf{v}} \\ &+ \frac{q_e}{m_e}\mathbf{E}^{HF}\cdot\frac{\partial f^{LF(2)}_e}{\partial \mathbf{v}} + \frac{q_e}{m_e}\mathbf{E}^{LF}\cdot\frac{\partial f^{HF(1)}_e}{\partial \mathbf{v}} = 0.\end{aligned} \tag{2.73}$$

The charge and current densities can be obtained from the linear wave equation by the spectral method and utilizing the inverse operator $\mathcal{H}_o^{-1}$, as done for the first order, keeping only terms at the lowest order in $k_\perp\rho_e$.

They are formally expressed by the equations (2.18)–(2.21) by substituting the superscript '(1)' with the superscript '(3), $L$' to indicate the linear contribution in the wave equation considered up to the third order in $\eta$. We can rewrite the equation (2.73) in the form

$$\mathcal{H}_o f^{HF(3),NL}_e = -\frac{q_e}{m_e}\mathbf{E}^{HF}\cdot\nabla_{\mathbf{v}} f^{LF(2)}_e - \frac{q_e}{m_e}\mathbf{E}^{LF}\cdot\nabla_{\mathbf{v}} f^{HF(1)}_e. \tag{2.74}$$

The integro-differential operator $\mathcal{H}_o$ has cylindrical symmetry in the velocity space around the direction of the magnetic field. The solution $f^{HF(3),NL}_e$ has the same symmetry, since the gradients and the boundary conditions in the velocity space do not break it. This means that the nonlinear component of the HF distribution function does not produce nonlinear current density components in the poloidal plane. The charge conservation allows obtaining the Fourier transform of the nonlinear toroidal current:

$$J^{HF(3),NL}_{e;z;\omega,k_y,k_z} = (\omega/k_z)\,\rho^{HF(3),NL}_{e;\omega,k_y,k_z}, \tag{2.75}$$

where $\rho^{HF(3),NL}_{e;\omega,k_y,k_z} = -en^{HF(3),NL}_{e;\omega,k_y,k_z}$ is the Fourier transform of the electron charge density. We thus need only to calculate the perturbed nonlinear density $n^{HF(3),NL}_{e;\omega,k_y,k_z}$.

To this end, we apply the operators $\mathcal{I}_\perp$ and $\mathcal{F}$ to equation (2.74) and obtain, measuring the electric fields in units of $A_o$

$$\begin{aligned}&g^{HF(3),NL}_{e;\omega,k_y,k_z} \\ &= \frac{i\eta\omega_o \mathrm{v}_{th,e}}{\omega - k_\parallel \mathrm{v}_\parallel}\left\{\int \mathrm{d}\Lambda' \tilde{E}_{\omega-\omega',k_y-k_y',k_z-k_z'^{HF}}\right. \\ &\cdot\left[\mathcal{I}_\perp\mathcal{F}\nabla_{\mathbf{v}} f^{LF(2)}_e\right]_{\omega',k_y',k_z'} + \int \mathrm{d}\Lambda'' \tilde{E}^{LF}_{\omega-\omega'',k_y-k_y'',k_z-k_z''} \\ &\left.\cdot\left[\mathcal{I}_\perp\mathcal{F}\nabla_{\mathbf{v}} f^{HF(1)}_e\right]_{\omega'',k_y'',k_z''}\right\}.\end{aligned} \tag{2.76}$$

The HF third-order nonlinear density perturbation $n^{HF(3),NL}_{e;\omega,k_y,k_z}$ is then derived by performing the integral of $g^{HF(3),NL}_{e;\omega,k_y,k_z}$ in the parallel velocity space, based on Landau's prescription to treat the relevant poles. As a result, we obtain:

$$\begin{aligned}&n^{HF(3),NL}_{e;\omega,k_y,k_z} \\ &= -\frac{2i\eta^2\omega_o^2 n_{eo}}{\Omega_e k_z \mathrm{v}_{th,e}}\int \mathrm{d}\Lambda' \tilde{E}^{HF}_{x;\omega-\omega',k_y-k_y',k_z-k_z'} \tilde{E}^{LF}_{y;\omega',k_y',k_z'} F_\perp\left(u,u'\right) \\ &+ \frac{2i\eta^2\omega_o^2 n_{eo}}{\Omega_e k_z \mathrm{v}_{th,e}}\int \mathrm{d}\Lambda' \tilde{E}^{HF}_{y;\omega-\omega',k_y-k_y',k_z-k_z'} \tilde{E}^{LF}_{x;\omega',k_y',k_z'} F_\perp\left(u,u'\right) \\ &+ \frac{2\eta^2\omega_o^2 n_{eo}}{k_z \mathrm{v}_{th,e}}\int \mathrm{d}\Lambda' \tilde{E}^{HF}_{z;\omega-\omega',k_y-k_y',k_z-k_z'} \tilde{E}^{LF}_{z;\omega',k_y',k_z'} \frac{F_\parallel\left(u,u'\right)}{k_z' \mathrm{v}_{th,}} \\ &- \frac{2i\eta^2\omega_o^2 n_{eo}}{\Omega_e k_z \mathrm{v}_{th,e}}\int \mathrm{d}\Lambda'' \tilde{E}^{LF}_{x;\omega-\omega'',k_y-k_y'',k_z-k_z''}\end{aligned}$$

$$\times \tilde{E}^{HF}_{y;\omega'',k_y'',k_z''} F_\perp(u,u'') + \frac{2\eta^2\omega_o^2 n_{eo}}{\Omega_e k_z v_{th,e}} \int d\Lambda'' \tilde{E}^{LF}_{y;\omega-\omega'',k_y-k_y'',k_z-k_z''} \times \frac{1}{k_z''} \partial_x \tilde{E}^{HF}_{z;\omega'',k_y'',k_z''} F_\perp(u,u'') + \frac{2\eta^2\omega_o^2 n_{eo}}{k_z v_{th,e}} \int d\Lambda'' \tilde{E}^{LF}_{z;\omega-\omega'',k_y-k_y'',k_z-k_z''} \times \tilde{E}^{HF}_{z;\omega'',k_y'',k_z''} \frac{F_\parallel(u,u'')}{k_z'' v_{th,e}}. \quad (2.77)$$

Here, the angular frequencies $\omega'$ and $\omega''$ belong, respectively, to the LF and HF range and we define:

$$u = \frac{\omega}{k_z v_{th,e}}, u' = \frac{\omega'}{k'_z v_{th,e}}, u'' = \frac{\omega''}{k''_z v_{th,e}}, \quad . \quad \Lambda' = d\omega' dk'_y dk'_z \text{ and } d\Lambda'' = d\omega'' dk''_y dk''_z$$

We recall that the LF electric field is of order $\eta$, as shown by equation (2.59), so that $n^{HF(3),NL}_{e;\omega,k_y,k_z}$ is a quantity of order $\eta^3$. Measuring the electric field in units of stV cm$^{-1}$, the nonlinear electron charge density perturbation at the third order is:

$$\rho^{HF(3),NL}_{e;\omega,k_y,k_z} = \frac{ie\omega_{pe}^2}{4\pi\Omega_e T_e k_z v_{th,e}} \int d\Lambda' E^{HF}_{x;\omega-\omega',k_y-k'_y,k_z-k'_z} E^{LF}_{y;\omega',k'_y,k'_z} F_\perp(u,u') - \frac{ie\omega_{pe}^2}{4\pi\Omega_e T_e k_z v_{th,e}} \int d\Lambda' E^{HF}_{y;\omega-\omega',k_y-k'_y,k_z-k'_z} E^{LF}_{x;\omega',k'_y,k'_z} F_\perp(u,u') - \frac{e\omega_{pe}^2}{4\pi T_e k_z v_{th,e}} \int d\Lambda' E^{HF}_{z;\omega-\omega',k_y-k'_y,k_z-k'_z} E^{LF}_{z;\omega',k'_y,k'_z} \frac{F_\parallel(u,u')}{k'_z v_{th,e}} \times \frac{ie\omega_{pe}^2}{4\pi\Omega_e T_e k_z v_{th,e}} \int d\Lambda'' E^{LF}_{x;\omega-\omega'',k_y-k_y'',k_z-k_z''} \times E^{HF}_{y;\omega'',k_y'',k_z''} F_\perp(u,u'') - \frac{e\omega_{pe}^2}{4\pi\Omega_e T_e k_z v_{th,e}} \int d\Lambda'' E^{LF}_{y;\omega-\omega'',k_y-k_y'',k_z-k_z''} \times \frac{1}{k_z''} \partial_x E^{HF}_{z;\omega'',k_y'',k_z''} F_\perp(u,u'') + - \frac{e\omega_{pe}^2}{4\pi T_e k_z v_{th,e}} \int d\Lambda'' E^{LF}_{z;\omega-\omega'',k_y-k_y'',k_z-k_z''} \times E^{HF}_{z;\omega'',k_y'',k_z''} \frac{F_\parallel(u,u'')}{k_z'' v_{th,e}}. \quad (2.78)$$

To compare our results with the standard theory of PI we express $\rho^{HF(3),NL}_{e;\omega,k_y,k_z}$ in terms of the linear component of the LF electric field:

$$\rho^{HF(3),NL}_{e;\omega,k_y,k_z} = \frac{ie\omega_{pe}^2}{4\pi\Omega_e T_e k_z v_{th,e}} \int d\Lambda' E^{HF}_{x;\omega-\omega',k_y-k'_y,k_z-k'_z} E^{LF,L}_{y;\omega',k'_y,k'_z} \times \frac{\chi'_e - \varepsilon'}{\chi'_e} F_\perp(u,u') - \frac{ie\omega_{pe}^2}{4\pi\Omega_e T_e k_z v_{th,e}} \int d\Lambda' E^{HF}_{y;\omega-\omega',k_y-k'_y,k_z-k'_z} E^{LF,L}_{x;\omega',k'_y,k'_z} \times \frac{\chi'_e - \varepsilon'}{\chi'_e} F_\perp(u,u') - \frac{e\omega_{pe}^2}{4\pi T_e k_z v_{th,e}} \int d\Lambda' E^{HF}_{z;\omega-\omega',k_y-k'_y,k_z-k'_z} E^{LF,L}_{z;\omega',k'_y,k'_z} \times \frac{\chi'_e - \varepsilon'}{\chi'_e} \frac{F_\parallel(u,u')}{k'_z v_{th,e}} \times \frac{ie\omega_{pe}^2}{4\pi\Omega_e T_e k_z v_{th,e}} \int d\Lambda'' E^{LF,L}_{x;\omega-\omega'',k_y-k_y'',k_z-k_z''} \times E^{HF}_{y;\omega'',k_y'',k_z''} \frac{\chi''_e - \varepsilon''}{\chi''_e} F_\perp(u,u'') - \frac{e\omega_{pe}^2}{4\pi\Omega_e T_e k_z v_{th,e}} \int d\Lambda'' E^{LF,L}_{y;\omega-\omega'',k_y-k_y'',k_z-k_z''} \times \frac{1}{k_z''} \partial_x E^{HF}_{z;\omega'',k_y'',k_z''} \frac{\chi''_e - \varepsilon''}{\chi''_e} F_\perp(u,u'') - \frac{e\omega_{pe}^2}{4\pi T_e k_z v_{th,e}} \int d\Lambda'' E^{LF,L}_{z;\omega-\omega'',k_y-k_y'',k_z-k_z''} E^{HF}_{z;\omega'',k_y'',k_z''} \times \frac{\chi''_e - \varepsilon''}{\chi''_e} \frac{F_\parallel(u,u'')}{k_z'' v_{th,e}}. \quad (2.79)$$

In the electrostatic limit of HF waves we need to substitute:

$$\frac{1}{k_z''} \partial_x E^{HF}_{z;\omega'',k_y'',k_z''} \to i E^{HF}_{x;\omega'',k_y'',k_z''}. \quad (2.80)$$

Moreover, all the electric fields are expressed by a potential, namely:

$$E^{HF}_{x;\omega,k_y,k_z} = -\partial_x \varphi^{HF}_{\omega,k_y,k_z}, E^{HF}_{y;\omega,k_y,k_z} = -ik_y \varphi^{HF}_{\omega,k_y,k_z}, E^{HF}_{z;\omega,k_y,k_z} = -ik_z \varphi^{HF}_{\omega,k_y,k_z}, \quad (2.81)$$

with analogous formulas for the LF range.

The HF electrostatic nonlinear wave equation is thus:

$$\left(1 - \sum_j \frac{\omega_{pj}^2}{\omega^2}\right) \left(\partial_x^2 - k_y^2 - k_z^2\right) \varphi^{HF}_{\omega,k_y,k_z} = \left[ \frac{1}{1 + i\gamma_e S(u_e)} \frac{\omega_{pe}^2}{\Omega_e^2} \frac{k_y^2 - \partial_x^2}{1 - \left(\frac{\omega + i\nu_e}{\Omega_e}\right)^2} + \frac{1}{\lambda_{De}^2} \frac{1 + u_e S(u_e)}{1 + i\gamma_e S(u_e)} \right] \varphi^{HF}_{\omega,k_y,k_z} - 4\pi \rho^{HF(3),NL}_{e;\omega,k_y,k_z}. \quad (2.82)$$

Here, $\rho^{HF(3),NL}_{e;\omega,k_y,k_z}$ is obtained from equation (2.79) with the substitutions indicated in equations (2.80) and (2.81) and expressing the electric field components in terms of the potentials.

Within the approximations leading to the dominant parallel dynamics of the electrons, the nonlinear charge density perturbation is:

$$\rho^{HF(3),NL}_{e;\omega,k_y,k_z} \cong -\frac{e\omega^2_{pe}}{4\pi\, T_e k_z \mathrm{v}_{th,e}} \times \int d\Lambda' E^{HF}_{z;\omega-\omega',k_y-k_y',k_z-k_z'} E^{LF}_{z;\omega',k_y',k_z'} \frac{F_{\parallel}(u,u')}{k_z' \mathrm{v}_{th,e}} - \frac{e\omega^2_{pe}}{4\pi\, T_e k_z \mathrm{v}_{th,e}} \int d\Lambda'' E^{LF}_{z;\omega-\omega'',k_y-k_y'',k_z-k_z''} \times E^{HF}_{z;\omega'',k_y'',k_z''} \frac{F_{\parallel}(u,u'')}{k_z'' \mathrm{v}_{th,e}}. \tag{2.83}$$

The perpendicular components of the current density in this case are neglected. The nonlinear current density along the direction of the magnetic field can be obtained from the charge conservation as,

$$J^{HF(3),NL}_{e;\omega,k_y,k_z} = \frac{\omega}{k_z} \rho^{HF(3),NL}_{e;\omega,k_y,k_z}. \tag{2.84}$$

For fixed ion background, the relevant nonlinear wave equation in the HF range is:

$$\frac{\mathrm{d}^2 E^{HF}_{z;\omega,k_y,k_z}}{\mathrm{d}x^2} = \beta^L(x,k_y,k_z,\omega) E^{HF}_{z;\omega,k_y,k_z} + \beta^{NL}(x,k_y,k_z,\omega,E_z), \tag{2.85}$$

where,

$$\beta^L(x,k_y,k_z,\omega) = k_y^2 + k_z^2 - \frac{\omega^2}{c^2} + \left(1 - \frac{\omega^2}{k_z^2 c^2}\right) \frac{1}{\lambda^2_{De}} \frac{1 + u_e S(u_e)}{1 + i\gamma_e S(u_e)}, \tag{2.86}$$

and

$$\beta^{NL}(x,k_y,k_z,\omega,E_z) = -i\left(1 - \frac{\omega^2}{k_z^2 c^2}\right) \frac{1}{\lambda^2_{De}} \frac{e}{2T_e} \left\{ \int \mathrm{d}\Lambda' E^{HF}_{z;\omega-\omega',k_y-k_y',k_z-k_z'} \times E^{LF}_{z;\omega',k_y',k_z'} \frac{F_{\parallel}(u,u')}{k_z'} + \int \mathrm{d}\Lambda'' E^{LF}_{z;\omega-\omega'',k_y-k_y'',k_z-k_z''} E^{HF}_{z;\omega'',k_y'',k_z''} \frac{F_{\parallel}(u,u'')}{k_z''} \right\}. \tag{2.87}$$

Finally, the nonlinear wave equations obtained taking into account the perpendicular dynamics of the electrons are:

$$\left(\frac{\omega^2}{c^2} - k_y^2 - k_z^2\right) E^{HF}_{x;\omega,k_y,k_z} - i\partial_x \left(k_y E^{HF}_{y;\omega,k_y,k_z} + k_z E^{HF}_{z;\omega,k_y,k_z}\right) = -\frac{4\pi\, i\omega}{c^2} \left[ J^{HF(1)}_{e;x;\omega,k_y,k_z} + \sum_j J^{HF(1)}_{j;x;\omega,k_y,k_z} \right], \tag{2.88}$$

$$\left(\partial_x^2 - k_z^2 + \frac{\omega^2}{c^2}\right) E^{HF}_{y;\omega,k_y,k_z} - k_y \left(i\partial_x E^{HF}_{x;\omega,k_y,k_z} - k_z E^{HF}_{z;\omega,k_y,k_z}\right) = -\frac{4\pi\, i\omega}{c^2} \left[ J^{HF(1)}_{e;y;\omega,k_y,k_z} + \sum_j J^{HF(1)}_{j;y;\omega,k_y,k_z} \right], \tag{2.89}$$

$$\left(\partial_x^2 - k_y^2 + \frac{\omega^2}{c^2}\right) E^{HF}_{z;\omega,k_y,k_z} - k_z \left(i\partial_x E^{HF}_{x;\omega,k_y,k_z} - k_y E^{HF}_{y;\omega,k_y,k_z}\right) = -\frac{4\pi\, i\omega}{c^2} \left[ J^{HF(1)}_{e;z;\omega,k_y,k_z} + \sum_j J^{HF(1)}_{j;z;\omega,k_y,k_z} + J^{HF(3),NL}_{e;z;\omega,k_y,k_z} \right]. \tag{2.90}$$

Here, $J^{HF(3),NL}_{e;z;\omega,k_y,k_z}$ is obtained by equations (2.84) and (2.78), and $\boldsymbol{J}^{HF(1)}_{e;\omega,k_y,k_z}$ and $\boldsymbol{J}^{HF(1)}_{i;\omega,k_y,k_z}$ are given, respectively, by equations (2.19)–(2.21) (with $\rho^{HF(1)}_{e;z;\omega,k_y,k_z}$ and $\rho^{HF(1)'}_{e;\omega,k_y,k_z}$ provided by equation (2.18), respectively, with and without the first term in the curly bracket) and by equation (2.22), utilizing the definition of $\eta$ and expressing the electric fields in units of stV cm$^{-1}$. The coupled system of the HF and LF integro-differential wave equations, the former being provided by equations (2.88)–(2.90) or their limits within the electrostatic approximation, equation (2.82), or within the approximations leading to dominant parallel electron dynamics, equation (2.85), and the latter being provided by equation (2.53), utilizing there the definition of $\eta$ and expressing the electric fields in units of stV cm$^{-1}$, are the main results of the present study. This has to be solved with the initial conditions in the LF range discussed above and the initial conditions in the HF range provided by the LH coupling codes concerning the spectral components of the pump wave and by the spectral analysis of the LH sidebands emerging from the noise. Compared to the standard eikonal model of PI driven by LH waves in inhomogeneous plasmas, this allows us to treat in detail the wavenumber spectrum of the pump wave, which in the standard model is reduced to a single component. In addition, the effect of finite illumination of the pump, which in the standard model is considered only by means of geometrical parameters of the area illuminated by the antenna, is embedded here in the full wavenumber spectrum of the LH pump wave. The convective loss effects, which in the standard model are often treated considering the phase mismatch of the interacting waves based on their parameters at the antenna mouth [15, 60], are embedded in the coupled LF–HF wave equations, considering the wave propagation in the overall interaction region, as also done within the framework of a more refined eikonal theory in [67]. Moreover, we consider here electromagnetic LH waves, which are often treated within the electrostatic approximation of the standard theory, with the exception of recent analysis in homogeneous plasma [65]. Finally, we take into account diffraction effects that are missing in the eikonal theory and can be important for LH sidebands with relatively low parallel wavenumber. Although in the present numerical implementation of the model this feature is not included, in principle,

**Table 2.** Summary of the model hypothesis. All the quantities are defined in the text of section 2 and in table 1. We note that, though the requirement $\omega_{HF} \ll \Omega_e$ is usually fulfilled in LHCD experiments, a much less severe requirement $\mathcal{O}\left[1-\omega^2/\Omega_e^2\right]^{-1}=1$ is sufficient for the model validity. In the same vein, the condition $\delta \ll 1$, usually verified to maximize the PI [68], can be substituted by the much less severe requirement $|k_y| < |k_x|$.

| | | | |
|---|---|---|---|
| $\eta, \lvert u_{\pm 1}\rvert, \delta \ll 1,\ \omega_{LF} \gg \omega^*_{e,i}$ | $\lvert k_\perp \rho_{th,e}\rvert, (k_y\rho_{th,i})^2 \ll 1,$ | $l_c < 2L_y, 2L_z;\ \lvert k_x^{-2}\mathrm{d}k_x/\mathrm{d}x\rvert_{LF} \ll 1$ | $\lvert k_x L\rvert < 10 \Rightarrow r_{E_\perp/E_\parallel} \ll 1$ |
| $\omega_{pi}, \Omega_i \ll \omega_{HF} \ll \Omega_e$ | $L^2 \gg 50\rho^2_{th,i}$ | $A_{j;\omega_o,k_{yo},k_{zo}} \gg A_{j;\omega_s,k_{ys},k_{zs}}, A_{j;\omega_q,k_{yq},k_{zq}}$ | $\lvert N_\parallel\rvert_{HF} > 1.5$ |

**Table 3.** Typical plasma and RF parameters that fulfill the model requirements.

| $B_o$ | $n_e$ $\left(10^{12}\ \mathrm{cm}^{-3}\right)$ | $T_e$ (eV) | $f_o$ | $\lvert k_\parallel\rvert$ $\left(\mathrm{cm}^{-1}\right)$ | $\lvert k_x\rvert$ | $\delta$ | $P_o$ | $L$ |
|---|---|---|---|---|---|---|---|---|
| 5.0 T | 0.6–30 | 2.5–100 | 5 GHz | 1.5–30 | $(2-10)\lvert k_\parallel\rvert$ | ∼0.15 | ∼2 kW cm$^{-2}$ | ∼1.0 cm |

**Table 4.** Typical plasma and RF parameters that fulfill the model requirements for dominant parallel dynamics of the electrons.

| $B_o$ | $n_e$ $\left(10^{12}\ \mathrm{cm}^{-3}\right)$ | $T_e$ (eV) | $f_o$ | $\lvert k_\parallel\rvert$ $\left(\mathrm{cm}^{-1}\right)$ | $\lvert k_x\rvert$ | $\delta$ | $P_o$ | $L$ |
|---|---|---|---|---|---|---|---|---|
| 5.0 T | 0.6–8.0 | 2.5–30 | 5 GHz | 1.5–15 | $(2-10)\lvert k_\parallel\rvert$ | ∼0.15 | ∼2 kW cm$^{-2}$ | ∼1.0 cm |

it might also treat sideband-sideband interactions instead of considering only sideband-pump interactions. In this vein, cascade PI phenomena may be evaluated. We summarize in table 2 the model hypothesis, introduced above, which is necessary to derive a set of coupled nonlinear LH integro-differential wave equations. In table 3 we indicate typical plasma and RF parameters that fulfill this model hypothesis. In table 4 we indicate typical plasma and RF parameters that fulfill the requirements of the simplified model that neglects the perpendicular dynamics of the electrons.

Despite the model constraints, the LH wave equations might reasonably describe nonlinear PI driven by LHCD in peripheral plasmas for many realistic experimental scenarios. We observe that the model cannot be considered as based on a full kinetic approach since it retains only kinetic effects compatible with the hypothesis made and uses a simplified collision operator. However, we observe that all the conditions listed in table 1 are usually verified in the peripheral plasma in LHCD experiments. Conversely, with the simplified wave equations considering only the parallel dynamics of the electrons, only the parallel drive of PI has a serious limitation due to the requirement $r_{E_\perp/E_\parallel} \ll 1$. This is not well justified for high plasma density, typically larger than $7-8\ 10^{12}\ \mathrm{cm}^{-3}$, so that the electrostatic approximation can be used and $r_{E_\perp/E_\parallel} \ll 1$ is equivalent to $\omega_{HF} \ll |\Omega_e k_z/k_x|$. The $\boldsymbol{E}\times\boldsymbol{B}$ drive of PI, discussed in the next section, becomes significant and then dominant for large plasma density [61, 73]. However, at this density level, the eikonal hypothesis is also reasonably justified for components with relatively small parallel wavenumbers, e.g. for the LH pump wave. The analysis of PI might thus be completed by interfacing the numerical code, which solves the set of nonlinear LH wave equations considering only parallel drive, with numerical codes that are based on the eikonal approximation and include the $\boldsymbol{E}\times\boldsymbol{B}$ drive, e.g. LHSTAR [60, 68]. On the other hand, in reactor scenarios, e.g. in ITER [80–82], at plasma density above the limit of the parallel drive modeling, which occurs near the separatrix, steep density and temperature gradients prevent the onset of PI, due to the convective losses and the large temperatures involved, quenching the PI drive. In this case, the parallel drive modeling can be applied standalone to evaluate the PI due to the LHCD power injection.

## 3. LH waves in homogeneous collisional and collisionless plasmas

Here, we first discuss the solutions of the linear and nonlinear dispersion equations in uniform collisionless plasmas derived from the modeling developed in section 2 and compare them with the archived literature results. We then analyze the role of collisions on nonlinear LH physics in homogeneous plasmas. Within the uniform plasma limit, the linear wave equations (2.23)–(2.25) give, for monochromatic waves with electric field $\mathcal{E} = Re\left[E_{\omega,k}e^{i(k\cdot r-\omega t)}\right]$, the equation:

$$\overline{\overline{\Lambda}}\cdot\boldsymbol{E}_{\omega,\boldsymbol{k}} = 0. \tag{3.1}$$

Here, the Cartesian component of the tensor $\overline{\overline{\Lambda}}$ in the reference frame defined in section 2, for $N_y = 0$ and $\nu_e = 0$ , are:

$$\begin{aligned}
\Lambda_{xx} &= n_z^2 - 1 - \frac{\omega_{pe}^2}{\Omega_e^2-\omega^2} + \sum_j \frac{\omega_{pj}^2}{\omega^2},\\
\Lambda_{xy} &= -i\frac{\omega_{pe}^2}{\Omega_e^2-\omega^2}\frac{\Omega_e}{\omega}\\
\Lambda_{xz} &= -N_xN_z,\ \Lambda_{yx} = +i\frac{\omega_{pe}^2}{\Omega_e^2-\omega^2}\frac{\Omega_e}{\omega}\\
\Lambda_{yy} &= N_x^2 + N_z^2 - 1 - \frac{\omega_{pe}^2}{\Omega_e^2-\omega^2} + \sum_j \frac{\omega_{pj}^2}{\omega^2},\\
\Lambda_{yz} &= -i\frac{\omega_{pe}^2}{\omega\Omega_e}\frac{N_x}{N_z}\left[1+uZ(u)\right]\\
\Lambda_{zx} &= -N_zN_x,\ \Lambda_{zy} = i\frac{\omega_{pe}^2}{\omega\Omega_e}\frac{N_x}{N_z}\left[1+uZ(u)\right]\\
\Lambda_{zz} &= n_x^2 - 1 - 2\frac{\omega_{pe}^2}{\omega^2}\frac{c^2}{N_z^2v_{th,e}^2}\left[1+uZ(u)\right] + \sum_j \frac{\omega_{pj}^2}{\omega^2}.
\end{aligned} \tag{3.2}$$

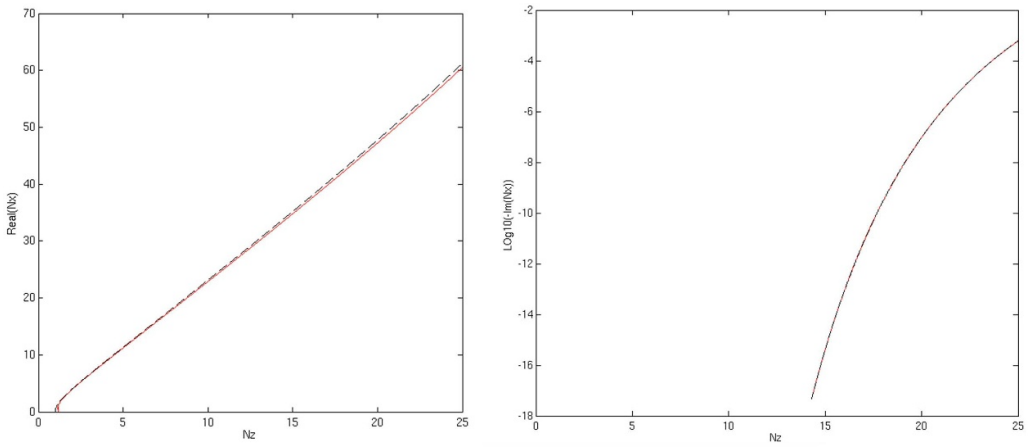


**Figure 2.** Real (left) and imaginary (right) parts of the perpendicular refractive index are plotted versus the parallel refractive index. Black dashed line corresponds to the solution of the wave equation obtained with fixed ion background and neglecting the electron dynamics perpendicular to the magnetic field. Red continuous line corresponds to the wave equation obtained at the lowest order in the parameter $k_\perp \rho_{th,e}$.

From equation (3.1), the following linear dispersion equation is obtained:

$$\det \overline{\overline{\Lambda}} = 0. \tag{3.3}$$

For given frequency and plasma parameters, the solutions of equation (3.3) provide the complex refractive index $N_x$ as a function of the real parallel refractive index $N_z$. The corresponding electric field polarization can then be obtained by solving equation (3.1).

Within the limit of dominant parallel electron dynamics and fixed ion background, the following dispersion equation is derived by the wave equation (2.26) for $N_y = 0$ and $\nu_e = 0$:

$$N_x^2 + N_z^2 - 1 + \left(1 - \frac{1}{N_z^2}\right) \frac{c^2}{\omega^2 \lambda_{De}^2} \left[1 + uZ(u)\right] = 0. \tag{3.4}$$

The solution is (for $N_z > 1$), considering the principal value of the square root:

$$N_x = \left\{1 - n_z^2 - \left(1 - \frac{1}{n_z^2}\right) \frac{c^2}{\omega^2 \lambda_{De}^2} \left[1 + uZ(u)\right]\right\}^{1/2}. \tag{3.5}$$

The electric field polarization is then obtained from equations (2.31) and (2.32):

$$E_y/E_x = 0, E_z/E_x = \left(N_z^2 - 1\right) / \left(N_x N_z\right). \tag{3.6}$$

In figures 2 and 3, we compare the results obtained by numerical solutions of the wave equation (3.1) with those expressed by equations (3.5) and (3.6). The RF and plasma parameters used are listed in table 5 below. Pure deuterium plasma has been considered.

A good agreement can be seen between the solutions of the two wave equations for $N_z > 1.5$, as required by the model hypothesis. We have not plotted the real part of the toroidal electric field, for $E_x = 1$ stV cm$^{-1}$, which is in practice identical for the two wave equations. $Im\left(E_z/E_x\right)$ is negligibly small, and only for $N_z > 20$ has the order of $10^{-6}$. Tiny differences, not detectable in this kind of plot, exist between the numerical solutions of the wave equation (3.1) for $N_y = 0$ and $\nu_e = 0$ and those obtained by numerical solutions of the wave equation derived considering the susceptibility tensors of the plasma species given in standard textbooks, e.g. equation (57) of [75], as calculated by the full kinetic theory.

We now calculate the nonlinear dispersion equation in uniform plasma considering four waves interactions. This is due to the parametric coupling of the LH pump waves with upper and lower sideband LH waves as mediated by ion-sound or ion-cyclotron quasi-modes. To compare our model with the results known in the archived literature, we first consider the electrostatic limit of LH waves in collisionless plasma.

The nonlinear interaction involves three electrostatic high-frequency monochromatic LH waves identified by their parallel electric fields, namely a pump wave $\mathcal{E}^o = \left[\boldsymbol{E}_o e^{i(k_o \cdot r - \omega_o t)} + c.c.\right]/2$, a lower sideband $\mathcal{E}^1 = \left[\boldsymbol{E}_1 e^{i(k_1 \cdot r - \omega_1 t)} + c.c.\right]/2$ and an upper sideband $\mathcal{E}^2 = \left[\boldsymbol{E}_2 e^{i(k_2 \cdot r - \omega_2 t)} + c.c.\right]/2$. In addition, we consider a single electrostatic LF monochromatic wave, characterized by a parallel electric field $\mathcal{E} = \left[\boldsymbol{E} e^{i(k \cdot r - \omega t)} + c.c.\right]/2$.

These electrostatic fields can be derived from electric potentials, so that we have, concerning the amplitudes, $\boldsymbol{E}_o = -i\boldsymbol{k}_o \phi_o$, $\boldsymbol{E}_1 = -i\boldsymbol{k}_1 \phi_1$, $\boldsymbol{E}_2 = -i\boldsymbol{k}_2 \phi_2$ and $\boldsymbol{E} = -i\boldsymbol{k}\phi$.

All the fields are measured in stV cm$^{-1}$ and the potentials in stV. We assume $Im(\omega_o) = 0$, i.e. a fixed pump amplitude, while the LH sidebands and the LF quasi-modes can damp or grow, i.e. $Im\left(\omega\right) \neq 0$. Concerning the real parts, it is assumed, without loss of generality, that $\omega_o > 0$ and $Re\left(\omega\right) = \omega_r > 0$. Suitable matching conditions are assumed for the four wave interactions, namely $\omega_1 = \omega - \omega_o$, $\boldsymbol{k}_1 = \boldsymbol{k} - \boldsymbol{k}_o$, $\omega_2 = \omega + \omega_o$, $\boldsymbol{k}_2 = \boldsymbol{k} + \boldsymbol{k}_o$. In the limit of uniform plasma, the following LF nonlinear equation is obtained, based on the kinetic equation and the perturbation theory, following the analysis performed in section 2:

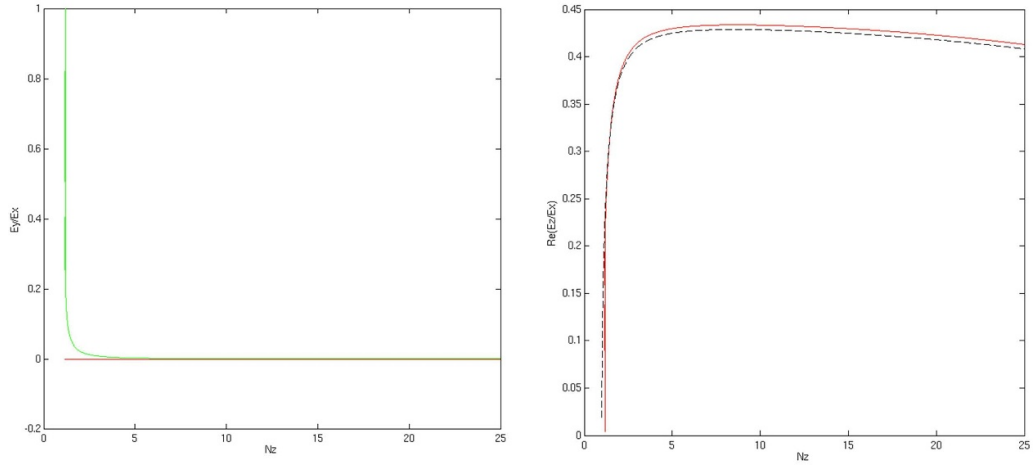


**Figure 3.** Poloidal electric field (left), for radial electric field $E_x = 1$ stV cm$^{-1}$ (real) is plotted versus $N_z$. Green line corresponds to the imaginary part, and red line on zero to the real part. Here, the wave equation obtained at the lowest order in the parameter $k_\perp \rho_e$ with un-magnetized ions is considered. Corresponding poloidal electric field obtained with fixed ion background and neglecting the electron dynamics perpendicular to the magnetic field is zero. Real part of the toroidal electric field (right), for radial electric field $E_x = 1$ stV cm$^{-1}$ (real) is plotted versus $N_z$. Red, continuous line corresponds to the wave equation obtained at the lowest order in the parameter $k_\perp \rho_e$ with un-magnetized ions. Black, dashed line corresponds to the wave equation obtained with fixed ion background and neglecting the electron dynamics perpendicular to the magnetic field.

**Table 5.** RF and plasma parameters used to compare the solutions of the linear wave equations.

| $f$ | $N_z$ | $B_o$ | $n_e$ | $T_e = T_i$ |
|---|---|---|---|---|
| 8.0 GHz | $1-25$ | 4.52 T | 5.0 $10^{12}$ cm$^{-3}$ | 25 eV |

$$\varepsilon\phi = -\frac{4\pi e}{k^2} n^{LF}_{e,NL}. \tag{3.7}$$

Here, $\varepsilon = 1 + \sum_\alpha \chi^{LF}_\alpha$ and the scalar susceptibilities of the plasma species $\alpha$, i.e. electrons and ions are defined, respectively, by equations (2.43) and (2.49). The nonlinear density perturbation $n^{LF}_{e,NL}$ is obtained by the beating of two HF fields, equation (2.46). The beating waves are limited to the three HF components defined above. One of the electric fields must correspond to the pump field since it has the largest amplitude. As a result, we obtain:

$$n^{LF}_{e,NL} = \frac{\omega^2_{pe}}{4\pi k_z m_e \mathrm{v}^4_e}\left[A_z E_{zo} E_{z1} + B_z E^*_{zo} E_{z2} + A_\perp (\boldsymbol{E}_{\perp 1} \times \boldsymbol{E}_{\perp o})_z + B_\perp (\boldsymbol{E}^*_{\perp o} \times \boldsymbol{E}_{\perp 2})_z\right]. \tag{3.8}$$

Here, we define:

$$A_z = \frac{F(u,u_o)}{k_{zo}} + \frac{F(u,u_1)}{k_{z1}}, B_z = \frac{F(u,u_o)}{-k_{zo}} + \frac{F(u,u_2)}{k_{z2}},$$
$$A_\perp = -i\frac{\mathrm{v}_{th,e}}{\Omega_e}\left[F_\perp(u,u_o) - F_\perp(u,u_1)\right]$$
$$B_\perp = -i\frac{\mathrm{v}_{th,e}}{\Omega_e}\left[F_\perp(u,u_2) - F_\perp(u,u_o)\right]$$
$$u = \frac{\omega}{k_z \mathrm{v}_e}, u_1 = \frac{\omega_1}{k_{z1}\mathrm{v}_e}, u_o = \frac{\omega_o}{k_{zo}\mathrm{v}_e}, u_2 = \frac{\omega_2}{k_{z2}\mathrm{v}_e}. \tag{3.9}$$

To compare this result with the expressions known in the literature, see e.g. equations (1) and (2) in [61] or equations (200) and (201) in [15]. We approximate the coefficients in equation (3.9), based on the ordering $|u| \ll |u_1|, |u_2|$. Using the identity $\omega_o k_z - \omega k_{zo} = \omega k_{z1} - \omega_1 k_z$ ,we obtain:

$$A_z \cong \frac{1}{\mathrm{v}_{th,e}}\left[\frac{k_z \mathrm{v}_{th,e}}{\omega_o k_z - \omega k_{zo}}\right]^2 \left[\omega_o S(u_o) + \omega_1 S(u_1) - \omega S(u)\right]. \tag{3.10}$$

Using the identity $\omega_o k_z - \omega k_{zo} = \omega_2 k_z - \omega k_{z2}$, we obtain:

$$B_z \cong \frac{1}{\mathrm{v}_{th,e}}\left[\frac{k_z \mathrm{v}_{th,e}}{\omega_o k_z - \omega k_{zo}}\right]^2 \left[-\omega_o S(u_o) + \omega_2 S(u_2) - \omega S(u)\right]. \tag{3.11}$$

Using the identity $\omega_o k_z - \omega k_{zo} = \omega k_{z1} - \omega_1 k_z$, we obtain:

$$A_\perp = -i\frac{\mathrm{v}_{th,e}}{\Omega_e}\frac{k_z}{\omega_o k_z - \omega k_{zo}}\left[\omega_o S(u_o) + \omega_1 S(u_1) - \omega S(u)\right]. \tag{3.12}$$

Using the identity $\omega_o k_z - \omega k_{zo} = \omega_2 k_z - \omega k_{z2}$, we obtain:

$$B_\perp = -i\frac{\mathrm{v}_{th,e}}{\Omega_e}\frac{k_z}{\omega_o k_z - \omega k_{zo}}\left[\omega_2 S(u_2) - \omega_o S(u_o) - \omega S(u)\right]. \tag{3.13}$$

In terms of the electric potential, the LF nonlinear density perturbation is given by,

$$n^{LF}_{e,NL} = \alpha_1 \phi_o \phi_1 + \alpha_2 \phi^*_o \phi_2, \tag{3.14}$$

where

$$\alpha_1 = -i\frac{n_{eo} e^2 k_{\perp 1} k_{\perp o} \sin\delta_1}{m^2_e \mathrm{v}^3_{th,e} |\Omega_e| (\omega k_{zo} - \omega_o k_z)}\left[\omega S(u) - \omega_1 S(u_1) - \omega_o S(u_o)\right] + \frac{n_{eo} e^2 k_{z1} k_{zo} k_z}{m^2_e \mathrm{v}^3_{th,e} (\omega k_{zo} - \omega_o k_z)^2}\left[\omega S(u) - \omega_1 S(u_1) - \omega_o S(u_o)\right]. \tag{3.15}$$

$\delta_1$ is the angle between $\boldsymbol{k}_{\perp 1}$ and $\boldsymbol{k}_{\perp o}$; more precisely $(\boldsymbol{k}_{\perp 1}\times\boldsymbol{k}_{\perp o})_z = \boldsymbol{k}_{\perp 1}\boldsymbol{k}_{\perp o}\sin\delta_1$.

$\alpha_2$ is obtained from $\alpha_1$ replacing $\omega_o, \boldsymbol{k}_o$ by $-\omega_o, -\boldsymbol{k}_o$ and the subscript 1 by 2, namely:

$$\alpha_2 = -i\frac{n_{eo}e^2 k_{\perp 2}k_{\perp o}\sin\delta_2}{m_e^2 v_{th,e}^3|\Omega_e|(\omega k_{zo}-\omega_o k_z)}\left[\omega S(u)-\omega_2 S(u_2)+\omega_o S(u_o)\right] - \frac{n_{eo}e^2 k_{z2}k_{zo}k_z}{m_e^2 v_{th,e}^3(\omega k_{zo}-\omega_o k_z)^2}\left[\omega S(u)-\omega_2 S(u_2)+\omega_o S(u_o)\right], \tag{3.16}$$

where the angle $\delta_2$ is defined by $(\boldsymbol{k}_{\perp 2}\times\boldsymbol{k}_{\perp o})_z = k_{\perp 2}k_{\perp o}\sin\delta_2$.

The LF nonlinear density perturbation given by equation (3.14) is thus identical to the expression given in [15] by equation (200), with the exception that here we have missed the polarization drift terms, which are usually considered negligible in the archived literature. Based on the kinetic equation and the perturbation theory and following the analysis performed in section 2, within the limit of uniform plasma, the following HF nonlinear equations for LH electrostatic sideband waves are derived:

$$\varepsilon_1\phi_1 = -\frac{4\pi e}{k_1^2}n_{e,NL,1}^{HF},\ \varepsilon_2\phi_2 = -\frac{4\pi e}{k_2^2}n_{e,NL,2}^{HF}. \tag{3.17}$$

Here, $\varepsilon_1 = \varepsilon^{HF}(\omega_1,\boldsymbol{k}_1)$ and $\varepsilon_2 = \varepsilon^{HF}(\omega_2,\boldsymbol{k}_2)$, where $\varepsilon^{HF}$ is the dielectric function in the HF range defined in section 2 in terms of the electron and ion susceptibilities. Nonlinear density perturbations $n_{e,NL,1}^{HF}$ and $n_{e,NL,2}^{HF}$ are obtained from the nonlinear charge density given by equation (2.79), dividing it by $-e$:

$$n_{e,NL,1}^{HF} = \alpha_3\phi_o^*\phi,\ n_{e,NL,2}^{HF} = \alpha_4\phi_o\phi.$$

Here,

$$\alpha_3 = \alpha_1\frac{\chi_e-\varepsilon}{\chi_e},\ \text{with}\ |\Omega_e|\to-|\Omega_e|\ \text{and}\ \alpha_4 = \alpha_2\frac{\chi_e-\varepsilon}{\chi_e},\ \text{with}\ |\Omega_e|\to-|\Omega_e|.$$

We thus obtain the following parametric dispersion equation for electrostatic LH waves:

$$f_p = -\varepsilon(\omega,\boldsymbol{k}) + \frac{\mu_1}{\varepsilon^{HF}(\omega_1,\boldsymbol{k}_1)} + \frac{\mu_2}{\varepsilon^{HF}(\omega_2,\boldsymbol{k}_2)} = 0, \tag{3.18}$$

where,

$$\mu_1 = \frac{4\pi e}{k_1^2}\frac{4\pi e}{k^2}\alpha_1\alpha_3|\phi_o|^2,\ \mu_2 = \frac{4\pi e}{k_2^2}\frac{4\pi e}{k^2}\alpha_2\alpha_4|\phi_o|^2. \tag{3.19}$$

This parametric dispersion equation differs from the parametric dispersion equation known in the archived literature [15, 60, 61] only due to the following approximations: (*i*) in the HF dielectric function we consider unmagnetized ions; (*ii*) in both the LF and HF range finite electron Larmor radius effects are neglected; (*iii*) the polarization drift term in the nonlinear interaction is neglected; (*iv*) the drift frequency in the LF linear susceptibility of both the electrons and ions is neglected. Numerical analysis of the solutions of the parametric dispersion equations indicates that, for typical RF and plasma parameters occurring in peripheral tokamak plasmas, all these approximations are well justified. Negligible differences occur between the solutions of the full parametric dispersion equation and the solutions of equation (3.11) concerning the growth rates of the instability and the frequency of the ISQM and ICQM. As an example, we show in figure 4, the growth rates and the frequency of ISQM versus the normalized wave number of these LF quasi-modes for the plasma parameters of table 6.

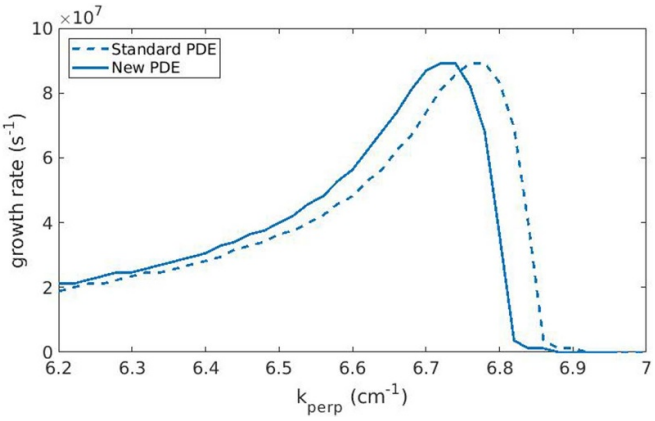


**Figure 4.** Comparison between the growth rates obtained solving the standard PDE (dashed line) and the PDE here derived (solid line) as a function of the perpendicular wavenumber of the LF ion-sound quasi-mode.

**Table 6.** RF and plasma parameters used to compare the solutions of the PDE. Pure deuterium plasma and 3.0 kW cm$^{-2}$ LH coupled power density have been considered.

| $f$ | $N_{\|o}, N_{yo}, N_z, N_y$ | $B_o$ | $n_e$ | $T_e = T_i$ |
|---|---|---|---|---|
| 8.0 GHz | 2,0, 8,0 | 4.52 T | 1.6 $10^{12}$ cm$^{-3}$ | 2.5 eV |

We consider a pump wave at the operating frequency $f_o = 8.0$ GHz, parallel refractive index $N_{\|o} = 2.0$, poloidal refractive index $N_{yo} = 0$ and 3.0 kW cm$^{-2}$coupled power density.

In the present study, we express the wave power in terms of kW m$^{-2}$ instead of the more habitually used kW m$^{-3}$. This is only due to the need to interface the ALGOR code with the RAYFP code, available in our Institute, implementing ray tracing coupled to a Fokker–Planck solver. It gives the LH power deposition and current drive, once the initial power density spectra versus the frequency, toroidal and poloidal wave numbers are provided. This code adopts as input the power density expressed in kW m$^{-2}$. The LF quasi-modes considered have zero poloidal wavenumber and normalized parallel wavenumber $N_{\|} = k_{\|}c/\omega_o$. The growth rate and the LF angular frequency, as calculated by numerical solutions of equation (3.18) are compared with those obtained with the standard PI modeling, neglecting the polarization drift but considering finite electron and ion Larmor radius effects in

both the LF and HF range. Since the poloidal numbers of the interacting waves are zero, the drift wave frequency is zero and only the parallel drive of PI occurs ($\delta_1 = \delta_2 = 0$). As shown in figure 4, only tiny differences can be detected between the solutions of the standard PDE and the solutions of equation (3.18), confirming that neglecting the finite Larmor radius effect of the electrons in both the LF and HF ranges and considering unmagnetized ions in the HF range is well justified.

Following [61], we now obtain approximate analytical solutions of the parametric dispersion equation for a collisional plasma within the limit of parallel dynamics of the electrons. The purpose of this calculation is to compare our results with the corresponding analytical solutions proposed in [66]. We assume that $|\varepsilon_2|$ is sufficiently large to neglect the LH upper (non-resonant) sideband. The LH lower sideband is assumed as a quasi-resonant mode, i.e. we assume $|\varepsilon_1| \ll 1$ and electrostatic, i.e. we assume $\left[N_{\|1}\right]^2 = k_{z1}^2 c^2/\omega_{1r}^2 \gg 1$ so that,

$$\varepsilon_1 \cong \frac{\partial \varepsilon_{1r}}{\partial \omega_{1r}} i\gamma + i\varepsilon_{1i} \cong \frac{\partial \varepsilon_{1r}}{\partial \omega_{1r}} i\left(\gamma + \gamma_{L1} + \gamma_{C1}\right), \tag{3.20}$$

where the subscripts $r$ and $i$ indicate, respectively, the real and imaginary part, $\gamma_{L1} > 0$ and $\gamma_{C1} > 0$ , which are, respectively, the LH sideband's Landau and collisional damping rates, which, for $\gamma_{L1}, \gamma_{C1} \ll |\omega_{1r}|$, can be approximated as,

$$\gamma_{L1} \cong \sqrt{\pi}\, \frac{\omega_{1r}^4}{|k_{z1}|^3 \mathrm{v}_e^3} e^{-\left(\frac{\omega_{1r}}{k_{z1}\mathrm{v}_e}\right)^2}, \quad \gamma_{C1} \cong \frac{\nu_e}{2}. \tag{3.21}$$

$\omega_{1r}^2 \cong \omega_{pe}^2 k_{z1}^2/k_1^2$ and $\gamma$ is the growth rate of the PI. We rewrite equation (3.18) neglecting the contribution of the upper sideband and assuming that $|\gamma_1 S(u_1)| \ll 1$.

We obtain the approximate parametric dispersion equation:

$$\varepsilon = \frac{\mu}{\varepsilon_1}, \tag{3.22}$$

with,

$$\mu = \left(\varepsilon - \chi_e\right) \frac{e^2 k_{zo}^2 \omega_{pe}^2}{2m_e^2 \mathrm{v}_e^4 k_z} |\phi_o|^2 \frac{k_{z1}^2}{k_1^2} \frac{A}{\left(\omega_1 + i\nu_e\right)^2}, \tag{3.23}$$

$$A \cong \frac{1}{\mathrm{v}_e} \left[\frac{k_z \mathrm{v}_e}{\omega_o k_z - \omega k_{zo}}\right]^2 \left[\omega_o S(u_o) + \omega_1 S(u_1) - \omega S(u)\right]. \tag{3.24}$$

Then, equations (3.20) and (3.21) give the growth rate:

$$\gamma = -\gamma_{L1} - \gamma_{C1} + \frac{1}{\partial \varepsilon_{1r}/\partial \omega_{1r}} Im\left(\frac{\mu}{\varepsilon}\right). \tag{3.25}$$

Concerning the low-frequency quasi-modes, we limit the analysis to ion-sound quasi-modes. For an order of magnitude estimate, we assume that the real angular frequency is given by the expression for magnetized ion-sound waves, namely $\omega_r = O(|k_z| c_s)$, where $c_s$ is the ion-sound velocity, given for single-ion species by $c_s = \sqrt{Z_i T_e/m_i}$. The dielectric function concerning the LF ion-sound quasi-mode can thus be simplified (for single-ion species with mass $m_i$ and charge number $Z_i$) as,

$$\varepsilon = 1 + \chi_e + \chi_i \cong 1 + \frac{\omega_{pi}^2 m_i}{k^2 Z_i T_e} - \frac{k_z^2}{k^2} \frac{\omega_{pi}^2}{\omega^2}. \tag{3.26}$$

Here, the asymptotic approximation has been adopted for the ions and the ion collisional frequency has been neglected since it is assumed to be much lower than the ion-sound frequency and the growth rate. We note that the asymptotic approximation for plasma ions is justified for growth rates sufficiently larger than the ion-sound angular frequency. A small argument approximation has been used concerning the plasma dispersion function for the electrons, consistently with the relevant model constraint, and we approximate $1 + i\gamma_e S(u) \cong 1 - \gamma_e \sqrt{\pi} \cong 1$. The real part of the dielectric function concerning the LH lower sideband wave is obtained utilizing both the electrostatic and the asymptotic approximation and neglecting the collisional frequency compared to the LH frequency:

$$\varepsilon_{1r} \cong 1 - \frac{k_{z1}^2}{k_1^2} \frac{\omega_{pe}^2}{\omega_{1r}^2}. \tag{3.27}$$

Therefore,

$$\partial \varepsilon_{1r}/\partial \omega_{1r} \cong 2/\omega_{1r} \cong -2/\omega_o. \tag{3.28}$$

Concerning the coefficient $A$, we can use, for the plasma dispersion function, the adiabatic approximation for the high-frequency terms and the power series for the LF terms and neglect the collisional frequency compared to the high frequency, thus obtaining,

$$A \cong -\frac{k_z \mathrm{v}_e^2}{\omega_o^2}. \tag{3.29}$$

Inserting in equation (3.25) the value of $\partial \varepsilon_{1r}/\partial \omega_{1r}$ as approximated by equation (3.28), the value of $\varepsilon$ as approximated by equation (3.26) and the value of $\mu$ as given in equation (3.23) with $\varepsilon$ and $\chi_e$ as in equation (3.26), $A$ as in equation (3.29) and approximating $\left(\omega_1 + i\nu_e\right)^2 \cong \omega_{1r}^2 \cong k_{z1}^2 \omega_{pe}^2/k_1^2$, we finally obtain the following equation for the growth rate $\gamma$, where $\omega_r$ is the real angular frequency of the ion-sound quasi-modes:

$$\left(\gamma + \gamma_{L1} + \gamma_{C1}\right)\left(\gamma^4 + 4\gamma^2 \omega_r^2\right) = \gamma \omega_r^3 \frac{e^2 |E_{zo}|^2}{4 m_e T_e \omega_o}. \tag{3.30}$$

To derive the above equation, we use the ordering $k^2 \lambda_{De}^2 \ll 1$. For single-ion species of mass $m_i$ and charge number $Z_i$ we thus obtain:

$$Im\left(\frac{\chi_e}{\varepsilon}\right) = Im\left(1 + k^2 \lambda_{De}^2 - \frac{k_z^2 c_s^2}{\omega^2}\right)^{-1} \cong Im\left(1 - \frac{k_z^2 c_s^2}{\left(\omega_r + i\gamma\right)^2}\right)^{-1} \cong -\frac{2y}{y^4 + 4y^2}, \tag{3.31}$$

where $y=\gamma/\omega_r$ so that $y^2 \gg 1-k_z^2c_s^2/\omega_r^2$.

Neglecting the Landau damping rate $\gamma_{L1}$ and the collisional frequency, we obtain the equation:

$$\gamma^4+4\gamma^2\omega_r^2=\omega_r^3\frac{e^2|E_{zo}|^2}{4m_eT_e\omega_o}. \tag{3.32}$$

The collisionless growth rate is thus:

$$\gamma=\omega_r\sqrt{\left(4+\frac{e^2|E_{zo}|^2}{4m_eT_e\omega_o\omega_r}\right)^{1/2}-2}\,. \tag{3.33}$$

This growth rate coincides with the growth rate calculated in [61] for PIs in collisionless plasma involving ISQM within the limit of dominant parallel interaction and for $\omega_o^2 \ll \omega_{pe}^2 \ll \Omega_e^2$. In collisional plasma and in the presence of Landau damping of the lower LH sideband, the growth rate can be expressed as $\gamma=\omega_r x$, where $x>0$ is the positive solution of the fourth degree equation obtained by equation (3.30):

$$x^4+px^3+4x^2+4px-q=0. \tag{3.34}$$

Here, we see that the normalized growth rates $x=\gamma/\omega_r$ are functions of only two parameters, namely:

$$p=\frac{\gamma_{L1}+\gamma_{C1}}{\omega_r}, q=\frac{e^2|E_{zo}|^2}{4m_eT_e\omega_o\omega_r}=\eta^2\frac{\omega_o}{\omega_r}. \tag{3.35}$$

The parameter $p$ is proportional to the rates of two dissipative phenomena, namely the Landau damping of the LH (lower) sideband and the collisional processes. This has a stabilizing effect on PI. The parameter $q$, namely the squared amplitude of the parallel component of the pump electric field in units $E_u=\left[4m_eT_e\omega_o\omega_r e^{-2}\right]^{1/2}$, acts as a PI drive. The parameter $q$ is proportional to the average power density $P_o$ of the LH pump wave (see appendix C). Neglecting electron Landau damping and thermal effects, as is reasonable in the SOL plasma for LH pump waves, we can evaluate the ratio $|E_{zo}|^2/\omega_o$ in terms of $P_o$ by means of equation (C40) of appendix C. The refractive index component $N_x$ has to be negative for LH pump power propagation towards the plasma core. To optimize the LH injected power penetration, the LH antenna spectrum is usually characterized by a negligible poloidal refractive index, so that $N_x \cong -N_\perp < 0$. The perpendicular refractive index can be calculated within the cold plasma theory. We approximate the Stix parameter $S=1-\sum_\alpha \omega_{p\alpha}^2/\left(\omega_o^2-\Omega_\alpha^2\right)\cong 1$ and assume that $|D|=\left|\sum_\alpha \omega_{p\alpha}^2\Omega_\alpha/\left[\omega_o\left(\omega_o^2-\Omega_\alpha^2\right)\right]\right| \ll 1$. The same result can be obtained for wave equation (2.87). To this end, we consider only the linear term and use the asymptotic approximation for the plasma dispersion function in $\beta_L$, the quasi-homogeneous plasma approximation, i.e. $\mathrm{d}^2E_{zo}/\mathrm{d}x^2 \cong -N_x^2\omega_o^2E_{zo}/c^2$ and neglect the poloidal refractive index, thus obtaining $N_x \cong -\left[\left(\omega_{pe}^2-\omega_o^2\right)\left(N_{zo}^2-1\right)\right]^{1/2}/\omega_o$.

As a result,

$$\frac{|E_{zo}|^2}{\omega_o}\cong\langle P_o\rangle\frac{8\pi}{c}\sqrt{\frac{N_{zo}^2-1}{\omega_{pe}^2-\omega_o^2}}, \tag{3.36}$$

so that the instability parameter is:

$$q=\frac{2\pi e^2}{m_ecT_e\omega_r}\langle P_o\rangle\sqrt{\frac{N_{zo}^2-1}{\omega_{pe}^2-\omega_o^2}}. \tag{3.37}$$

Efficient LH power coupling typically requires $\omega_{pe}^2 \cong (2-3)\,\omega_o^2$ in the plasma region near the antenna mouth, though passive active multijunction (PAM) launchers [83] allows relatively low (∼5%) reflection coefficients even near the LH cutoff [84]. In the peripheral plasma region, the largest PI growth rates are expected. Assuming $\omega_{pe}^2 \cong 2\omega_o^2$, the PI driving term $q$ is proportional to $f_o^{-1}T_e^{-3/2}$. This suggests operating at high frequency and high electron temperature to minimize the PI growth rate.

These were indeed the key conditions to reduce PI and achieve LH interaction in the plasma core at reactor relevant central density in the FTU tokamak [11]. Concerning the solutions of equation (3.34), we observe that the analytical roots of the polynomials of the fourth order were obtained during the 16th century by Lodovico Ferrari, collaborator of Girolamo Cardano, who published the solutions in the 1545 book *Artis magnae sive de regulis algebraicis liber unus* [85]. Efficient methods to compute the roots of quartic equations with real coefficients as equation (3.34) are described in [86]. Due to the Descartes rule, equation (3.34) has at most a single positive root. The polynomial $P(x)$ at the l.h.s. of equation (3.25) is such that $P(0)=-q$ and $P\left(\sqrt[4]{q}\right)>0$, so the positive root does exist in the interval $\left]0,\sqrt[4]{q}\right[$. The analytical formula for such a root is,

$$x=-\frac{p}{4}-\frac{1}{2}\sqrt{T_1+S_1}+\frac{1}{2}\sqrt{2\,T_1-S_1+\frac{(16p+p^3)}{4\sqrt{T_1+S_1}}}. \tag{3.38}$$

Here, we define the following parameters:

$$\begin{aligned}
P_1&=-4\left(16-12p^2-12q\right)^3\\
&\quad+\left(128+288p^2+288q-27p^2q\right)^2\\
Q&=128+288p^2+288q-27p^2q+\sqrt{P_1}\\
R&=4-3p^2-3q\\
S_1&=4\sqrt[3]{2}\,R/3\,\sqrt[3]{Q}+\sqrt[3]{Q}/3\sqrt[3]{2}\\
T_1&=-8/3+p^2/4.
\end{aligned}$$

Standard numerical routines can be used to calculate the roots of a polynomial (like *roots* of MATLAB). Then, one can pick up the positive root. This procedure might be even faster and more accurate than the numerical routines implementing the analytical formula (3.38) and has been used here to calculate the growth rates in figure 5. It is important to note that the growth rates calculated from equation (3.34) correct those obtained from equation (26) of [66]. Here, the collisional PDE is derived considering LF nonlinear density perturbations calculated not self-consistently with the LF electric field equation, therefore missing the important contribution of the plasma ion species. Figure 5 shows a plot of the PI

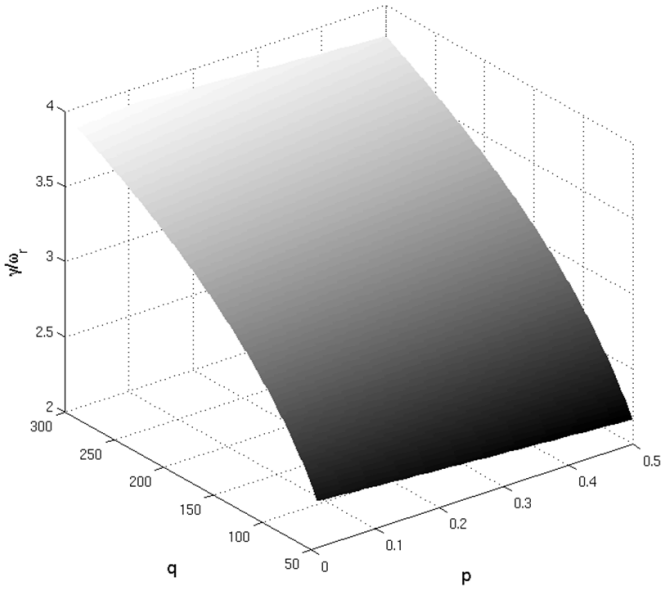


**Figure 5.** Growth rate, normalized to the angular frequency of the ion-sound quasi-modes, is plotted versus the dissipation parameter $p$ and the instability drive parameter $q$.

growth rates normalized to the ion-sound angular frequency as a function of the two parameters $p$ and $q$, for a reasonable range of these parameters. As a result, the PI growth rates are typically of the order of a few times $\omega_r$. To give an idea of the values of $p$ and $q$ expected in LHCD scenarios, we consider first the LHCD experiment planned in ITER [87], operating at 5.0 GHz LH wave frequency and with ∼12 eV electron temperature envisaged in the SOL before the region of steep gradients near the separatrix. Assuming $k_z = 6\ \mathrm{cm}^{-1}$, so that $\omega_r \cong 1.4\ 10^7\ \mathrm{rad\,s}^{-1}$ for deuterium plasma, the above electric field reference unit has a value of $E_u \cong 0.41\ \mathrm{stV\,cm}^{-1}$. We predict a value of $|E_{zo}| \cong 6.7\ \mathrm{stV\,cm}^{-1}$ in front of the LH launcher in ITER, with a power density injection of $3.3\ \mathrm{kW\,cm}^{-2}$, peak value of the parallel refractive index $N_{\|o} = 1.9$ and operating at about twice the cutoff density, namely at $n_e \cong 0.62\ 10^{12}\ \mathrm{cm}^{-3}$. The value of the parameter $q$ is thus about 280, corresponding to $\eta \cong 0.35$. The electron-ion collisional frequency is [88],

$$\nu_e = \frac{4\sqrt{2\pi}\,\Lambda e^4}{3 m_e^{1/2} T_e^{3/2}} \sum_i Z_i^2 n_i, \tag{3.39}$$

where the physical quantities are in cgs units, the sum is over all the ion species with charge number $Z_i$ and density $n_i$ and $\Lambda$ is a Coulomb logarithm relevant for electron-ion collisions. For single-ion species, the latter can be evaluated as [89],

$$\Lambda = 31.3 - \ln\left(n_e^{\frac{1}{2}} T_e^{-1}\right). \tag{3.40}$$

Here, the electron density is expressed in $\mathrm{cm}^{-3}$ and $T_e$ in eV. For pure deuterium plasma, considering the above ITER parameters we thus obtain $\nu_e \cong 0.9\ 10^6\ \mathrm{s}^{-1}$.

However, due to the presence of impurities in the density and temperature regime envisaged, an effective charge $Z_{\mathrm{eff}} = 3$ can be expected near the LH launcher. An estimate of the collision frequency might thus be $\nu_e \cong 2.5\ 10^6\ \mathrm{s}^{-1}$. Hence, the parameter $p$ (neglecting $\gamma_{L1}$) might be about 0.1. Typical RF and plasma parameters of the LHCD experiment in the FTU tokamak [90, 91] are the operating frequency of 8.0 GHz, a peak value of the parallel refractive index $N_{\|o} = 1.8$, power density 3.0 kW $\mathrm{cm}^{-2}$ coupled to the plasma at about twice the cutoff density, namely at $n_e \cong 1.6\ 10^{12}\ \mathrm{cm}^{-3}$ where the electron temperature is expected to be of the order of 5 eV. Assuming $k_z = 15\ \mathrm{cm}^{-1}$, so that $\omega_r \cong 1.8\ 10^7\ \mathrm{rad\,s}^{-1}$ for deuterium plasma, the above electric field unit has the value in front of the launcher of $E_u \cong 0.34\ \mathrm{stV\,cm}^{-1}$. In front of the LH launcher in FTU we obtain $|E_{zo}| \cong 6.1\ \mathrm{stV\,cm}^{-1}$. Therefore, the value of the parameter $q$ is about 260, corresponding to $\eta \cong 0.30$. The collision frequency is $\nu_e \cong 7.8\ 10^6\ \mathrm{s}^{-1}$, assuming pure deuterium plasma, so that the parameter $p$ (neglecting $\gamma_{L1}$) is about 0.2.

As shown in figure 5, the effect of the collisions on the growth rates seems marginal, reducing the growth by a few percent. However, the LH sideband power amplification is an exponential function of twice the growth rates, so the overall effect might not be negligible. In addition, other approximations are made that can affect the growth rates with an even larger amount w.r.t. the collisions. We note that a possible reason for the very different dependence of the growth rate on the dissipation w.r.t. the instability parameter is that $p \ll q$. Taking into account this ordering, an approximate solution of equation (3.34) for $p = 0$ and $q^{1/4} \gg 1$ is $x_o \cong q^{1/4} \gg 1$, and an approximate solution for $p \ll 1$ is $x \cong (1 - p/4)\, q^{1/4}$. The analytical approximation of the growth rates given in [66] by equation (26) overestimates the effects of the collisions in reducing the PI growth rates. To illustrate this point, let us assume $\omega_{pe}^2 \gg \omega_o^2$, deuterium plasma at density $n\ \left(\mathrm{cm}^{-3}\right)$, and temperatures (eV) $T_e = T_i = T$ sufficiently low that the electron Landau damping rate of the lower sideband is negligible compared to the collisional damping rate. Simple expressions for the electron and ion collisional frequencies are, respectively, $\nu_e = 2.9\ 10^{-6}\ n\lambda T^{-3/2}$ and $\nu_i = 4.8\ 10^{-8}\ n\lambda T^{-3/2}\ \mu^{-1/2}$ where $\lambda$ is the Coulomb logarithm and $\mu$ is the deuteron mass in units of the proton mass [92]. Equation (26) of [56] can thus be written as $\gamma/\omega_r = (1 - ap)\left[(4+q)^{1/2} - 2\right]^{1/2}$, where $a \cong 86$.

The PI growth rates are reduced by the collisional effects much more than predicted by the solutions of equation (3.34) and no PIs are expected for almost all the values of $p$ in figure 1, i.e. for $p > 0.0117$. We show further numerical solutions of the PDE given by equation (3.18) obtained within the limit of dominant parallel dynamics of the electrons. The solutions are calculated as the poles of $|f_P|^{-1}$ where the function $f_P$ is defined by equation (3.18). We consider a typical FTU scenario with 5.0 T static magnetic field, considering an injected LH power density of 3.0 kW $\mathrm{cm}^{-2}$ operating at 8.0 GHz frequency with a peak parallel refractive index of $N_{zo} = k_{zo}c/\omega_o = 1.8$ and assuming a normalized parallel wavenumber of the LF quasi-modes as given by $k_z c/\omega_o = 10$. The poloidal wavenumbers of the interacting waves are set to zero. The perpendicular wavenumber of the lower LH

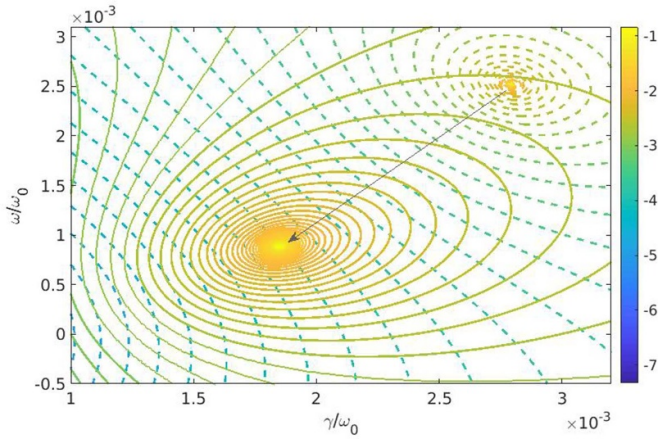


**Figure 6.** Contour plots of the function $\mathrm{Log}_{10}\left|f_P^{-1}\right|$, where $f_P$ is defined in equation (3.18), as calculated in the plane of real (ordinates) and imaginary (abscissae) parts of the LF quasi-mode angular frequency in units of the angular frequency $\omega_o$ of the LH pump wave in FTU with $B_o = 5.0$ T. We assume that $n_e = 2.0\ 10^{12}$ cm$^{-3}$, $T_e = T_i = 2.5$ eV (dashed lines) and $n_e = 5.0\ 10^{12}$ cm$^{-3}$, $T_e = T_i = 15$ eV (continuous lines). Respective solutions of the electrostatic PDE, which are given by the poles of $\left|f_P^{-1}\right|$ (connected by an arrow in the figure), are $\omega = 1.27\ 10^8$ rad s$^{-1}$, $\gamma = 1.4\ 10^8$ s$^{-1}$ and $\omega = 4.45\ 10^7$ rad s$^{-1}$, $\gamma = 9.25\ 10^7$ s$^{-1}$. Analytical growth rates, given by equation (3.37, are, respectively, $\gamma = 3.15\ 10^8$ s$^{-1}$ and $\gamma = 7.0\ 10^7$ s$^{-1}$ if the collisions are neglected and $\gamma = 3.09\ 10^8$ s$^{-1}$ and $\gamma = 6.85\ 10^7$ s$^{-1}$ if the collisions are taken into account. Properties of the LH pump and sideband waves used in the calculations are described in the te

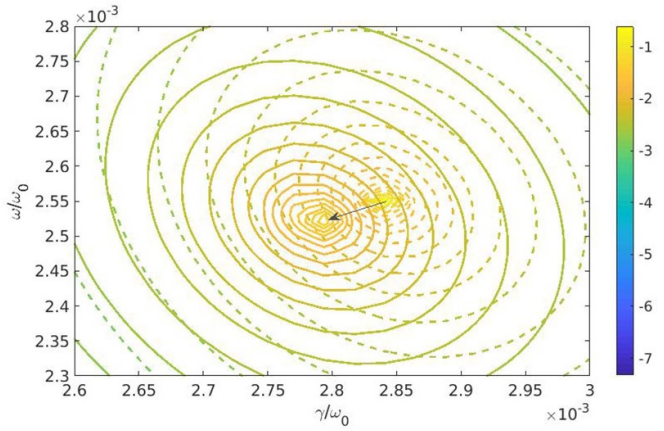


**Figure 7.** Contour plots of the function $\mathrm{Log}_{10}\left|f_P^{-1}\right|$, where $f_P$ is defined in equation (3.44), as calculated in the plane of real (ordinates) and imaginary (abscissae) parts of the angular frequency of the quasi-modes in units of the angular frequency $\omega_o$ of the LH pump wave in FTU, with $B_o = 5.0$ T, for $n_e = 2.0\ 10^{12}$ cm$^{-3}$ and $T_e = T_i = 2.5$ eV in collisionless (dashed lines) and collisional (continuous lines) plasma. The respective solutions of the electrostatic PDE, which are given by the poles of $\left|f_P^{-1}\right|$ (connected by an arrow in the figure), are $\omega = 1.28\ 10^8$ rad s$^{-1}$, $\gamma = 1.43\ 10^8$ s$^{-1}$ and $\omega = 1.27\ 10^8$ rad s$^{-1}$, $\gamma = 1.40\ 10^8$ s$^{-1}$. The analytical growth rates, given by equation (3.383.37), are found, respectively, $\gamma = 3.18\ 10^8$ s$^{-1}$ and $\gamma = 3.09\ 10^8$ s$^{-1}$. Injected LH power and the frequency and wavenumbers of the interacting waves are the same as in figure 6.

sideband is chosen as being equal to the solution of the real part of the linear LH electrostatic dispersion equation, for angular frequency and parallel wavenumber given by the matching conditions. In figure 6, we show that at higher temperatures one obtains a reduction in the growth rate of the instability. In figure 7, we compare the solutions of the PDE with and without collisions. As a result, the stabilizing effect of the collision is marginal, of the order of 2% of the growth rate. The numerical results also suggest that the growth rates evaluated by analytical formulas might be overestimated by a factor ∼2.

For RF and plasma parameters of figure 1(a) of [66] we obtain from the solution of equation (3.34) the growth rate $\gamma/\omega_o = 2.76\ 10^{-3}$, i.e. a factor ∼30 larger than the peak value of $\gamma/\omega_o$ shown in figure 1(a) of [66]. The numerical solution of the PDE (3.18) within the limit of dominant parallel dynamics of the electrons gives $\gamma/\omega_o = 3.70\ 10^{-3}$. This suggests that larger mistakes affected the analytical formula in [66]. The role of the collisions becomes essential in determining the power density threshold for the onset of the PI instability. We now derive a general analytical expression for this threshold, assuming that the electrostatic approximation is justified for the lower LH sideband and that the parallel dynamics of the electrons is dominant. The latter condition is well justified in the extreme peripheral plasma region near the LH antenna mouth. We thus assume that $\left[N_{\|1}\right]^2 = k_{z1}^2 c^2/\omega_{1r}^2 \gg 1$. We start from the growth rate expression (3.25), at the instability threshold $\gamma = 0$.

Based on equation (3.28) and considering again $(\omega_1 + i\nu_e)^2 \cong \omega_{1r}^2 \cong k_{z1}^2\omega_{pe}^2/k_1^2$ we obtain:

$$0 = -\gamma_{L1} - \gamma_{C1} - \frac{\omega_o}{2} Im\left[\left(1 - \frac{\chi_e}{\varepsilon}\right)\frac{e^2 A}{2m_e^2 v_e^4 k_z}|E_{zo}|^2\right]. \tag{3.41}$$

We improve the approximations used above to calculate the growth rate of PI, namely we consider the following approximations:

$$[1 + uS(u)] \cong 1 + i\sqrt{\pi}\,\frac{\tilde{\omega}}{|k_z|\,v_e}, \tag{3.42}$$

$$A \cong -\frac{k_z v_e^2}{\omega_o^2}\left(1 + i\sqrt{\pi}\,\frac{\tilde{\omega}}{|k_z|\,v_e}\right), \tag{3.43}$$

$$\chi_e \cong \left[1/k^2\lambda_{De}^2\right]\left(1 + i\sqrt{\pi}\,\frac{\tilde{\omega}}{|k_z|\,v_e}\right), \tag{3.44}$$

$$\varepsilon = 1 + \chi_e + \chi_i \cong 1 + \frac{\left(1 + i\sqrt{\pi}\,\frac{\tilde{\omega}}{|k_z|v_{th,e}}\right)}{k^2\lambda_{De}^2} + \frac{1}{k^2\lambda_{D,i}^2}\left[1 + \frac{\omega}{|k_z|\,v_{th,i}}\sum_{n=-\infty}^{+\infty} Z\left(\frac{\omega - n\Omega_i}{|k_z|\,v_{th,i}}\right) I_n(\lambda_i)\, e^{-\lambda_i}\right]. \tag{3.45}$$

Here, $\tilde{\omega} = \omega_r + i\,\nu_e$ and $\omega = \omega_r$ since the collision rate for the ions can be neglected. We consider single-ion species with

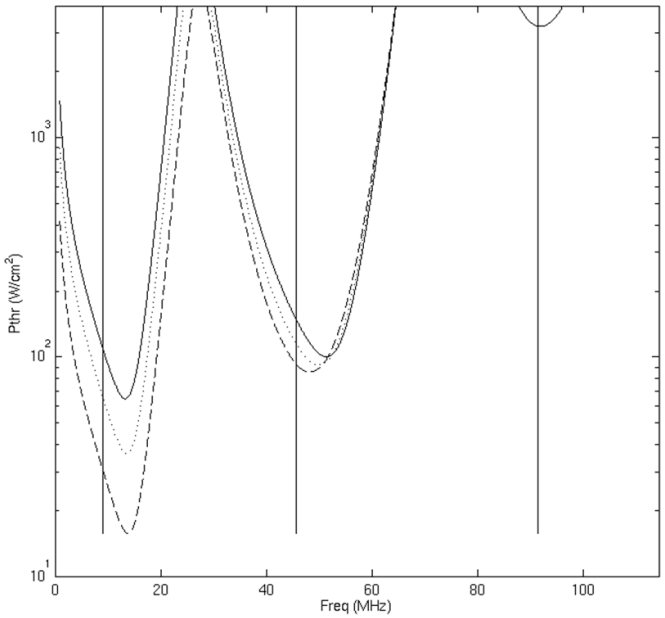


**Figure 8.** Power density at the threshold for PI, as given by equation (3.48), is plotted versus the frequency of the quasi-modes that can be excited by the LHCD power injection in FTU. Relevant plasma and RF data are reported in table 3. We consider here the parallel wavenumber $k_z = 30\ \mathrm{cm}^{-1}$ of the LF modes. Three plasma densities are considered, namely $n_e = 2\ n_{co}$ (dashed line), $n_e = 3\ n_{co}$ (dotted line) and $n_e = 4\ n_{co}$ (continuous line). Vertical lines indicate the frequency $k_z \mathrm{v}_{th,i}/(2\pi)$ (line on the left), the ion cyclotron frequency $\Omega_i/(2\pi)$ (central line) and its first harmonics (line on the right). Available LHCD power density in FTU is much larger than the threshold to drive ISQM and ICQM near the fundamental ion cyclotron frequency. However, ICQM with frequency near the first ion cyclotron harmonics frequency requires a power density $\sim 3\ \mathrm{kW\ cm}^{-2}$, near the maximum available, operating at the larger density $4\ n_{co}$.

mass $m_i$ and charge number $Z_i$. Assuming $k^2\lambda_{De}^2 \ll 1$ and $|\tilde{\omega}| \ll |k_z|\,\mathrm{v}_{th,e}$, we obtain the following expression for the PI threshold value of the squared electric field toroidal component in collisional plasma:

$$|E_{zo,thrc}|^2 = \frac{4m_e^2 \mathrm{v}_{th,e}^2 \omega_o}{e^2} \frac{(\gamma_{L1} + \gamma_{C1})}{Im\left(\frac{Z_i\Gamma}{\tau + Z_i\Gamma}\right)}\,. \tag{3.46}$$

Here, we define $\tau = T_i/T_e$ and

$$\Gamma = 1 + \frac{\omega}{|k_z|\,\mathrm{v}_{th,i}} \sum_{n=-\infty}^{+\infty} Z\left(\frac{\omega - n\Omega_i}{|k_z|\,\mathrm{v}_{th,i}}\right) I_n(\lambda_i)\, e^{-\lambda_i}. \tag{3.47}$$

The threshold for PI of the average power density in collisional plasma is thus obtained by equations (3.36) and (3.45):

$$P_{thrc} = \frac{m_e c}{\pi e^2} T_e \frac{(\gamma_{L1} + \gamma_{C1})}{Im\left(\frac{Z_i\Gamma}{\tau + Z_i\Gamma}\right)} \sqrt{\frac{\omega_{pe}^2 - \omega_o^2}{N_{zo}^2 - 1}}. \tag{3.48}$$

In figure 8, we show the above power threshold as a function of the frequency of the quasi-modes with parallel wavenumber $k_z = 30\ \mathrm{cm}^{-1}$ for plasma and RF data of near the LHCD antenna in FTU, which are reported in table 7. We have verified that the model constraints summarized in table 1, with the additional constraints for the dominant parallel dynamics of the electrons, are fulfilled. Minima of $P_{\mathrm{thrc}}$ are found near the characteristic frequency of ISQM, namely $k_z \mathrm{v}_{th,i}/(2\pi)$ and near the characteristic frequency of the ICQM, i.e. near the ion cyclotron frequency and its first harmonics. In this case, the electron Landau damping rate $\gamma_{L1}$ of the lower sideband is negligible and the threshold power is only determined by the collisional damping $\gamma_{C1} \cong \nu_e/2$.

**Table 7.** Plasma and RF data of the LHCD experiment in FTU. The plasma parameters correspond to the plasma near the LHCD antenna. Deuterons are the main ion species. $n_{co} = 7.9\ 10^{11}\ \mathrm{cm}^{-3}$ is the cutoff density.

| $B_o$ (T) | $T_e$ (eV) | $\tau$ | $n_e$ | $Z_{eff}$ | $f_o$ (GHz) | $N_{zo}$ |
|---|---|---|---|---|---|---|
| 6.0 | 2.5 | 1.5 | $(2 \div 4)\ n_{co}$ | 3.0 | 8.0 | 1.8 |

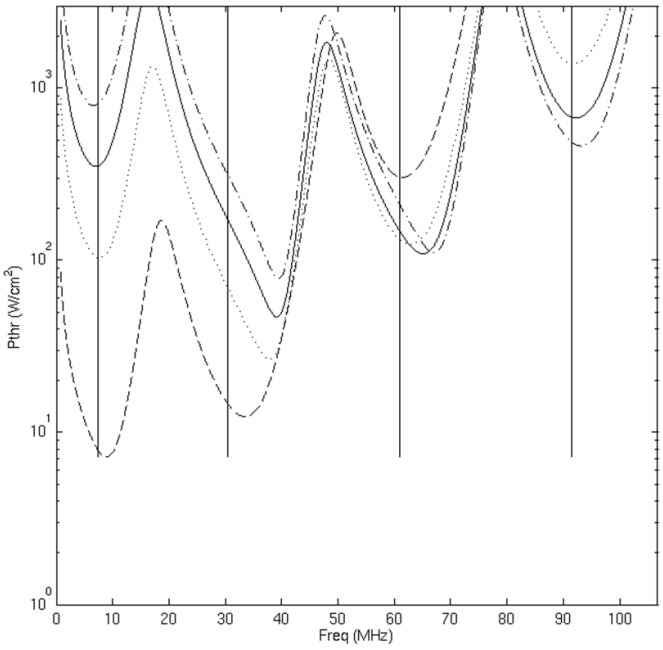


**Figure 9.** Power density at the threshold for PI, as given by equation (3.48), is plotted versus the frequency of the quasi-modes that can be excited by the LHCD power injection in ITER. Relevant plasma and RF data are reported in table 4. We consider here the parallel wavenumber $k_z = 10\ \mathrm{cm}^{-1}$ of the LF modes. Four plasma densities are considered, namely, in units of $10^{12}\ \mathrm{cm}^{-3}$, $n_e = 1.1$ (dashed line), $n_e = 4.1$ (dotted line) and $n_e = 7.1$ (continuous line) and $n_e = 10.1$ (dash-dotted line). Vertical lines indicate, from the left to the right, the frequency $k_z \mathrm{v}_{th,i}/(2\pi)$, the ion cyclotron frequency $\Omega_i/(2\pi)$ (second line from the left) its first harmonics (third line from the left) and its second harmonics (fourth line from the left).

In figure 9, we show the power threshold as a function of the frequency of the quasi-modes with parallel wavenumber $k_z = 10\ \mathrm{cm}^{-1}$ for typical plasma and RF data of the LHCD experiment planned for ITER, which are reported in table 8. We have verified that the model constraints summarized in table 1 are fulfilled. The power density threshold is much lower than the power density planned for LHCD in ITER and can

**Table 8.** Plasma and RF data of the LHCD experiment planned in ITER. The plasma parameters are those expected in the overall SOL region up to the steep increase of the density and temperature near the separatrix. Deuterons are the main ion species. The LH cutoff density for ITER is $n_{co} = 3.1\ 10^{11}\ \mathrm{cm}^{-3}$.

| $B_o$ (T) | $T_e$ (eV) | $T_i$ (eV) | $n_e$ $\left(10^{12}\mathrm{cm}^{-3}\right)$ | $Z_{\mathrm{eff}}$ | $f_o$ (GHz) | $N_{zo}$ |
|---|---|---|---|---|---|---|
| 6.0 | 11.7 | 21.6 | $1.1-10.1$ | 2.0 | 5.0 | 1.9 |

be excited by both ISQM and ICQM, near the fundamental, first harmonics and second harmonics of the ion cyclotron frequency. The planned power density is up to 3.3 kW $\mathrm{cm}^{-2}$, so it is possible that the ICQM near the third harmonics of the ion cyclotron frequency can also be excited. However, we have not extended the analysis up to the relevant frequency of about 120 MHz since the condition $|\omega/(k_z \mathrm{v}_{th,e})|_{LF} \ll 1$ is marginally fulfilled for such a relatively large value.

## 4. Numerical solutions of the nonlinear wave equation

We propose here the numerical solutions of the nonlinear coupled wave equations (2.53) and (2.85) as calculated by the updated version (currently version 7.2) of the numerical code ALGOR [93], written in MATLAB. We evaluate the spectral broadening in the frequency and in the parallel refractive index due to the nonlinear amplification of the noise produced by the RF power source, limiting the simulation to those frequencies where PIs are driven by the ISQM channel, as in [73]. We consider an experimental scenario typical for LH power injection in the FTU tokamak [90]. The profiles for the electron density and temperature are shown in figure 10, assuming the last closed magnetic surface (LCMS) at 2.5 cm from the LH antenna mouth. We consider an electron density at the LH grill of $1.6 \times 10^{12}\ \mathrm{cm}^{-3}$ (we assume about twice the cutoff density) and an electron density of $9.83 \times 10^{12}\mathrm{cm}^{-3}$ at the LCMS, an electron temperature at the LH grill of 2.5 eV and an LCMS electron temperature of 20 eV. Deuterium plasma is considered and thermal equilibrium between ions and electrons is assumed, i.e. $\tau = 1$. The line frequency of the RF source is $f_0 = 8.0$ GHz, the LH coupled power is 300 kW and the antenna radiating surface is 98.0 $\mathrm{cm}^2$, i.e. we simulate a single module of the FTU LH grill [91]. We compute the coupled power spectrum at the antenna mouth as the solution of the antenna power coupling problem [22] with an antenna facing a linear plasma density profile, which approximates the density profile in the first centimeter of the SOL. We consider a phase shift of 90 degrees between adjacent rectangular waveguides belonging to the same row of the LH grill. The parallel and poloidal refractive indexes corresponding to the peak values of the coupled power spectrum are $n_{zo} = 2$ and $n_{yo} = 0$, respectively.

We consider noise from an RF power source with a spectral energy density proportional to the reciprocal of the square of the frequency (red noise) and a power level of $-30$ dB (relative

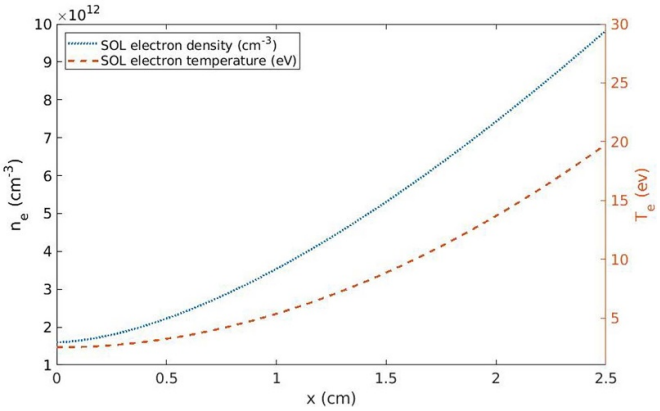


**Figure 10.** Density profile (dotted line) in $\mathrm{cm}^{-3}$ and the temperature profile (dashed line) in eV considered in the simulations for the SOL of FTU.

to the pump power) at a frequency shift of about 500 kHz from the pump line frequency $f_0$. A constant magnetic field $\boldsymbol{B}_0 = 4.52\,\hat{\boldsymbol{z}}$ in the SOL is assumed.

We consider the slab geometry described in section 2. To simplify the spectral representation of the pump wave, we represent here the pump as a delta function in frequency (centered at $f_0$) and in poloidal refractive index (centered at $n_{yo} = 0$), while we retain its full spectrum in the parallel refractive index. We perform a spectral discretization of the problem on a meshgrid with 2583 spectral components. We consider 21 points in frequency around the pump line frequency $f_0$ with a uniform step size $\Delta f = 526$ kHz, 41 points in the parallel refractive index with a uniform step size $\Delta n_z = 0.5$, 3 points in the poloidal refractive index with a uniform step size $\Delta n_y = 0.5$ and a spatial discretization with 251 points in the radial direction with a uniform step size of 0.01 cm. The complex amplitude of the parallel component of the high-frequency electric field $E_z^{HF}(x, \omega,\ k_y, k_z)$ has the following discrete representation:

$$E_z^{HF}(x, k_y, k_z, \omega) = \sum\nolimits_{l,m,n} \left[\tilde{\psi}_{l,m,n}(x)\,\delta(\omega-\omega_l)\,\delta(k_y-k_m)\,\delta(k_z-k_n) + c.c.\right], \tag{4.1}$$

where $\omega_l = \omega_0 + l * \Delta\omega$ with $\omega_0 = 2\pi f_0$, $\Delta\omega = 2\pi\ \Delta f$, $l \in \mathbb{Z}$ and $-10 \leqslant l \leqslant 10$; $k_m = m * \Delta k_y$ with $\Delta k_y = (\omega_0/c) * \Delta n_y$, $m \in \mathbb{Z}$ and $-1 \leqslant m \leqslant 1$; $k_n = n * \Delta k_z$ with $\Delta k_z = (\omega_0/c) * \Delta n_z$, $n \in \mathbb{Z}$ and $-20 \leqslant n \leqslant 20$. Writing the nonlinear wave equation for each discrete spectral component, we obtain a homogeneous system of nonlinearly coupled wave equations. Each equation is a homogeneous ordinary differential equation given by:

$$\partial_x^2 \tilde{\psi}_{l,m,n}(x) = \left(\beta^L(x, \omega_l, k_m, k_n) + \tilde{\beta}^{NL}(x, \omega_l, k_m, k_n)\right)\tilde{\psi}_{l,m,n}(x). \tag{4.2}$$

Here,

$$\beta^{L}(x,\omega_l,k_m,k_n)=\left(k_m^2+k_n^2-\frac{\omega_l^2}{c^2}\right)+\left(k_n^2-\frac{\omega_l^2}{c^2}\right)\times\frac{k_{De}^2(x)}{k_n^2}\frac{1+\tilde{u}_{l,n}(x)\,S(\tilde{u}_{l,n}(x))}{1+i\tilde{\gamma}_n(x)\,S(\tilde{u}_{l,n}(x))},\tag{4.3}$$

with $k_{De}(x)=1/\lambda_{De}(x)$, $\lambda_{De}(x)=\left[k_B T_e(x)/(4\pi n_{eo}(x)e^2)\right]^{1/2}$, $\tilde{\omega}_l(x)=(\omega_l+i\nu_e(x))$, $\tilde{u}_{l,n}(x)=\tilde{\omega}_l(x)/(k_n \mathrm{v}_{th,e}(x))$, $\tilde{\gamma}_n(x)=i\nu_e(x)/(k_n \mathrm{v}_{th,e}(x))$ and,

$$\tilde{\beta}^{NL}(x,\omega_l,k_m,k_n)=-\frac{e^2}{2(k_B T_e(x))^2}\frac{\omega_{pe}^2(x)}{\tilde{\omega}_l^2(x)}\times\frac{\left(k_n^2-\frac{\omega_l^2}{c^2}\right)}{(1+i\gamma_n S(\tilde{u}_{l,n}(x)))}\times\sum_{a,b,c}\left|\tilde{\psi}_{a,b,c}(x)\right|^2 G^{LF}_{l-a,m-b,n-c}(x)\times H^{l,n,a,c}_{l-a,n-c}(x),\tag{4.4}$$

where the summation is over every HF spectral component $(a,b,c)$ in the meshgrid with $(a,b,c)\neq(l,m,n)$ and,

$$G^{LF}_{l-a,m-b,n-c}(x)=\frac{1}{k_{n-c}}\left(\frac{\varepsilon(x,\tilde{\omega}_{l-a},k_{m-b},k_{n-c})-\chi_e(x,\tilde{\omega}_{l-a},k_{m-b},k_{n-c})}{\varepsilon(x,\tilde{\omega}_{l-a},k_{m-b},k_{n-c})}\right),\tag{4.5}$$

$$H^{l,n,a,c}_{l-a,n-c}(x)=\frac{F\left(\left(u^{LF}_{l-a,n-c}(x),u^{HF}_{l,n}(x)\right)\right)}{k_n}-\frac{F\left(u^{LF}_{l-a,n-c}(x),\left(u^{HF}_{a,c}(x)\right)^*\right)}{k_c},\tag{4.6}$$

where according to the general selection rules (arising from the discretization of the two nested convolutions of the nonlinear term (2.60)) $\omega^{LF}_{l-a}=\omega^{HF}_l-\omega^{HF}_a$, $k^{LF}_{m-b}=k^{HF}_m-k^{HF}_b$, $k^{LF}_{n-c}=k^{HF}_n-k^{HF}_c$ (where we have simply highlighted with an apex the spectral separation in the frequency domain), we have that $\tilde{\omega}_{l-a}=\omega^{LF}_{l-a}+i\nu_e(x)=(l-a)*\Delta\omega+i\nu_e(x)$, $k_{m-b}=k^{LF}_{m-b}=(m-b)*\Delta k_y$, $k_{n-c}=k^{LF}_{n-c}=(n-c)*\Delta k_z$ and $u^{LF}_{l-a,n-c}(x)=\tilde{\omega}_{l-a}/(k_{n-c}\mathrm{v}_{th,e}(x))$, $u^{HF}_{l,n}(x)=\tilde{u}_{l,n}(x)=\tilde{\omega}_l/(k_n \mathrm{v}_{th,e}(x))$, $\tilde{\omega}_a=(\omega_a+i\nu_e(x))$ and $u^{HF}_{a,c}(x)=\tilde{u}_{a,c}(x)=\tilde{\omega}_a/(k_c \mathrm{v}_{th,e}(x))$. We solve this nonlinear system with an iterative method, using as initial guess the solution of the linear wave equation for the pump wave. The iterative method is based on a numerical scheme that exploits the natural spectral separation in frequency between the pump wave and the sideband waves [73]. In each iteration, the nonlinear wave equation is solved first for all the sideband spectral components and then for all the pump spectral components. The nonlinear coupling is limited only between the pump wave and the sideband waves, i.e. the nonlinear interactions between the spectral components of the sideband waves and between the spectral components of the pump wave are not considered (the latter is excluded by the zero limit of the coupling function for zero frequency of the intermediate mode). In this way, in each iteration, all the sidebands see the same pump (computed at the previous iteration) and all pump spectral components see the same sidebands (computed at the previous iteration). We have found that this scheme ensures the convergence of the nonlinear system of coupled equations. Moreover, we integrate numerically each wave equation (4.2) with an algorithm based on an implicit Runge–Kutta method with variable order and with variable integration step [94], controlling the numerical convergence with thresholds on both the relative error ($1\times10^{-6}$) and the absolute error ($1\times10^{-9}$). Moreover, in order to evaluate the ion susceptibility in equation (4.5), we solve the system of ordinary differential equations (2.56) and (2.57) to obtain the relevant complex radial wavenumber $k_x$ of the LF ion-sound quasi-modes resulting from the beating of two HF electric fields. As initial conditions, concerning the pump wave equations, we consider for each spectral component the amplitude and the derivative of the solution $E_z(x)$ of the antenna power coupling problem [24] with a facing linear plasma density profile.

For the sideband wave equations, we consider a red noise produced by the RF source, and for each spectral component the amplitude of the parallel electric field $E_z(x)$ and the gradient $\partial_x E_z(x)$ are computed in the same way that was done for the pump wave (since we consider here an antenna coupled noise). Moreover, we limited the $N_\parallel$ domain according to a full accessibility condition to the LCMS plasma layer in order to avoid the spectral components lost in the mode conversion of an LH wave to a fast wave. Thus, for all spectral components here considered, the condition $\left|N_\parallel\right|>1.24$ must be satisfied (in the present meshgrid, we have $\left|N_\parallel\right|\geqslant1.5$). Moreover, we define the pump depletion at the radial position $x$ as:

$$Pump\_depletion(x)=1-P_x(x)/P_x^{LIN}(x),\tag{4.7}$$

where $P_x(x)$ is the radial power flux density, evaluated at $x$ radial position, obtained from the solution of the nonlinear coupled system of equations for the pump wave; $P_x^{LIN}(x)$ is the radial power flux density, evaluated at the same $x$ radial position, computed from the solution of the linear solution of the wave equation for the pump wave, i.e. the wave equation (2.85) without the nonlinear term. The quantity (4.7) measures the power that the pump wave loses for nonlinear effects due to the transfer of power to the sideband waves. In figure 11, it is shown that the trend of the radial component $P_x$ of the power flux density vector $P$ for the pump wave versus the radial position $x$ for both the linear and the nonlinear case and the corresponding pump depletion, as defined in (4.7). We reach numerical convergence of the solution of the nonlinear system in four iterations, with pump depletion at the LCMS of about 3%. We observe that the numerical convergence here is quite fast since we simulated a scenario with low pump depletion. In scenarios with stronger PI, the numerical convergence may be reached with more iterations and longer simulation times. In figure 12, the spectral broadening of the coupled power spectrum in the frequency domain can be observed. The predicted asymmetry of the power spectrum is dominated by the lower sidebands. This asymmetry is typical of PI and it is usually observed in the measured RF spectra when PI occurs [11, 60,

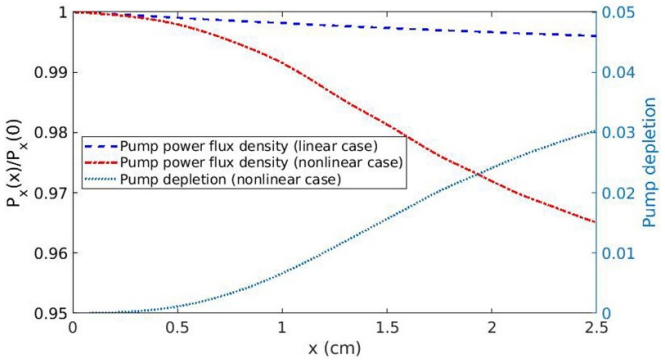


**Figure 11.** Radial component of the power flux vector for the pump wave versus the radial position $x$ for both the linear (dashed line) and the nonlinear (point dashed line) case and the corresponding pump depletion (dotted line).

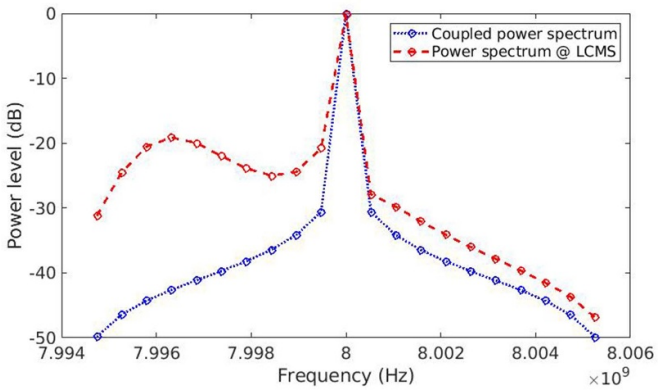


**Figure 12.** Coupled power spectrum (dotted line) at the LH antenna mouth and nonlinear broadened power spectrum (dashed line) at the LCMS, both represented in the frequency domain. Spectral broadening is the result of the nonlinear interaction of the pump wave at the operating line frequency $f_0 = 8.0$ GHz with the sideband LH waves.

88]. In figure 13, the spectral broadening of the parallel refractive index can be observed. The predicted broadening improves previous results [73]. The amplified spectral components up to $N_{||} \sim 10$ may determine the power deposition in the outer part of the plasma column. Figures 12 and 13 are typical results of a nonlinear modeling allowing the estimation of the transfer of the pump power to new sideband spectral components. Since the FTU experimental scenario considered here has a pump depletion at the LCMS of about 3%, only a small fraction of the coupled power is predicted to be transferred to each sideband. We have checked that all the model constraints are fulfilled. Here, we show that the more critical parameters can be checked. In figure 14, we plot the maximum values of the angle $\delta$, the quantity $|\omega\, k_x/(\Omega_e k_z)|$, the expansion parameter $\eta$ and the LF quantity $\left|\left(1/k_x^2\right)\partial\, k_x/\partial x\right|$ versus the radial position evaluated over all spectral components of the sideband waves. Since all the values are always much less than unity, the relevant hypotheses are satisfied in the simulation. In figure 15, it is shown that, as a representative solution for the sideband waves, the spatial amplification of a few selected spectral components of the lower sideband corresponds to the frequency of the relative maximum at ∼7.996 GHz observed in figure 12. In figure 16, it is shown that, as a representative solution for the pump wave, the spatial trend for the three selected spectral components corresponds to the peak of the coupled power spectrum. The components with a longer wavelength in the radial direction are those where the WKB validity fails. Finally, in order to appreciate the difference in the spatial amplification of the sideband waves driven unstable by PI as computed by the ALGOR code, and that one as predicted from the standard theory [15], we solve the standard PDE in the complex angular frequency, obtaining the growth rates for plasma parameters corresponding to those of the plasma edge in the simulation.

Moreover, we use the method indicated in [15, 60] to evaluate the effects of convective losses due to plasma inhomogeneity and due to finite illumination by the LH pump wave. As a result, concerning the leading LH sideband, the ALGOR code predicts a spatial amplification of about 40 dB while the standard theory predicts a larger amplification of about 60 dB.

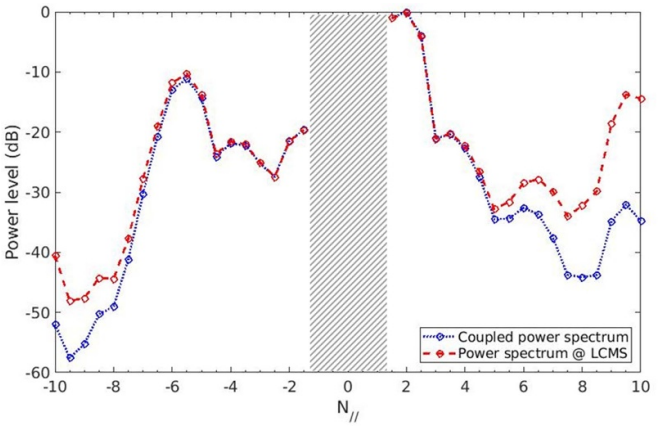


**Figure 13.** Coupled power spectrum (dotted line) at the LH antenna mouth and the broadened power spectrum (dashed line) at the LCMS, both represented in the parallel refractive index domain. Gray central band indicates the spectral components of the spectrum that were ignored in the simulations since they correspond to slow waves that do not satisfy the accessibility condition to the LCMS.

We have calculated the amplification of other LH sidebands based on the standard theory of PI and found that this amplification is overestimated by orders of magnitude with respect to the new modeling, so that significant pump depletion would be predicted by the standard modeling, much larger than the 3% found by the new modeling.

## 5. Discussion and conclusions

The importance of PI in the LHCD physics of tokamak plasmas motivates an accurate theoretical modeling of this nonlinear effect. The objective of the present study has been to overcome the limits and the incorrectness of the standard theory of the PI in inhomogeneous plasma [15, 60, 67, 68] and provide a correct assessment of the role of the collisions, which were overestimated by previous, incorrect analysis [66]. This

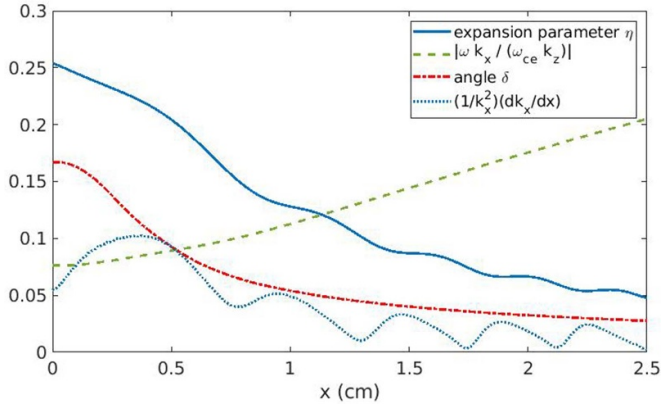


**Figure 14.** Most critical parameters for the model validity, evaluated taking their maximum values over all simulated spectral components, plotted here as a function of the radial position $x$: the expansion parameter $\eta$, the quantity $|\omega\, k_x/\,(\Omega_e k_z)|$, the angle $\delta$ and the quantity $\left|\left(1/k_x^2\right)\partial\, k_x/\partial x\right|$.

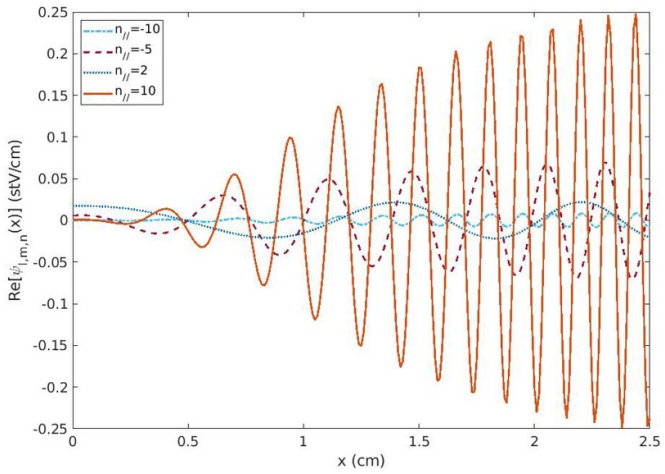


**Figure 15.** Spatial (radial) trend of the real part of the complex amplitude for selected spectral components of the sideband wave with $l = -7$ (corresponding to the frequency ∼7.996 GHz at the peak shown in figure 12), $m = 0$ and $n = 1,\ 11,\ 25,\ 41$.

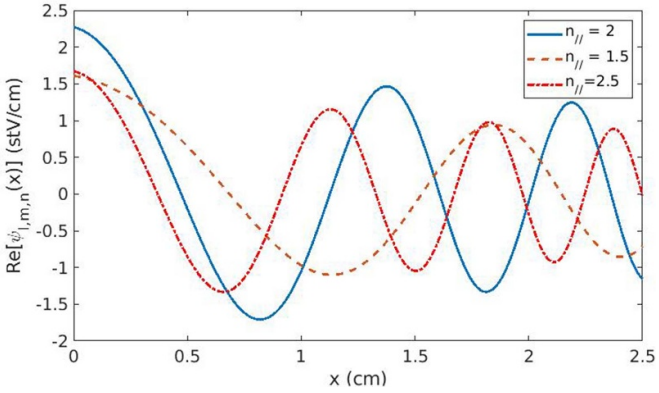


**Figure 16.** Spatial (radial) trend of the real part of the complex amplitude for selected spectral components of the pump wave with $l = 0,\ m = 0$ and $n = 24,\ 25,\ 26$.

required developing a full-wave approach, improving previous modeling [20, 73]. As a main result, a new set of nonlinear coupled integro-differential equations in the LF and HF ranges, respectively equations (2.53) and (2.88)–(2.90), has been derived in section 2 from a kinetic model of collisional plasma and the Maxwell equations, based on the spectral method and the perturbation theory up to the third order. The effects of the collisions have been included here in the kinetic equation by a simple BGK particle conserving operator, which seems sufficient to capture the correct LH physics in the present study, as suggested by the analysis in appendix A. As in the standard PI theory for inhomogeneous plasma, the 1D slab model is adopted, assuming a constant equilibrium magnetic field. 2D modeling and spatial variation of the static magnetic field are essential to describe the wave propagation and its effects in the plasma core. In the peripheral plasma, where PI occurs, it is expected that the nonlinear driving of the instabilities does not change significantly in the presence of these effects, unless important poloidal asymmetries and important poloidal components of the launched LH waves are present. However, these should be avoided in a well-designed LHCD experiment in a tokamak device. The plasma ions, in the HF range are assumed, as usual in the LH wave modeling, to be a cold, unmagnetized fluid. We show in section 3 that this assumption is reasonably well justified. An important feature of our modeling is that finite electron Larmor radius effects have been neglected. For typical peripheral plasmas in tokamak devices, where PI driven by LHCD power injection occurs, the ordering $\rho_{th,e} \ll \lambda_{D,e}$ usually holds. The kinetic equation used here as well as in the standard modeling of PI only concerns collective effects that occur on scale lengths much larger than the electron Debye length.

In this vein, the condition $|k_\perp|\,\rho_{th,e} \ll 1$ that we assume here should not be considered as a limit of the theory but a prerequisite for any LH modeling based on the kinetic equation for the plasma electrons. We also neglect the drift frequencies compared to the characteristic frequencies of the ISQM and ICQM channels of PI, which is reasonable, as the latter are orders of magnitude larger. Moreover, if the eikonal hypothesis is not well justified, a regime that we assume to occur for $|k_x L| < 10$, we derive the electron charge and current densities in the HF range based on the cold plasma approximation. In this regard, we note that in this case the cold plasma approximation is justified and has been used to derive the linear LH full-wave equation for the analysis of LHCD scenarios in [69], where the perturbed current densities are calculated by the cold conductivity tensor. The cold plasma approximation was also used in the full-wave propagation analysis of the injected LH power in the presence of steep density profiles [95]. A complete list of the specific model constraints is proposed in table 2 of section 2. These are usually fulfilled in peripheral tokamak plasmas in LHCD experiments, as suggested by the typical plasma and RF parameters listed in table 3. As a benchmark of the new theory, in section 3 we have compared, in the homogeneous and collisionless plasma limit, the solutions of both the linear dispersion equation and the nonlinear parametric dispersion equation for electrostatic LH waves, as derived

from our modeling, with those obtained within the framework of a full kinetic model within the archived literature. In particular, the solutions of the linear dispersion equation are, in practice, identical. Concerning the parametric dispersion equation derived from our theory, it differs from the known expression in the standard theory of PI [15, 60, 61] only due to the following approximations: (*i*) in the HF dielectric function we consider unmagnetized ions; (*ii*) in both the LF and HF range finite electron Larmor radius effects are neglected; (*iii*) the polarization drift term in the nonlinear interaction is neglected; (*iv*) the drift frequency in the LF linear susceptibility of both the electrons and ions is neglected. These approximations are well justified in peripheral plasma conditions. For typical experimental scenarios, tiny differences emerge in the PDE numerical solutions, i.e. in the growth rates and frequencies of the LH sideband waves driven unstable, as a function of the parallel wavenumber. On the other hand, our modeling has many advantages compared to the standard theory of PI in inhomogeneous plasmas, in addition to overcoming the lack of validity of the eikonal hypothesis used in that theory. This allows us to treat, in detail, the overall wavenumber spectrum of the pump wave, which in the standard model is reduced to a single component. The effects of finite illumination of the pump, which in the standard model are considered only by means of the geometrical parameters of the area illuminated by the antenna, are embedded here in the complete poloidal and toroidal wavenumber spectrum of the LH pump wave. The convective loss effects, which in the standard model are often treated considering the phase mismatch of the interacting waves based on their parameters at the antenna mouth [15, 60], are embedded in the coupled LF-HF wave equations, considering the wave propagation in the overall interaction region. This was also done within the framework of a more refined eikonal theory in [67] concerning electrostatic LH waves, though still affected by the incorrectness and limits of that approach. Here, we consider electromagnetic LH waves. These are treated within the electrostatic approximation of the standard theory, and only a recent analysis in homogeneous plasma [65] suggested a non-negligible stabilization effect due to the electromagnetic corrections. Finally, the model proposed can take into account diffraction effects that are missing in the eikonal theory and can be important for LH sidebands with relatively low parallel wavenumber. Although in the present numerical implementation of the model this feature is not included, it might in principle also treat sideband-sideband interactions instead of considering only sideband-pump interactions. In this vein, cascade PI phenomena might also be evaluated.

The new modeling improves significantly previous full-wave LH theories of PI, proposed in [20, 73]. In the former, a fluid model was used to evaluate the time evolution of an LH power pulse with two spectral components in the parallel wave number, thus not considering a steady-state condition, which is necessary for a comparison with LHCD experiments. In the latter, only adiabatic electrons in the HF range were considered and the electron dynamics perpendicular to the magnetic field was neglected, missing the effect of $\boldsymbol{E} \times \boldsymbol{B}$ drive of PI. Limiting the ion dynamics in the LF range to the parallel motion also allowed us to treat only the ISQM channel of PI. Moreover, due to an approximate treatment of the poles in the velocity space involved in the kinetic model, based on the adiabatic approximation, it is not possible to deduce the correct PDE even within the limit of dominant parallel drive of PI. In the present implementation of the new model in the numerical code ALGOR, updating older versions [73, 93], only the parallel electric field $E_{\|}$ of the LH pump wave is considered. In fact, it is the dominant PI drive with respect to the $\boldsymbol{E} \times \boldsymbol{B}$ term in the low-density regimes, typically up to $\sim 10^{19}$ cm$^{-3}$, as long as the angle $\delta$ of the perpendicular wavenumber of the LH pump and the LH sidebands is sufficiently small [61, 73]. To maximize the amplification of the LH sidebands by considering the convective losses, and the finite region illuminated by the LH antenna, an optimal value of only $\delta \cong 0.14$ has been indeed suggested [68]. For larger plasma density the eikonal hypothesis is reasonably justified. Therefore, the PI modeling can be completed by interfacing the numerical code ALGOR with the code LHSTAR [60]. The latter calculates the effects of PI in LHCD physics based on the eikonal hypothesis. However, we observe that in reactor scenarios like ITER, for plasma densities exceeding the above limit, a region of steep gradients of density and temperature, near the separatrix, is envisaged. In this case, strong convective losses are expected to quench the PI and the large electron temperatures $T_e$ expected also reduce the PI drive. Therefore, the present modeling can also be used standalone as a suitable guide for the design of LHCD systems for future reactor relevant machines, concerning the PI effects. The numerical solutions of the new set of nonlinear integro-differential wave equations, proposed in section 4, exhibit frequency spectra with features similar to those observed in LHCD experiments, such as spectral broadening and asymmetry around the pump wave frequency, with larger amplifications of the LH sideband at lower frequencies. A check of the validity of the model constraints as well as of the energy conservation, which is reasonably well fulfilled within the unavoidable limit of numerical noise, makes us confident about the reliability of the model implementation by ALGOR. A comparison of the amplification of LH sidebands driven unstable by PI as calculated by ALGOR and by the method indicated in [15, 60] to evaluate the effects of convective losses and finite illumination by the LH pump wave has also been performed. As a result, ALGOR predicts a much smaller amplification (about 20 dB less). This is due to the fact that the standard theory evaluates the amplification on the basis of the growth rates calculated at the initial point of the nonlinear interactions, i.e. near the antenna mouth. There, the pump wave electric field has the largest value. However, the model implemented in ALGOR considers the space evolution of the LH pump wave electric field, driving the PI. It decreases following the wave propagation in the peripheral plasma. It is thus not surprising that the standard modeling of PI in inhomogeneous plasma overestimates the LH sideband amplification. We have also assessed the role of the collisions in PI. We show that they are marginal concerning the PI for typical levels of the LH pump power density. In this vein, we have pointed out that previous analysis, performed in [66], overestimated the stabilizing effect of the collisions, due to a model error, completely

neglecting the important ion contribution to determine consistently the LF electric field. A new analytical expression for the growth rate of the PI, within the limit of dominant parallel drive, has been derived, correcting the analogous formula proposed in [66], which greatly overestimates the effect of the collisions.

We have found that the role of the collisions becomes essential near the threshold power for the onset of PI. An analytical expression for this threshold has been proposed.

Possible improvements in the modeling are listed in the following. The ALGOR code must be updated to include the contribution of the $E \times B$ drive and the aforementioned cascade effects. The effects of LH scattering off density fluctuations should be included in the model, as they might provide, in synergy with nonlinear effects, a more accurate analysis of LHCD experiments. A 2D model in space will be developed, overcoming the limits of the slab model. In this regard, we note that high-frequency waves typically give rise to bending wave fronts so that treating the equations in one dimension only merely describes the physics up to a point. It is also planned to take into account the spatial variation of the equilibrium magnetic field, which has been assumed here to be constant. However, it is not expected that these effects might significantly change the nonlinear LH physics in peripheral plasmas. For a complete LHCD modeling, it is also necessary to develop an interface between ALGOR and ray-tracing codes coupled to Fokker–Planck solvers, e.g. RAYFP [96], in order to evaluate the LHCD power deposition and current drive in the plasma core. Strong turbulence effects, already suggested in [20], might occur in front of the LH launcher, where the expansion parameter in some LHCD scenarios might only marginally satisfy the weak turbulence conditions. A full nonlinear model, e.g. within the fluid theory or by a suitable PIC (particle in cell) algorithm, might be used to properly treat these effects. Finally, a careful theoretical analysis of the LHCD spectral noise, which is the seed of the PI, possibly complemented by experimental measurements, should be performed. We plan to apply the present modeling with at least some of the above improvements to analyze experimental scenarios, for example those of [11], [59] and [97] as well as the LHCD scenarios envisaged for ITER [87] or other reactor relevant tokamaks.

However, we believe that the present study provides a significant improvement over the standard modeling of PI and is a candidate to represent the state of the art in this field. The above improvements, now ongoing, should indeed provide a high-fidelity modeling of the LHCD physics.

## Data availability statement

All data that support the findings of this study are included within the article (and any supplementary files).

## Acknowledgments

The authors are grateful to Roberto Cesario for his valuable suggestions. C Castaldo thanks Annika Ekedhal, Gerardo Giruzzi, Marc Goniche and Tuong Hoang for their warm hospitality during his visit to the CEA-IRFM Institute in 2010, when the present study started. He is also grateful to them for their useful comments during the presentation of the first version of the model.

## Appendix A. The collision operator

In section 3, we show that the collisions play a marginal role in PI if the LH pump power is much larger than the threshold for their onset. However, they are important to determine the power threshold for PI and it is reasonable to admit that they affect the LH nonlinear behavior for low LH power regimes. In this vein, it is important to investigate if the 1D particle-conserving BGK collision operator, as given by equation (2.1), is sufficiently accurate to model the LH physics. Here, we show that the collisions do not change significantly the nonlinear coupling function and the LF linear plasma electron response. They affect the LH physics near the PI threshold due to the collisional damping of the LH sideband waves. We thus first verify that the LH collisional damping is calculated with reasonable accuracy utilizing the proposed collision operator. We note that the LH collisional damping is calculated by linear codes within the weak-damping limit usually adding a suitable imaginary part to the dispersion relation. In the GENRAY code [98], for this purpose, as suggested in [32], the electron mass $m_e$ is replaced by $m_e\left(1+i\nu_{ei}/\omega_r\right)$ in the cold plasma dispersion relation used in the ray equations of the eikonal theory. Within the limits $\omega_{pe}\ll|\Omega_{ce}|$, $\omega_{pi}\ll|\omega|$ and $\nu_{ei}\ll|\omega|$, for LH quasi-electrostatic waves, the relevant dispersion relation is thus as follows:

$$\varepsilon = 1-\frac{\omega_{pe}^2}{\omega^2}\frac{k_\parallel^2}{k_\perp^2}\left(1-i\frac{\nu_{ei}}{\omega_r}\right). \tag{A1}$$

As a result, the collisional damping rate is $\gamma_C=\nu_{ei}/2$, which is identical to the value given by equation (3.21) utilizing the collision operator defined in equation (2.1), though a more general collisional rate $\nu_e$ is present there (it might include, in principle, also the effects of the electron–neutral and electron–electron collisions).

The simple collision operator given by equation (2.1) thus provides essentially the same collisional damping rate of the LH simulation code GENRAY, widely used for many years to study the LHCD experiments in several tokamak plasma scenarios, up to quite recent predictive study for the LHCD design [99] in the CFETR planned tokamak fusion reactor [100].

As a further assessment of the accuracy of the collision operator used, we compare the collisional damping in the HF range with the result obtained by the following more accurate BGK 1D linear collisional operator:

$$\left(\frac{\partial g_e}{\partial t}\right)_{\text{coll}} = -\nu_e\left(g_e-g_{eo}\frac{n_e}{n_{eo}}\right)+2\nu_e\left(\frac{\mathrm{v}_z^2}{\mathrm{v}_{th,e}^2}-\frac{1}{2}\right)\frac{g_{eo}}{n_{eo}}\int_{-\infty,\mathcal{L}}^{+\infty}\mathrm{dv}_z\left(\frac{\mathrm{v}_z^2}{\mathrm{v}_{th,e}^2}-\frac{1}{2}\right)g_e. \tag{A2}$$

This operator conserves the particle number and the kinetic energy and is zero in equilibrium conditions, i.e. for $g_e=g_{eo}=n_{eo}\pi^{-1/2}\mathrm{v}_{th,e}^{-1}\exp\left(-\mathrm{v}_z^2/\mathrm{v}_{th,e}^2\right)$.

The perturbed force density acting on the electrons, due to the collisions, is parallel to the magnetic field, namely $F_z=-m_e\nu_e n_{eo}u_z$, where $u_z=\int_{-\infty}^{+\infty}\mathrm{dv}_z\, g_e/\, n_{eo}$. The sum of the force densities acting on the ions and neutrals must be opposite to $F_z$, leading to momentum conservation. However, we have assumed that the ions behave as a fixed background (we can also extend this assumption for the neutrals), so that no energy exchange is allowed between them and the mobile electrons. Consistently, we have,

$$\int_{+\infty}^{-\infty}\mathrm{dv}_z\frac{1}{2}m_e\mathrm{v}_z^2\left(\frac{\partial g_e}{\partial t}\right)_{\text{coll}}=0. \tag{A3}$$

The first-order, linear kinetic equation in the HF range is:

$$\frac{\partial g_e}{\partial t}+\mathrm{v}_z\frac{\partial g_e}{\partial z}+\frac{q_e}{m_e}E_z\frac{\partial g_{eo}}{\partial \mathrm{v}_z}=\left(\frac{\partial g_e}{\partial t}\right)_{\text{coll}}. \tag{A4}$$

For monochromatic LH waves $E_z=E_{z1}e^{-i(\omega_1 t-k_1\cdot r)}$ we obtain the following, from equations (A2) and (A4):

$$\begin{aligned} g_e=\frac{i}{\omega_1+i\nu_e-k_{z1}\mathrm{v}_z}\Bigg[&+\frac{q_e}{m_e}E_{z1}\frac{\mathrm{v}_z}{\mathrm{v}_{th,e}^2}\frac{n_{eo}}{\sqrt{\pi}\,\mathrm{v}_{th,e}}\exp\left(-\mathrm{v}_z^2/\mathrm{v}_{th,e}^2\right)+\nu_e\frac{n_e}{\sqrt{\pi}\,\mathrm{v}_{th,e}}\exp\left(-\mathrm{v}_z^2/\mathrm{v}_{th,e}^2\right)\\ &+2\nu_e\left(\frac{\mathrm{v}_z^2}{\mathrm{v}_{th,e}^2}-\frac{1}{2}\right)\frac{1}{\sqrt{\pi}\,\mathrm{v}_{th,e}}\exp\left(-\mathrm{v}_z^2/\mathrm{v}_{th,e}^2\right)\left(\frac{n_{eo}K_\parallel}{T_e}-\frac{n_e}{2}\right)\Bigg]. \end{aligned} \tag{A5}$$

Here, we define the perturbed quantity $K_{\parallel}$ as,

$$K_{\parallel} = \frac{1}{n_{eo}} \int_{+\infty}^{-\infty,\mathcal{L}} \mathrm{d}\mathrm{v}_z \frac{1}{2} m_e \mathrm{v}_z^2 g_e. \tag{A6}$$

Following Landau's prescription, the integration of the equation (A5) gives,

$$\begin{aligned} n_e = &-i\frac{q_e n_{eo}}{m_e k_{z1} \mathrm{v}_{th,e}^2} E_{z1} \frac{1}{\sqrt{\pi}} \int_{-\infty,\mathcal{L}}^{+\infty} \mathrm{d}z \frac{z e^{-z^2}}{z-u} - i n_e \frac{\nu_e}{k_{z1}\mathrm{v}_{th,e}} \frac{1}{\sqrt{\pi}} \int_{-\infty,\mathcal{L}}^{+\infty} \mathrm{d}z \frac{e^{-z^2}}{z-u} - i\frac{\nu_e}{k_{z1}\mathrm{v}_{th,e}} \\ &\times \left(\frac{2n_{eo}K_{\parallel}}{T_e} - n_e\right) \frac{1}{\sqrt{\pi}} \int_{-\infty,\mathcal{L}}^{+\infty} \mathrm{d}z \frac{e^{-z^2}}{z-u} \left(z^2 - \frac{1}{2}\right). \end{aligned} \tag{A7}$$

Here, $u = (\omega_1 + i\nu_e)/(k_{z1} v_{th,e})$. We rewrite the above equation utilizing the definitions:

$$\mathcal{J}_n = \frac{1}{\sqrt{\pi}} \int_{-\infty,\mathcal{L}}^{+\infty} \mathrm{d}z \frac{e^{-z^2}}{z-u} z^n,\ E_{z1} = E_o \mathcal{E}_{z1},\ \gamma_e = \frac{\nu_e}{k_{z1}\mathrm{v}_{th,e}}. \tag{A8}$$

Here, $E_o > 0$ is the squared root of the time average of the squared parallel electric field of the LH pump wave, with angular frequency $\omega_o$, at the peak value corresponding to the parallel wave number $N_{\parallel o}$. We also recall the definition of the expansion parameter:

$$\eta = \frac{eE_o}{m_e \mathrm{v}_{th,e} \omega_o}. \tag{A9}$$

We thus obtain from equation (A7), defining $u_o = \omega_o/(k_z \mathrm{v}_{th,e})$:

$$n_e = i\eta u_o \mathcal{E}_{z1} n_{eo} \mathcal{J}_1 - i\gamma_e n_e \mathcal{J}_o - i\gamma_e \left(\frac{2n_{eo}K_{\parallel}}{T_e} - n_e\right)\left(\mathcal{J}_2 - \frac{\mathcal{J}_o}{2}\right). \tag{A10}$$

From equations (A5) and (A6) we have:

$$K_{\parallel} = T_e \left[\eta u_o \mathcal{E}_{z1} \mathcal{J}_3 - i\gamma_e \frac{n_e}{n_{eo}} \mathcal{J}_2 - i\gamma_e \left(\frac{2T_{\parallel}}{T_e} - \frac{n_e}{n_{eo}}\right)\left(\mathcal{J}_4 - \frac{\mathcal{J}_2}{2}\right)\right]. \tag{A11}$$

In terms of the variables $x = n_e/n_{eo}$ and $y = K_{\parallel}/T_e$ we rewrite the linear system (A10), (A11) in the form:

$$x = i\eta u_o \mathcal{E}_{z1} \mathcal{J}_1 - i\gamma_e \mathcal{J}_o x - i\gamma_e (2y - x)\left(\mathcal{J}_2 - \frac{\mathcal{J}_o}{2}\right), \tag{A12}$$

$$y = \eta u_o \mathcal{E}_{z1} \mathcal{J}_3 - i\gamma_e \mathcal{J}_2 x - i\gamma_e (2y - x)\left(\mathcal{J}_4 - \frac{\mathcal{J}_2}{2}\right). \tag{A13}$$

The calculations of $\mathcal{J}_n$ with the integer $n$, so that $0 \leqslant n \leqslant 4$, give:

$$\mathcal{J}_o = S(u), \tag{A14}$$

$$\mathcal{J}_1 = 1 + uS(u), \tag{A15}$$

$$\mathcal{J}_2 = u[1 + uS(u)], \tag{A16}$$

$$\mathcal{J}_3 = \frac{1}{2} + u^2[1 + uS(u)], \tag{A17}$$

$$\mathcal{J}_4 = \frac{1}{2}u + u^3[1 + uS(u)]. \tag{A18}$$

For Landau damping rate and collisional damping rate much smaller than the angular wave frequency, i.e. for weak damping, the perturbation theory can be applied. The anti-Hermitian part of the dielectric tensor can be expressed as a sum of the contribution due to Landau interaction and the collisional interaction. Therefore, the Landau damping can be calculated setting

to zero the collisional rate and the collisional damping can be calculated within the limit of vanishing Landau damping, namely for $|u| \gg 1$. The latter ordering gives, considering the asymptotic expansion of the plasma dispersion function:

$$\mathcal{J}_o \cong -\frac{1}{u}, \mathcal{J}_1 \cong -\frac{1}{2u^2}, \mathcal{J}_2 \cong -\frac{1}{2u}, \mathcal{J}_3 \cong -\frac{3}{4u^2}, \mathcal{J}_4 \cong -\frac{3}{4u}. \tag{A19}$$

The equations (A12) and (A13) give:

$$x = -\frac{i\eta u_o \mathcal{E}_{z1}}{u^2} + i\frac{\gamma_e}{u}x, \tag{A20}$$

$$y = -\frac{3\eta u_o \mathcal{E}_{z1}}{4u^2} + i\frac{\gamma_e}{u}y. \tag{A21}$$

To determine the collisional damping rate only the former equation is necessary. It gives the perturbed electron density:

$$n_e = -i\frac{en_{eo}E_{z1}}{m_e k_{z1} \mathrm{v}_{th,e}^2} \frac{k_{z1}^2 \mathrm{v}_{th,e}^2}{(\omega_1 + i\nu_e)^2} \frac{1}{1 - i\frac{\nu_e}{\omega_1 + i\nu_e}} \cong -i\frac{en_{eo}k_{z1}E_{z1}}{m_e\omega_1^2}\left(1 - i\frac{\nu_e}{\omega_{1,r}}\right). \tag{A22}$$

The approximation on the r.h.s. of the above equation is obtained from the orderings $|\omega_{1,i}| \ll |\omega_{1,r}|$ (weak damping) and $\nu_e \ll |\omega_{1,r}|$.

For quasi-homogeneous plasma, so that the eikonal approximation is valid, the approximated linear wave equation in the HF range, within the electrostatic limit, is obtained from equation (2.26):

$$k_1^2 E_{z1} - 4\pi i k_{z1} e n_e = 0, \tag{A23}$$

where $n_e$ is given by equation (A22).

The above equation can be cast in the form:

$$\varepsilon_1 E_{z1} = 0. \tag{A24}$$

The dielectric function $\varepsilon_1$ is given by:

$$\varepsilon_1 = 1 - \frac{\omega_{pe}^2}{\omega_1^2}\frac{k_{z1}^2}{k_1^2}\left(1 - i\frac{\nu_e}{\omega_{1,r}}\right). \tag{A25}$$

The perturbation theory gives:

$$\omega_{1,r}^2 \cong \omega_{pe}^2 \frac{k_{z1}^2}{k_1^2}, \tag{A26}$$

and

$$\omega_{1,i} = -\frac{\nu_e}{2}. \tag{A27}$$

Therefore, the collisional damping rate is again $\gamma_{C1} = \nu_e/2$.

Concerning the LF range, the linear electron density perturbation is formally given by equation (2.42) both in the case of the Fourier transform and in the case of the response to monochromatic waves. In the former, the LF angular frequency $\omega$ is real, while in the latter, an imaginary part is allowed, to account for damping or growth rates. In both cases, the small argument approximation can be used for the plasma dispersion function and we obtain:

$$n_e^{(2)L} \cong 2in_{eo}\frac{eE_z}{m_e k_z \mathrm{v}_{th,e}^2}\left[1 + i\sqrt{\pi}\frac{\omega}{k_z \mathrm{v}_{th,e}}\right]. \tag{A28}$$

We recall that the following orderings hold:

$$|\omega| / (|k_z| \mathrm{v}_{th,e}), \nu_e / (|k_z| \mathrm{v}_{th,e}) \ll 1.$$

Equation (A28) is obtained including first-order terms in the small ratios defined above. As a result, the LF linear electron density perturbation does not depend on the collisional frequency up to the second order in $\nu_e / (|k_z| \mathrm{v}_{th,e})$ and, within this order, is the same for collisionless plasma. We show now that the nonlinear second-order electron density perturbation is pooly affected by the presence of the collisions and can be approximated reasonably well by the expression obtained for collisionless plasma.

The present discussion is limited to the parallel coupling function $F_{\parallel}$. Similar conclusions concern the perpendicular coupling function $F_{\perp}$ as well as the third-order nonlinear density perturbation. We report here the full parallel coupling function that can be derived also retaining in the gradients of the velocity distribution the contribution to the collisions, namely:

$$F_{\parallel}\left(u_e,u_e'\right)=\frac{2}{1+i\gamma_e S\left(u_e\right)}\left[u_e\frac{1+u_eS\left(u_e\right)}{u_e'-u_e}+\frac{u_e'}{2}\frac{S\left(u_e'\right)-S\left(u_e\right)}{\left(u_e'-u_e\right)^2}\right]$$
$$-\frac{2i\gamma_e'}{1+i\gamma_e'S\left(u_e'\right)}\left[\frac{1+u_eS\left(u_e\right)}{u_e'-u_e}+\frac{1}{2}\frac{S\left(u_e'\right)-S\left(u_e\right)}{\left(u_e'-u_e\right)^2}\right]\frac{1+u_e'S\left(u_e'\right)}{1+i\gamma_eS\left(u_e\right)}, \tag{A29}$$

where $u_e=\left(\omega+i\nu_e\right)/\left(k_z\mathrm{v}_{th,e}\right)$ $u_e'=\left(\omega'+i\nu_e\right)/\left(k_z'\mathrm{v}_{th,e}\right)$ and $\gamma_e'=\nu_e/\left(k_z'\mathrm{v}_{th,e}\right)$.

As observed in section 2, only the beating of two HF fields (one of them being a component of the pump due to the ordering $|E_{z,\mathrm{sideband}}|\ll|E_{z,\mathrm{pump}}|$) has to be considered in the nonlinear density perturbation given in section 2. Therefore, the angular frequencies in the definitions of the variables $u$ and $u'$ of the coupling function $F\left(u,u'\right)$ belong, respectively, to the LF and HF range. The orderings $|u|,|\gamma|,|\gamma'|\ll1$ hold and, for the large majority of LH waves, it is also verified that $|\omega'/\left(k_z'v_{th,e}\right)|>2$. Therefore, we obtain, neglecting second-order terms in $|u|,|\gamma|,|\gamma'|$, adopting the asymptotic expansion for $S(u')$ and the small argument approximation for $S\left(u\right)$

$$F_{\parallel}\left(u,u'\right)\cong\frac{1}{u'}\left[4u-\frac{1}{u'}-i\sqrt{\pi}\,sgn\left(k_z\right)+i\pi\frac{\nu_e}{k_zv_{th,e}}\right]. \tag{A30}$$

For a given LF spectral component (with angular frequency $\omega$, poloidal wavenumber $k_y$ and toroidal wavenumber $k_z$) any given spectral component of the LH sideband contributes twice to the integral in equation (2.46), beating with any given pump component (with angular frequency $\omega_o$, poloidal wavenumber $k_{yo}$ and toroidal wavenumber $k_{zo}$), with parallel electric field denoted as $E_{zo}$, dropping the wavenumbers indices. Let us denote $E_{z1}$ as the parallel electric field of an LH sideband spectral component with angular frequency $\omega_1=\omega-\omega_o$, poloidal wavenumber $k_{y1}=k_y-k_{yo}$ and toroidal wavenumber $k_{z1}=k_z-k_{zo}$.

The two contributions of the beating $E_{zo}E_{z1}$ comes from $\omega'=\omega_o,\ k_y'=k_{yo},\ k_z'=k_{zo}$ and$\omega'=\omega_1,\ k_y'=k_{y1},\ k_z'=k_{z1}$. Therefore, the total contribution to the integral due to the beating $E_{zo}E_{z1}$ is given by:

$$E_{zo}E_{z1}\left(\frac{F_{\parallel}\left(u,u_o\right)}{k_zk_{zo}}+\frac{F_{\parallel}\left(u,u_1\right)}{k_zk_{z1}}\right)=\frac{E_{zo}E_{z1}}{k_z}\left\{\frac{1}{u_ok_{zo}}\left[4u-\frac{1}{u_o}-i\sqrt{\pi}\,sgn\left(k_z\right)+i\pi\frac{\nu_e}{k_z\mathrm{v}_{th,e}}\right]\right.$$
$$\left.+\frac{1}{u_1k_{z1}}\left[4u-\frac{1}{u_1}-i\sqrt{\pi}\,sgn\left(k_z\right)+i\pi\frac{\nu_e}{k_z\mathrm{v}_{th,e}}\right]\right\}$$
$$\cong-E_{zo}E_{z1}\frac{\mathrm{v}_{th,e}^2}{\omega_o^2}\left[1+\mathcal{O}\left(\frac{\nu_e}{\omega_o}\right)+\mathcal{O}\left(\left|\frac{\omega}{k_z\mathrm{v}_{th,e}}\right|\right)\right]. \tag{A31}$$

In figure A1, we plot as a function of the frequency of the quasi-modes the real part of the following quantity:

$$A=\frac{\omega_o^2}{v_{th,e}^2}\left(\frac{F_{\parallel}\left(u,u_o\right)}{k_zk_{zo}}+\frac{F_{\parallel}\left(u,u_1\right)}{k_zk_{z1}}\right)\cong-1+\mathcal{O}\left(\frac{\nu_e}{\omega_o}\right)+\mathcal{O}\left(\left|\frac{\omega}{k_z\mathrm{v}_{th,e}}\right|\right). \tag{A32}$$

The plasma and RF parameters considered are summarized in table A1. These values are typical for ITER scenarios [76, 77], except obviously the parallel wavenumber of the LF quasi-modes.

The mode coupling is affected by the collisions by less than 1% concerning the real part. In figure A2, we show the imaginary part of A. It is mainly due to the correction to the approximate expression coming from the term of the order $|\omega/\left(k_z\mathrm{v}_{th,e}\right)|$. The effect of the collision is marginal and can be seen more precisely only by zooming the figure.

Let us now denote $E_{z2}$ as the parallel electric field of an LH sideband spectral component with angular frequency $\omega_2=\omega+\omega_o$, poloidal wavenumber $k_{y2}=k_y+k_{yo}$ and toroidal wavenumber $k_{z2}=k_z+k_{zo}$.

The two contributions of the beating $E_{zo}^*E_{z2}$ comes from $\omega'=-\omega_o,\ k_y'=-k_{yo},\ k_z'=-k_{zo}$ and $\omega'=\omega_2,\ k_y'=k_{y2},\ k_z'=k_{z2}$. Therefore, the total contribution to the integral due to the beating $E_{zo}^*E_{z2}$ is given by:

$$E_{zo}^*E_{z2}\left(-\frac{F_{\parallel}\left(u,u_o^*\right)}{k_zk_{zo}}+\frac{F_{\parallel}\left(u,u_2\right)}{k_zk_{z2}}\right)=\frac{E_{zo}^*E_{z2}}{k_z}\left\{-\frac{1}{u_o^*k_{zo}}\left[4u-\frac{1}{u_o^*}-i\sqrt{\pi}\,sgn\left(k_z\right)+i\pi\frac{\nu_e}{k_z\mathrm{v}_{th,e}}\right]\right.$$
$$\left.+\frac{1}{u_2k_{z2}}\left[4u-\frac{1}{u_2}-i\sqrt{\pi}\,sgn\left(k_z\right)+i\pi\frac{\nu_e}{k_z\mathrm{v}_{th,e}}\right]\right\}$$
$$\cong-E_{zo}^*E_{z2}\frac{\mathrm{v}_{th,e}^2}{\omega_o^2}\left[1+\mathcal{O}\left(\frac{\nu_e}{\omega_o}\right)+\mathcal{O}\left(\left|\frac{\omega}{k_z\mathrm{v}_{th,e}}\right|\right)\right]. \tag{A33}$$

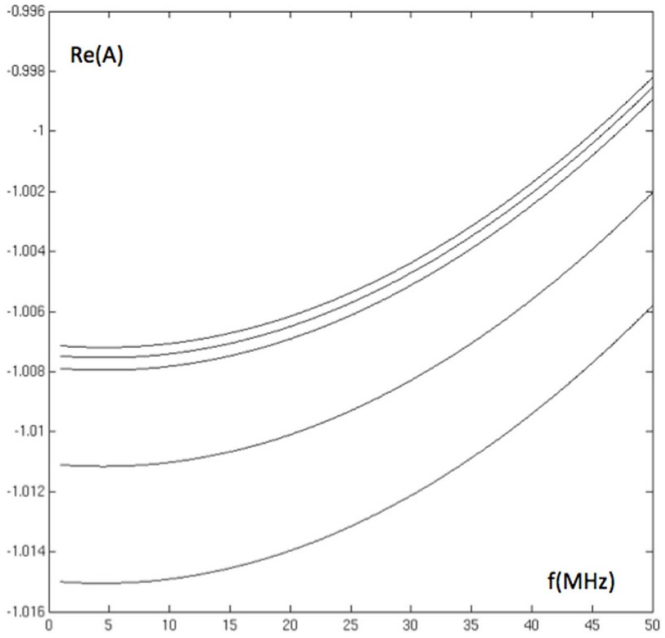


**Figure A1.** We plot the real part of the quantity A defined in equation (A31) as a function of the frequency of the quasi-modes. Plasma and RF parameters are reported in table A1. From the top curve to the bottom curve the density is increased following the values indicated in table A1, and the collision rates increase, following the set of values given in its caption.

**Table A1.** Plasma and RF parameters used in figure A1. Here, $N_{\|} = k_{\|}c/\omega_{\rm o}$, where $k_{\|}$ is the parallel wavenumber of the LF quasi-modes. The collision frequencies associated with the increasing values of the plasma density are (in $10^6$ s$^{-1}$ units) 0.216, 1.04, 2.04, 9.75 and 19.1.

| $T_e$ (eV) | $n_e$ ($10^{12}$ cm$^{-3}$) | $Z_{\rm eff}$ | $f_{\rm o}$ (GHz) | $N_{\|{\rm o}}$ | $N_{\|}$ |
|---|---|---|---|---|---|
| 11.7 | 0.1, 0.5, 1.0, 5.0, 10.0 | 1.5 | 5.0 | 1.85 | 20.0 |

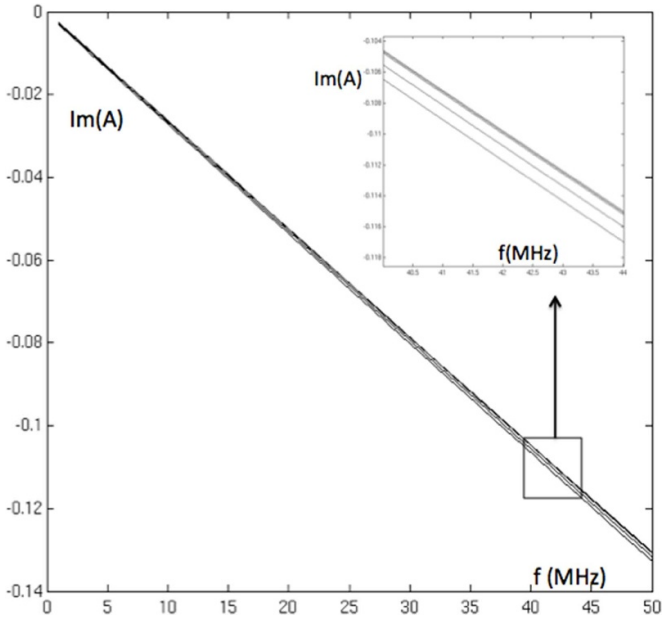


**Figure A2.** We plot the imaginary part of the quantity A defined in equation (A31) as a function of the frequency of the quasi-modes. Plasma and RF parameters are reported in table A1. From the top curve to the bottom curve the density is increased following the values indicated in table A1, so that the collision rates increase. However, their effect is marginal, of the order of 0.1% compared to Re(A) and can only be seen by zooming the figure, as in the inset shown.

Plots of the real and imaginary parts of quantity $B$ defined below accord with the same observations made concerning quantity $A$:

$$B=\frac{\omega_o^2}{\mathrm{v}_{th,e}^2}\left(-\frac{F_{\parallel}(u,u_o^*)}{k_z k_{zo}}+\frac{F_{\parallel}(u,u_2)}{k_z k_{z2}}\right)\cong -1+\mathcal{O}\left(\frac{\nu_e}{\omega_o}\right)+\mathcal{O}\left(\left|\frac{\omega}{k_z \mathrm{v}_{th,e}}\right|\right). \tag{A34}$$

We may conclude that the collisions contribute to the nonlinear electron density perturbation only marginally. The BGK operator, while conserving the necessary quantity, neglects small angle scattering and cannot predict the enhanced relaxation that occurs in the velocity ranges in which the distribution varies sharply. To account for small angle scattering by a diffusion term, a collisional operator for like particles was proposed by Dougherty [101]. In 1D velocity space, its general nonlinear form for plasma electrons is:

$$\left(\frac{\partial g}{\partial t}\right)_c=-\nu_{ee}(n,T)\frac{\partial}{\partial \mathrm{v}_z}\left[\frac{T(g)}{m}\frac{\partial g}{\partial \mathrm{v}_z}+(\mathrm{v}_z-U_z(g))\,g\right]. \tag{A35}$$

Here, the density $n$, the average velocity $U_z$ and the temperature $T$, are given respectively as:

$$n=\int_{-\infty}^{+\infty}\mathrm{dv}_z g,\; U_z=\frac{1}{n}\int_{-\infty}^{+\infty}\mathrm{dv}_z \mathrm{v}_z g,\; T=\frac{m}{n}\int_{-\infty}^{+\infty}\mathrm{dv}_z(\mathrm{v}_z-U_z(g))^2 g\,.$$

If the electron distribution can be written as $g=g_o+\delta g$ where $\delta g$ is a small perturbation and $g_o$ is the Maxwellian with density $n_{eo}$, temperature $T_e$ and zero mean velocity, then one may write the linear collisional operator as follows:

$$\left(\frac{\partial g}{\partial t}\right)_{c,D}=-\nu_{ee}(n_{eo},T_e)\frac{\partial}{\partial \mathrm{v}_z}\left[\frac{T_e}{m}\frac{\partial \delta g}{\partial \mathrm{v}_z}+\frac{\delta T}{m}\frac{\partial g_o}{\partial \mathrm{v}_z}+\mathrm{v}_z\delta g-\delta U_z g_o\right], \tag{A36}$$

where,

$$\delta T=\frac{m}{n_{eo}}\int_{-\infty}^{+\infty}\mathrm{dv}_z\left(\mathrm{v}_z{}^2-\frac{T_e}{m}\right)\delta g=\frac{m}{n_{eo}}\int_{-\infty}^{+\infty}\mathrm{dv}_z \mathrm{v}_z{}^2\delta g-\frac{T_e}{n_{eo}}n_e,$$
$$n_e=\int_{-\infty}^{+\infty}\mathrm{dv}_z\delta g,\delta U_z=\frac{1}{n_{eo}}\int_{-\infty}^{+\infty}\mathrm{dv}_z \mathrm{v}_z\delta g.$$

The 1D linear kinetic equation for the perturbed distribution $\delta g$ in the HF range with the linearized Dougherty collision operator given above is:

$$\frac{\partial \delta g}{\partial t}+\mathrm{v}_z\frac{\partial \delta g}{\partial z}-\frac{e}{m}E_{z1}\frac{\partial g_o}{\partial \mathrm{v}_z}=\left(\frac{\partial g}{\partial t}\right)_{c,D}. \tag{A37}$$

For monochromatic waves $E_{z1}=A_{z1}\exp[-i(\omega_1 t-\boldsymbol{k}_1\cdot\boldsymbol{r})]$ we have:

$$-i(\omega_1-k_{z1}v_z)\,\delta g+2\frac{e}{m}A_{z1}\frac{\mathrm{v}_z}{\mathrm{v}_{th,e}^2}g_o=-\nu_{ee}\frac{\partial}{\partial \mathrm{v}_z}\left[\frac{T_e}{m}\frac{\partial \delta g}{\partial \mathrm{v}_z}+\frac{\delta T}{m}\frac{\partial g_o}{\partial \mathrm{v}_z}+\mathrm{v}_z\delta g-\delta U_z g_o\right]. \tag{A38}$$

We define the variable $z=\mathrm{v}_z/\mathrm{v}_{th,e}$ and the parameter $u=\omega_1/(k_{z1}\mathrm{v}_{th,e})$, so the above equation can be rewritten in term of dimensionless perturbed distribution $\delta f(z)=\mathrm{v}_{th,e}\delta g(\mathrm{v}_{th,e}z)/n_{eo}$. We obtain:

$$(z-u)\,\delta f-\frac{2ieA_{z1}}{mk_{z1}\mathrm{v}_{th,e}^2}\frac{1}{\sqrt{\pi}}ze^{-z^2}=i\frac{\nu_{ee}}{k_{z1}\mathrm{v}_{th,e}}\left[\frac{1}{2}\frac{\partial^2}{\partial z^2}\delta f+\frac{\partial}{\partial z}z\delta f+\frac{\delta T}{2T_e}\frac{1}{\sqrt{\pi}}\frac{\partial^2 e^{-z^2}}{\partial z^2}-\frac{\delta U_z}{\mathrm{v}_{th,e}}\frac{1}{\sqrt{\pi}}\frac{\partial e^{-z^2}}{\partial z}\right]. \tag{A39}$$

In terms of the perturbed distribution function $\delta f$ the quantities $\delta T/(2T_e)$ and $\delta U_z/v_{th}$ are, respectively:

$$\frac{\delta T}{2T_e}=\int_{-\infty,\mathcal{L}}^{+\infty}dz\,z^2\delta f-\frac{n_e}{2n_{eo}},\;\frac{\delta U_z}{\mathrm{v}_{th,e}}=\int_{-\infty,\mathcal{L}}^{+\infty}dz\,z\,\delta f,\;\frac{n_e}{n_{eo}}=\int_{-\infty,\mathcal{L}}^{+\infty}dz\,\delta f. \tag{A40}$$

The Landau prescription, suggested above by the symbol $\mathcal{L}$ in the integrals above, must be used to treat the possible poles of $\delta f$. The integro-differential equation for the perturbed distribution $\delta f$ should be solved with the boundary conditions $\lim_{z\to+\infty}\delta f = \lim_{z\to-\infty}\delta f = 0$. However, an approximate solution can be obtained considering that the collision operator on the r.h.s. of equation (A36) is a small perturbation of the operator on the l.h.s. due to the ordering $\nu_{ee} \ll |k_{z1}|\, v_{th}$. Therefore, the solution of equation (A36) up to the zero order in the small parameter $\gamma_{ee} = \nu_{ee}/\left(|k_{z1}|\, \mathrm{v}_{th,e}\right) \ll 1$ is:

$$\delta f^{(o)} = a_{z1}\frac{1}{\sqrt{\pi}}\frac{z e^{-z^2}}{z-u}, \quad \text{where } a_{z1} = \frac{2ieA_{z1}}{mk_{z1}\mathrm{v}_{th,e}^2}. \tag{A41}$$

The solution correct up to the first order in $\gamma_{ee}$ is obtained by replacing $\delta f$ with $\delta f^o$ on the r.h.s of equation (A39) and in the integrals in equation (A39).

Therefore, we obtain:

$$\delta f^{(1)} = \delta f^{(o)} + i\frac{\gamma_{ee}}{z-u}\left[\frac{1}{2}\frac{\partial^2}{\partial z^2}\delta f^{(o)} + \frac{\partial}{\partial z}z\delta f^{(o)} + \left(\frac{\delta T}{2T_e}\right)^{(o)}\frac{1}{\sqrt{\pi}}\frac{\partial^2 e^{-z^2}}{\partial z^2} - \left(\frac{\delta U_z}{\mathrm{v}_{th,e}}\right)^{(o)}\frac{1}{\sqrt{\pi}}\frac{\partial e^{-z^2}}{\partial z}\right], \tag{A42}$$

where,

$$\left(\frac{\delta T}{2T_e}\right)^{(o)} = \int_{-\infty,\mathcal{L}}^{+\infty} dz\, z^2\, \delta f^{(o)} - \frac{1}{2}\left(\frac{n_e}{n_{eo}}\right)^{(o)}, \quad \left(\frac{\delta U_z}{\mathrm{v}_{th,e}}\right)^{(o)} = \int_{-\infty,\mathcal{L}}^{+\infty} dz\, z\, \delta f^{(o)}, \quad \left(\frac{n_e}{n_{eo}}\right)^{(o)} = \int_{-\infty,\mathcal{L}}^{+\infty} dz\, \delta f^{(o)}.$$

The Landau prescription must be used to treat the pole of $\delta f^{(o)}$. We can now calculate the normalized perturbed density correct up to the first order in $\gamma_{ee}$, and obtain:

$$\left(\frac{n_e}{n_{eo}}\right)^{(1)} = a_{z1}\mathcal{J}_1 + i\gamma_{ee}a_{z1}\left[-u\frac{1}{2}\frac{\mathrm{d}^2}{\mathrm{d}u^2}\mathcal{J}_1 - u\frac{1}{6}\frac{\mathrm{d}^3}{\mathrm{d}u^3}\mathcal{J}_o + \left(\mathcal{J}_3 - \frac{1}{2}\mathcal{J}_1\right)(4\mathcal{J}_2 - 2\mathcal{J}_o) + 2\mathcal{J}_2\mathcal{J}_1\right]. \tag{A43}$$

As discussed above, the collisional damping can be obtained neglecting the electron Landau damping, i.e. within the limit $u \gg 1$, so that the asymptotic expansion of the plasma dispersion function holds. We recall that,

$$\mathcal{J}_1 \cong -\frac{1}{2u^2}. \tag{A44}$$

In addition, we have:

$$\mathcal{J}_3 - \frac{1}{2}\mathcal{J}_1 \cong -\frac{1}{2u^2}, \tag{A45}$$

$$4\mathcal{J}_2 - 2\mathcal{J}_o = 0, \tag{A46}$$

$$2\mathcal{J}_2\mathcal{J}_1 \cong \frac{1}{2u^3}, \tag{A47}$$

$$\frac{\mathrm{d}^2}{\mathrm{d}u^2}\mathcal{J}_1 \cong -\frac{3}{u^4}, \tag{A48}$$

$$\frac{\mathrm{d}^3}{\mathrm{d}u^3}\mathcal{J}_o \cong \frac{6}{u^4}. \tag{A49}$$

Therefore,

$$-u\frac{1}{2}\frac{\mathrm{d}^2}{\mathrm{d}u^2}\mathcal{J}_1 - u\frac{1}{6}\frac{\mathrm{d}^3}{\mathrm{d}u^3}\mathcal{J}_o \cong \frac{1}{2u^3}. \tag{A50}$$

We thus obtain:

$$-u\frac{1}{2}\frac{\mathrm{d}^2}{\mathrm{d}u^2}\mathcal{J}_1 - u\frac{1}{6}\frac{\mathrm{d}^3}{\mathrm{d}u^3}\mathcal{J}_o + \left(\mathcal{J}_3 - \frac{1}{2}\mathcal{J}_1\right)(4\mathcal{J}_2 - 2\mathcal{J}_o) + 2\mathcal{J}_2\mathcal{J}_1 \cong \frac{1}{u^3}. \tag{A51}$$

The density perturbation up to the first order in $\gamma_{ee}$ is thus given by:

$$\left(\frac{n_e}{n_{eo}}\right)^{(1)} = -\frac{2ieA_{z1}}{mk_{z1}\mathrm{v}_{th,e}^2}\left(\frac{1}{2u^2} - i\gamma_{ee}\frac{1}{u^3}\right). \tag{A52}$$

The wave equation gives, within the electrostatic limit:

$$k^2A_{z1} - 4\pi\, ik_{z1}e\left[-in_{eo}\frac{eA_{z1}}{m}\frac{k_{z1}}{\omega_1^2} - n_{eo}\frac{\nu_{ee}}{\omega_1}\frac{eA_{z1}k_{z1}}{m\omega_1^2}\right] = 0. \tag{A53}$$

This equation can be cast in the form of the dispersion equation:

$$\varepsilon_1 A_{z1} = 0, \tag{A54}$$

where the dielectric function is:

$$\varepsilon_1 = 1 - \frac{\omega_{pe}^2}{\omega_1^2}\frac{k_{z1}^2}{k^2} + i\frac{\omega_{pe}^2k_{z1}^2}{k^2\omega_1^2}\frac{\nu_{ee}}{\omega_1}. \tag{A55}$$

The relevant damping rate, calculated as usual by the perturbation theory, is $\nu_{ee}/2$. To summarize the results of this appendix, the simple BGK operator used in our kinetic equation seems appropriate to describe the effects of the collisions in the nonlinear LH wave physics. The collisions do not affect significantly both the linear LF electron response and the nonlinear LF electron density perturbation. Their role is marginal for LH pump power much larger than the threshold for the onset of PI. However, the latter is determined by the collisions, due to the PI quenching effect produced by the collisional damping. It is thus reasonable to assume that the collisions play an important role in the nonlinear LH physics for sufficiently low LH pump power, near the PI threshold and that they affect the LH nonlinear physics through the collisional damping. The particle-conserving BGK operator proposed in our kinetic model provides a collisional damping rate of $\nu_e/2$, which is in agreement with the value $\nu_{ei}/2$ obtained by the model of collisions implemented in the numerical code GENRAY, if the characteristic collision rate $\nu_e$ coincides with $\nu_{ei}$. A more complex and accurate BGK collision operator, which conserves both the energy and the number of particles, gives the same collisional damping with respect to the simpler operator proposed in our kinetic model.

A 1D linearized Dougherty collisional operator, which describes the like particle collisions, including small scattering effects and particle diffusion, gives a collisional damping equal to $\nu_{ee}/2$. This result can easily be incorporated in our model, if we assume that $\nu_e = \nu_{ei} + \nu_{ee}$. In the same vein, by defining $\nu_e = \nu_{ei} + \nu_{ee} + \nu_{en}$, we can also include the effects of the collisions with the neutrals by introducing the electron-neutral characteristic collision rate $\nu_{en}$.

## Appendix B. Drift waves

The drift waves are quasi-electrostatic normal plasma modes that propagate mainly in the poloidal plane with angular frequency $\omega \cong \omega_e^*$, where $\omega_e^* = k_y\mathrm{v}_{th,e}^2/(2L_n|\Omega_e|)$ is the electron diamagnetic drift angular frequency. $L_n$ is the characteristic length of variation of the density. Their wavenumbers are such that $|k_z|\,\mathrm{v}_i \ll |\omega| \ll |k_z|\,\mathrm{v}_e$ and $0.1\rho_i^{-1} < |k_y| < \rho_i^{-1}$, for the main ion species $i$. We observe that the drift waves can provide, in principle, an efficient channel of PI for LH waves [15]. However, for LHCD experiments in tokamaks, they are not considered in the archived literature. The following qualitative analysis suggests indeed that the coupling of the LH sidebands with the pump wave, as driven by drift waves, is poor. The above ordering $\rho_i^{-1} > |k_y| > 0.1\ \rho_i^{-1}$ indicates indeed that the drift waves are characterized by relative large poloidal wave number. The perpendicular wavenumber $\boldsymbol{k}_{o\perp}$ of the LH pump wave is usually aligned in the radial direction to maximize the power density flow towards the plasma core. Therefore, due to the matching condition $\boldsymbol{k}_s = \boldsymbol{k} \pm \boldsymbol{k}_o$ the LH sidebands nonlinearly coupled to the pump wave should have perpendicular wavenumbers in practice aligned in the poloidal direction in the low-density peripheral plasma near the LH launcher. These sidebands propagate mainly in the poloidal plane, so that PIs are strongly limited due to the convective losses and the fact that the LH sidebands quickly propagate outside the region illuminated by the LH antenna, and thus the wave-wave interaction quenches. We also observe that the LF linear response of both the electrons and ions should include, in principle, the effects of the density gradient through the diamagnetic drift angular frequencies.

The ion scalar susceptibility should be defined as [15],

$$\chi_i = \frac{1}{k^2\lambda_{D,i}^2}\left[1 + \frac{\omega - \omega_i^*}{k_z\mathrm{v}_{th,i}}\sum_{n=-\infty}^{+\infty} S\left(\frac{\omega - n\Omega_i}{k_z\mathrm{v}_{th,i}}\right) I_n(\lambda_i)\, e^{-\lambda_i}\right], \tag{B1}$$

where $\omega_i^* = k_y\mathrm{v}_{th,i}^2/(2L_n\Omega_i)$ is the ion diamagnetic drift angular frequency. The model constraint $\delta \ll 1$ implies $|k_y| \ll k_\perp$, so that $|\omega_i^*| \ll k_\perp\rho_e\mathrm{v}_{th,e}\tau/(2Z_iL_n)$, where $\tau = T_i/T_e$ is in the range of a few units and $Z_i$ is the ion charge, which is one for

the hydrogen isotopes that are the main ion species. In peripheral tokamak plasmas, with magnetic field of the order of 4 T, maximum electron temperature of the order of 50 eV, $L_n$ of the order of 1 cm and $k_\perp$ not exceeding the order of 100 $\mathrm{cm}^{-1}$, the order of magnitude of $k_\perp \rho_e \mathrm{v}_{th,e} \tau / (2 Z_i L_n)$ is not larger than 0.5 $10^6$ $\mathrm{rad\,s}^{-1}$, so that $|\omega_i^*| / (2\pi) \ll 0.1$ MHz, i.e. a frequency negligible compared to the typical frequency of the LF quasi-modes driven by LH waves. The electron susceptibility should be defined as [15],

$$\chi_e = \frac{1}{k^2 \lambda_{D,e}^2} \left[ 1 + \frac{\omega + \omega_e^*}{k_z \mathrm{v}_{th,e}} \sum_{n=-\infty}^{+\infty} S\left( \frac{\omega - n\Omega_e}{k_z \mathrm{v}_{th,e}} \right) I_n(\lambda_e) e^{-\lambda_e} \right]. \tag{B2}$$

The electron diamagnetic drift frequency is also much less than 0.1 MHz. Therefore, to evaluate the LF linear electron and ion density perturbations the effects of the diamagnetic drift frequency can be neglected.

## Appendix C. LH waves for dominant parallel dynamics of the electrons and fixed ion background

If the perpendicular dynamics of the electrons is neglected, kinetic equation (2.7) can be solved by application of the operators $\mathcal{F}$ and $\mathcal{I}_\perp$. As a result we obtain:

$$g^{HF(1)}_{e;\omega,k_y,k_z} = 2i\eta \frac{n_{eo}}{\mathrm{v}_{th,e}} \frac{\omega_o}{k_z \mathrm{v}_{th,e}} \frac{1}{\sqrt{\pi}} \frac{\zeta e^{-\zeta^2}}{\zeta - u_e} \tilde{E}^{HF}_{z;\omega,k_y,k_z} - \frac{i\nu_e}{k_z \mathrm{v}_{th,e}^2} \frac{n_e^{(1)}}{\sqrt{\pi}} \frac{e^{-\zeta^2}}{\zeta - u_e}, \tag{C1}$$

where $g^{HF(1)}_{e;\omega,k_y,k_z} = \mathcal{F}\mathcal{I}_\perp f_e^{HF(1)}$, $\zeta = \mathrm{v}_z / \mathrm{v}_{th,e}$ and $u_e = (\omega + i\nu_e) / (k_z \mathrm{v}_{th,e})$. The perturbed density at the first order in $\eta$ is obtained by integration in the 1D velocity space, following the Landau prescription concerning the pole at the denominator.

As a result, we have:

$$n^{HF(1)}_{e;\omega,k_y,k_z} = \frac{2i\eta n_{eo}}{1 + i\gamma_e S_\sigma(u)} \frac{\omega_o}{k_z \mathrm{v}_{th,e}} \left[ 1 + u_e S_\sigma(u_e) \right] \tilde{E}^{HF}_{z;\omega,k_y,k_z}. \tag{C2}$$

The electron charge density perturbation is $\rho^{HF(1)}_{e;\omega,k_y,k_z} = -e n^{HF(1)}_{e;\omega,k_y,k_z}$ and the toroidal electron current density as deduced from the charge conservation, is:

$$J^{HF(1)}_{e;\omega,k_y,k_z} = -e \frac{\omega}{k_z} n^{HF(1)}_{e;\omega,k_y,k_z}. \tag{C3}$$

The charge density perturbation and the toroidal current density perturbation of the electrons at the first order in $\eta$ have been calculated by a method also valid for inhomogeneous plasma and coincide with the corresponding quantities evaluated in section 2 by a different method, within the limit of negligible perpendicular dynamics of the electrons.

The Maxwell equations, as written in Gaussian units, with the effects of a plasma medium embedded in the current density and in the charge density, give the local energy conservation law:

$$\nabla \cdot \boldsymbol{P} + \frac{\partial W}{\partial t} + \boldsymbol{E} \cdot \boldsymbol{J} = 0. \tag{C4}$$

Here, $\boldsymbol{P} = c\ (\boldsymbol{E} \times \boldsymbol{B}) / 4\pi$ is the Poynting vector and $W = \left( E^2 + B^2 \right) / 8\pi$ is the energy density of the electromagnetic field. In equation (D1) all the vector and scalar quantities are real. Within the frame of the spectral analysis, these quantities, here indicated by the function $\psi(r,t)$, are given by the inverse Fourier transforms:

$$\psi(\boldsymbol{r},t) = \int\int\int \mathrm{d}\omega\, \mathrm{d}k_y\, \mathrm{d}k_z\, \psi_{\omega,k_y,k_z}(x)\, e^{-i(\omega t - k_y y - k_z z)}. \tag{C5}$$

The Fourier transforms $\psi_{\omega,k_y,k_z}(x)$ are defined as in equation (2.2) of section 2, where the adopted plasma slab geometry is defined. Although no explicit indication is provided, the boundary values of the integrals are intended hereinafter as defined in section 2. For $\psi(r,t)$ real $\psi_{-\omega,-k_y,-k_z} = \psi^*_{\omega,k_y,k_z}$. The steady-state condition, implicit above for real $\omega$, implies that the integral of the energy density in the poloidal plane $YZ$ is constant, namely:

$$\iint \mathrm{d}\, y \mathrm{d}\, z \frac{\partial W}{\partial t} = 0. \tag{C6}$$

We can thus derive from the energy conservation an equation for the energy flux across a poloidal plane, during a time interval $T$ (centered on an instant $t$), which we assume to be much larger than any period of the HF electromagnetic field:

$$\int_{t-T/2}^{t+T/2} \mathrm{d}\tau \iint \mathrm{d}y\,\mathrm{d}z \frac{\partial P_x}{\partial x} = -\int_{t-\frac{T}{2}}^{t+\frac{T}{2}} \mathrm{d}\tau \iint \mathrm{d}y\,\mathrm{d}z\, \boldsymbol{E}\cdot\boldsymbol{J}. \tag{C7}$$

We observe that,

$$\iint \mathrm{d}y\,\mathrm{d}z \nabla\cdot\boldsymbol{P} = \iint \mathrm{d}y\ \mathrm{d}z \frac{\partial P_x}{\partial x}. \tag{C8}$$

Here, we also assume that $T$ is much larger than any period of the HF electromagnetic field but much lower than any LF period. We recall that the periodic structure in the LF range emerges from the beating of HF waves. Performing the space-time integrals indicated above (D1) by means of the spectral analysis, we thus obtain for the time interval $T$:

$$\frac{\partial}{\partial x}\langle P_x\rangle = -(2\pi)^3 \int\int\int \mathrm{d}\omega\,\mathrm{d}k_y\,\mathrm{d}k_z \boldsymbol{E}_{\omega,k_y,k_z}(x)\cdot\boldsymbol{J}^*_{\omega,k_y,k_z}(x). \tag{C9}$$

Here, the angular frequency integral is limited to the HF range and we define,

$$\langle P_x\rangle = \int_{t-\frac{T}{2}}^{t+\frac{T}{2}} \mathrm{d}\tau \int\int dy\,dz P_x = 2\pi^2 c \int\int\int \mathrm{d}\omega\,\mathrm{d}k_y\,\mathrm{d}k_z \left[\boldsymbol{E}_{\omega,k_y,k_z}(x) \times \boldsymbol{B}^*_{\omega,k_y,k_z}(x)\right]_x. \tag{C10}$$

We also consider electromagnetic fields given by a superposition of discrete monochromatic waves, i.e. with real components of the form:

$$\psi(\boldsymbol{r},t) = \frac{1}{2}\sum_{\omega,k_y,k_z}\left[\psi_{\omega,k_y,k_z}(x)\ e^{-i(\omega t-k_y y-k_z z)} + c.c\right], \tag{C11}$$

where the symbol $c.\,c.$ indicates, as usual, the complex conjugate of the term on the left and $\psi_{\omega,k_y,k_z}(x)$ is the complex amplitude.

In this case, we obtain the following from equation (C4):

$$\frac{\partial}{\partial x}\langle P_x\rangle = -\frac{1}{4}\sum_{\omega,k_y,k_z}\left[\boldsymbol{E}_{\omega,k_y,k_z}(x)\cdot\boldsymbol{J}^*_{\omega,k_y,k_z}(x) + c.c.\right]. \tag{C12}$$

Here,

$$\langle P_x\rangle = \frac{1}{TL_yL_z}\int_{-T/2}^{T/2}\mathrm{d}t\int_{-L_y/2}^{+L_y/2}\mathrm{d}y\int_{-L_z/2}^{+L_z/2}\mathrm{d}z P_x(\boldsymbol{r},t) = \frac{c}{16\pi}\sum_{\omega,k_y,k_z}\left\{\left[\boldsymbol{E}_{\omega,k_y,k_z}(x)\times\boldsymbol{B}^*_{\omega,k_y,k_z}(x)\right]_x + c.c.\right\}. \tag{C13}$$

We recall that the time interval $T$ is much larger than the periods of the HF monochromatic waves and much lower than the LF periods and that the lengths $L_y$ and $L_z$ are much larger, respectively, of the HF poloidal and toroidal wavelengths. The Maxwell equations can be used to obtain the full electromagnetic field from the toroidal components within the framework of the slab model adopted and the condition that the current density is parallel to the static magnetic field, which is fulfilled in the HF range within the model hypothesis discussed in section 2. To this end, we first consider the Maxwell equations that do not contain the charge density and the toroidal current density, namely:

$$ik_yE_z - ik_zE_y = i(\omega/c)B_x, \tag{C14}$$
$$ik_zE_x - \partial_xE_z = i(\omega/c)B_y, \tag{C15}$$
$$-ik_yE_x + \partial_xE_y = i(\omega/c)B_z, \tag{C16}$$
$$ik_yB_z - ik_zB_y = -i(\omega/c)E_x, \tag{C17}$$
$$ik_zB_x - \partial_xB_z = -i(\omega/c)E_y. \tag{C18}$$

Equations (C14)–(C16) are obtained by the Faraday equation; equations (C17) and (C18) are obtained by the Ampere–Maxwell law, considering only the components along X and Y, respectively, and considering that the relevant current density

is negligible, namely $J_x = J_y = 0$. The plasma ions, within the model constraints, are considered as a fixed neutralizing background in the HF range. Equations (C14)–(C18) hold both for Fourier transformed quantities and for discrete monochromatic electromagnetic field components. We first express the X and Y components of the electromagnetic field in terms of $E_z$, $B_z$ and their derivatives with respect to $x$. From equation (C15), we have:

$$E_x = -\left(i/k_z\right)\partial_x E_z + \left(1/N_z\right)B. \tag{C19}$$

Substituting this expression in equation (C17) we obtain:

$$B_y = \frac{1}{N_z^2 - 1}\left[N_y N_z B_z - \frac{ic}{\omega}\partial_x E_z\right], \tag{C20}$$

and equation (C19) gives:

$$E_x = \frac{1}{N_z^2 - 1}\left[N_y B_z - \frac{ic}{\omega}N_z \partial_x E_z\right]. \tag{C21}$$

From equation (C14) we have:

$$E_y = \left(k_y/k_z\right)E_z - \left(1/N_z\right)B_x\,. \tag{C22}$$

Substituting this expression in equation (C18) we obtain:

$$B_x = -\frac{1}{N_z^2 - 1}\left[N_y E_z + \frac{ic}{\omega}N_z \partial_x B_z\right], \tag{C23}$$

and equation (C22) gives:

$$E_y = \frac{1}{N_z^2 - 1}\left[N_y N_z E_z + \frac{ic}{\omega}\partial_x B_z\right]. \tag{C24}$$

We then substitute $E_x$ from equation (C21) and $E_y$ from equation (C24) in equation (C16) and obtain:

$$\partial_x^2 B_z = \frac{\omega^2}{c^2}\left(N_z^2 + N_y^2 - 1\right)B_z. \tag{C25}$$

The HF fields require $N_z^2 \geqslant N_{z,\,crit}^2 > 1$ where $N_{z,\mathrm{crit}}$ is the critical parallel refractive index so that the mode conversion of LH waves into whistler waves occurs (we have assumed that $|N_z| > 1.5$) so that equation (C25) only admits evanescent solutions. Unphysical growing solutions are not considered.

They occur and are discarded, for example, also when the cold plasma dispersion equation gives negative values for the squared perpendicular refractive index. We also exclude evanescent solutions and obtain $B_z = 0$.

Therefore, the electromagnetic field can be expressed in terms of $E_z$ and $\partial_x E_z$ utilizing equations (C20), (C21), (C23) and (C24):

$$B_x = -\frac{N_y E_z}{N_z^2 - 1}, \tag{C26}$$

$$B_y = -\frac{i\left(c/\omega\right)}{N_z^2 - 1}\partial_x E_z, \tag{C27}$$

$$B_z = 0, \tag{C28}$$

$$E_x = -\frac{i\left(c/\omega\right)}{N_z^2 - 1}N_z \partial_x E_z, \tag{C29}$$

$$E_y = \frac{N_y N_z E_z}{N_z^2 - 1}. \tag{C30}$$

Taking into account equations (C26)–(C30), the Maxwell equations also provide the wave equation in the HF range for $E_z$, namely:

$$\frac{\mathrm{d}^2 E_{z;\omega,k_y,k_z}}{\mathrm{d}x^2} = \left(k_y^2 + k_z^2 - \frac{\omega^2}{c^2}\right)E_{z;\omega,k_y,k_z} + \frac{4\pi i}{k_z}\left(k_z^2 - \frac{\omega^2}{c^2}\right)\rho_{e;\omega,k_y,k_z}^{HF(1)}. \tag{C31}$$

This equation is identical to equation (2.26) of section 2.

We can express the average $x$-component of the Poynting vector, as defined in (C10) considering Fourier transforms, in terms of the toroidal electric field only:

$$\langle P_x\rangle = -2\pi^2 c\int\int\int \mathrm{d}\omega\,\mathrm{d}k_y\,\mathrm{d}k_z\,\frac{i\,(c/\omega)}{n_z^2-1}E_{z;\omega,k_y,k_z}\partial_x E^*_{z;\omega,k_y,k_z}. \tag{C32}$$

From equation (C10), since $J_x = J_y = 0$, we obtain:

$$\frac{\partial}{\partial x}\langle P_x\rangle = -(2\pi)^3\int\int\int \mathrm{d}\omega\,\mathrm{d}k_y\,\mathrm{d}k_z\,E_{z;\omega,k_y,k_z}(x)\,J^*_{z;\omega,k_y,k_z}(x)\,. \tag{C33}$$

Due to the charge conservation we obtain:

$$\frac{\partial}{\partial x}\langle P_x\rangle = -(2\pi)^3\int\int\int \mathrm{d}\omega\,\mathrm{d}k_y\,\mathrm{d}k_z\,E_{z;\omega,k_y,k_z}(x)\,\frac{\omega}{k_z}\,\rho^*_{z;\omega,k_y,k_z}(x)\,. \tag{C34}$$

Following the same method, we can derive the conservation equation of the power density radial flow for electromagnetic fields, charge and current densities given by a superposition of discrete waves of the following form:

$$\psi(\boldsymbol{r},t) = \frac{1}{2}\sum_{\omega,k_y,k_z}\left[\psi_{\omega,k_y,k_z}(x)\;e^{-i(\omega t-k_y y-k_z z)} + c.c\right]. \tag{C35}$$

In this case, the radial component of the average Poynting vector is:

$$\begin{aligned}\langle P_x\rangle &= \frac{c}{16\pi}\sum_{\omega,k_y,k_z}\left\{\left[\boldsymbol{E}_{\omega,k_y,k_z}(x)\times\boldsymbol{B}^*_{\omega,k_y,k_z}(x)\right]_x + c.c.\right\}\\ &= -\frac{c}{16\pi}\sum_{\omega,k_y,k_z}\left\{E_{z;\omega,k_y,k_z}(x)\;\frac{i\,(c/\omega)}{n_z^2-1}\partial_x E^*_{z;\omega,k_y,k_z}(x) + c.c.\right\},\end{aligned} \tag{C36}$$

and the relevant conservation law is:

$$\frac{\partial}{\partial x}\langle P_x\rangle = -\frac{1}{4}\sum_{\omega,k_y,k_z}\left[E_{z;\omega,k_y,k_z}(x)\;J^*_{z;\omega,k_y,k_z}(x) + c.c.\right]. \tag{C37}$$

Taking into account the charge conservation we obtain:

$$\frac{\partial}{\partial x}\langle P_x\rangle = -\frac{1}{4}\sum_{\omega,k_y,k_z}\left[E_{z;\omega,k_y,k_z}(x)\;\frac{\omega}{k_z}\rho^*_{\omega,k_y,k_z}(x) + c.c.\right]. \tag{C38}$$

This equation has to be verified by the numerical solutions $E_{z;\,\omega,k_y,k_z}(x)$ of the set of nonlinear integro-differential LH wave equations. If the power absorption due to the electron Landau damping or the collisional damping can be neglected, the power of the sideband waves increases at the expense of the injected 'pump' waves, and $\langle P_x\rangle = const.$

For quasi-uniform plasma, such that the eikonal approximation holds, the electromagnetic fields can be expressed as a superposition of quasi-monochromatic components in the following form:

$$\psi(\boldsymbol{r},t) = \frac{1}{2}\sum_{\omega,k_x,k_y,k_z}\left[\psi_{\omega,k_x,k_y,k_z}(x)\;e^{-i(\omega t-S(x)-k_y y-k_z z)} + c.c\right], \tag{C39}$$

where the eikonal function $S(x)$ is real and $\partial_x E^*_{z;\omega,k_y,k_z} \cong -ik_x E^*_{z;\omega,k_x,k_y,k_z}$, with $k_x = \partial S/\partial x$.

Therefore, in this case,

$$\langle P_x\rangle \cong -\frac{c}{8\pi}\sum_{\omega,k_x,k_y,k_z}\frac{N_x}{N_z^2-1}\left|E_{z;\omega,k_x,k_y,k_z}\right|^2. \tag{C40}$$

Moreover, $N_x = k_x c/\omega$ is real and, for normal plasma modes, is obtained as a function of $\omega, k_y, k_z$ and $x$ by the local linear dispersion equation based on the Hermitian part of the dielectric tensor. For inward power density flow $N_x < 0$.

## ORCID iDs

C Castaldo https://orcid.org/0000-0003-2869-393X
F Napoli https://orcid.org/0000-0002-7606-8488

## References

[1] Friedberg J 2007 *Plasma Physics and Fusion Energy* (Cambridge University Press)
[2] Fisch N J 1978 *Phys. Rev. Lett.* **41** 873
[3] Fisch N J 1987 *Rev. Mod. Phys.* **59** 175
[4] Bernabei S *et al* 1982 *Phys. Rev. Lett.* **49** 1255
[5] Porkolab M *et al* 1984 *Phys. Rev. Lett.* **53** 450
[6] Karney C, Fisch N J and Jobes F C 1985 *Phys. Rev.* A **32** 2554
[7] Cardinali A *et al* 2018 *Sci. Rep.* **8** 10318
[8] Pericoli-Ridolfini V *et al* 1999 *Phys. Rev. Lett.* **82** 93
[9] Kirov K K *et al* 2009 LH wave absorption and current drive studies by application of modulated LHCD at JET *Proc. 36th European Phys. Society Conf. on Plasma Physics (Sofia Bulgaria)*
[10] Wallace G *et al* 2009 Observation of lower hybrid wave absorption in the scrape-off layer of a diverted tokamak *Proc. 18th Topical Conf.* (*Gent, Belgium*) (*Radiofrequency Power in Plasmas*) ed V Bobkov and J M Noterdaeme (AIP) p 395
[11] Cesario R *et al* 2010 *Nat. Commun.* **1** 55
[12] Wallace G M *et al* 2011 *Nucl. Fusion* **51** 083032
[13] Baek S G *et al* 2018 *Phys. Rev. Lett.* **121** 055001
[14] Porkolab M 1974 *Phys. Fluids* **17** 1432
[15] Liu C S and Tripathi V K 1986 *Phys. Rep.* **130** 143
[16] Stix T H 1965 *Phys. Rev. Lett.* **15** 878
[17] Karney C F F 1979 *Phys. Fluids* **22** 2188
[18] Porkolab M, Bernabei S, Hooke W M, Motley R W and Nagashima T 1977 *Phys. Rev. Lett.* **38** 230
[19] Takase Y, Porkolab M, Schuss J J, Watterson R L, Fiore C L, Slusher R E and Surko C M 1985 *Phys. Fluids* **28** 983
[20] Castaldo C, Lazzaro E, Lontano M and Sergeev A M 1997 *Phys. Lett.* A **230** 336
[21] Cesario R, Cardinali A, Castaldo C, Paoletti F and Mazon D 2004 *Phys. Rev. Lett.* **92** 175002
[22] Brambilla M 1976 *Nucl. Fusion* **16** 47
[23] Irzak M A and Shcherbinin O N 1995 *Nucl. Fusion* **35** 1341
[24] Milanesio D *et al* 2007 TOLPHA: an accurate and efficient numerical tool for analysis and design of LH antennas *AIP Conf. Proc.* **933** 301
[25] Hillairet J, Voyer D, Ekedahl A, Goniche M, Kazda M, Meneghini O, Milanesio D and Preynas M 2010 *Nucl. Fusion* **50** 125010
[26] Preinhaelter J, Urban J, Vahala L and Vahala G 2012 *Nucl. Fusion* **52** 083005
[27] Watterson R, Takase Y, Bonoli P T, Porkolab M, Slusher R E and Surko C M 1985 *Phys. Fluids* **28** 2622
[28] Ceccuzzi S *et al* 2011 Validation of lower hybrid coupling codes (Brambilla, GRILL3D-U, TOLPHA) with the FTU conventional grill *38th EPS Conf. on Plasma Physics* p 1.097
[29] Ignat D W 1981 *Phys. Fluids* **24** 1110
[30] Bonoli P T and Ott E 1982 *Phys. Fluids* **25** 359
[31] Bonoli P T 1984 *IEEE Trans. Plasma Sci.* **PS-12** 95
[32] Bonoli P T and Englade R C 1986 *Phys. Fluids* **29** 2937
[33] Bonoli P T, Porkolab M, Takase Y and Knowlton S F 1988 *Nucl. Fusion* **28** 991
[34] Peysson Y *et al* 2016 *Plasma Phys. Control. Fusion* **58** 044008
[35] Bernstein I 1975 *Phys. Fluids* **18** 320
[36] Takahashi H 1994 *Phys. Plasmas* **1** 2254
[37] Esterkin A R and Piliya A D 1992 *Nucl. Fusion* **32** 927
[38] Esterkin A R and Piliya A D 1992 *Plasma Phys. Control. Fusion* **34** 1957
[39] Kupfer J P and Moreau D 1992 *Nucl. Fusion* **32** 1845
[40] Bizarro J P 1993 *Nucl. Fusion* **33** 831
[41] Kupfer K, Moreau D and Litaudon X 1993 *Phys. Fluids* B **5** 1227
[42] Kupfer K, Moreau D and Litaudon X 1993 *Phys. Fluids* B **5** 4391
[43] Bizarro J P, Ferreira J S, Rodrigues P, Arslanbekov R and Peysson Y 1995 *Phys. Rev. Lett.* **75** 1308
[44] Peysson Y, Arslanbekov R, Basiuk V, Carrasco J, Litaudon X, Moreau D and Bizarro J P 1996 *Phys. Plasmas* **3** 3668
[45] Bizarro J P S, Ferreira J S and Nakach R 1999 *Phys. Plasmas* **6** 1131
[46] Pereverzev G 1992 *Nucl. Fusion* **32** 1091
[47] Wright J C *et al* 2005 *Nucl. Fusion* **45** 1411
[48] Ott E 1979 *Phys. Fluids* **22** 1732
[49] Andrews P L and Perkins F W 1983 *Phys. Fluids* **26** 2546
[50] Casolari A and Cardinali A 2016 *Entropy* **18** 175
[51] Brambilla M 1999 *Kinetic Theory of Plasma Waves* (Oxford University Press)
[52] Pericoli-Ridolfini V, Apicella M L, Calabrò G, Cianfarani C, Giovannozzi E and Panaccione L 2011 *Nucl. Fusion* **51** 113023
[53] Decker J, Peysson Y, Artaud J-F, Nilsson E, Ekedahl A, Goniche M, Hillairet J and Mazon D 2014 *Phys. Plasmas* **21** 092504
[54] Martin E H, Lau C, Wallace G M, Shiraiwa S and Mumgaard R T 2019 *Nucl. Fusion* **59** 076006
[55] Lau C, Martin E H, Shiraiwa S and Wallace G M 2020 *Nucl. Fusion* **60** 036001
[56] Biswas B, Bonoli P, Ram A and White A 2023 *Nucl. Fusion* **63** 016029
[57] Baek S G *et al* 2021 *Nucl. Fusion* **61** 106034
[58] Bertelli N *et al* 2013 *Plasma Phys. Control. Fusion* **56** 074003
[59] Ding B J *et al* 2018 *Nucl. Fusion* **58** 126015
[60] Cesario R *et al* 2014 *Nucl. Fusion* **54** 043002
[61] Zhao A and Gao Z 2013 *Nucl. Fusion* **53** 083015
[62] Porkolab M 1977 *Phys. Fluids* **20** 2058
[63] De Marco F 1985 Review of current drive experiments at the lower hybrid frequency *Course and Workshop on Applications of RF waves to Tokamak Plasmas* (*Varenna, Italy*) vol I, ed S Bernabei *et al* (International School of Plasma Physics) p 316
[64] Fujiyama H, Watanabe Y and Akazaki M 1980 *J. Phys. Soc. Jpn.* **49** 1981
[65] Liu Z, Gao Z and Zhao A 2020 *Phys. Plasmas* **27** 042503
[66] Castaldo C, Di Siena A, Fedele R, Napoli F, Amicucci L, Cesario R and Schettini G 2016 *Nucl. Fusion* **56** 016003
[67] Chen L and Berger R 1977 *Nucl. Fusion* **17** 779
[68] Cesario R, Cardinali A, Castaldo C, Paoletti F, Fundamenski W and Hacquin S (the JET-EFDA Workprogramme Contributors) 2006 *Nucl. Fusion* **46** 462
[69] Peysson Y, Sébelin E, Litaudon X, Moreau D, Miellou J-C, Shoucri M M and Shkarofsky I P 1998 *Nucl. Fusion* **38** 939
[70] Wright J C *et al* 2007 *AIP Conf. Proc.* **933** 285
[71] Yang C, Bonoli P T, Wright J C, Ding B J, Parker R, Shiraiwa S and Li M H 2014 *Plasma Phys. Control. Fusion* **56** 125003
[72] Frank S J, Lee J P, Wright J C, Hutchinson I H and Bonoli P T 2022 *J. Plasma Phys.* **88** 1
[73] Napoli F, Castaldo C, Cesario R and Schettini G 2013 *Plasma Phys. Control. Fusion* **55** 095004
[74] Bhatnagar P, Gross E P and Krook M K 1954 *Phys. Rev.* **94** 511
[75] Stix T H 1992 *Waves in Plasmas* (AIP) ch 10

[76] Abrahmovitz M and Stegun I A 1970 *Handbook of Mathematical Functions* (Dover Publications, Inc.) ch 9
[77] Fried B D and Conte S D 1961 *The Plasma Dispersion Function* (Academic)
[78] Verdon A L, Cairns I H, Melrose D B and Robinson P A 2008 Properties of lower hybrid waves *Proc. Int. Astron. Union* **4** 569–73
[79] Callen H B and Welton T A 1951 Irreversibility and Generalized Noise Phys. Rev. **83** 34–40
[80] Ikeda K 2007 *Nucl. Fusion* **47** S1–S414
[81] Colas L, Milanesio D, Faudot E, Goniche M and Loarte A 2009 *J. Nucl. Mater.* **390–391** 959–62
[82] Carpentier S, Pitts R A, Stangeby P C, Elder J D, Kukushkin A S, Lisgo S, Fundamenski W and Moulton D 2011 *J. Nucl. Mater.* **415** S165–9
[83] Bibet P, Litaudon D and Moreau D 1995 *Nucl. Fusion* **35** 1213
[84] Pericoli-Ridolfini V *et al* 2005 *Nucl. Fusion* **45** 1085
[85] Cardano G 1993 *Ars Magna or the Rules of Algebra* translated ed T Richard Witmer (Dover)
[86] Neumark S 1965 *Solutions of Cubic & Quartic Equations* 1st edn (Pergamon) Library of Congress Catalog Card No. 65–25339, reprint Elsevier 2014
[87] Belo J H C M, Goniche M, Hillairet J and Bizarro J 2015 *Fusion Eng. Des.* **96–97** 70
[88] Aleynikov P and Breizman B 2015 *Nucl. Fusion* **55** 043014
[89] Sivukhin D V 1966 Coulomb collisions in a fully ionized plasma *Reviews of Plasma Physics* vol 4 (Consultants Bureau)
[90] Gormezano C, de Marco F, Mazzitelli G, Pizzuto A, Righetti G B and Romanelli F (the FTU Team) 2004 Chapter 1: The FTU Program *Fusion Sci. Technol.* **45** 297–302
[91] Aquilini M *et al* 2004 Chapter 11: The heating and current drive systems of the FTU *Fusion Sci. Technol.* **45** 459–82
[92] Huba J D 2016 *NRL Plasma Formulary* NRL/PU/6790-16-614 (Naval Research Laboratory)
[93] Napoli F 2014 Interazione non lineare delle onde di lower hybrid con il plasma di bordo di un tokamak *Doctoral Dissertation* Engineering Department, Roma Tre University (available at: http://hdl.handle.net/2307/4331)
[94] Shampine L F and Reichelt M W 1997 The MATLAB ODE suite *SIAM J. Sci. Comput.* **18** 1–22
[95] Cardinali A and Santini F 2011 *Plasma Phys. Control. Fusion* **53** 125001
[96] Cardinali A 2000 Quasilinear absorption of the lower hybrid wave in tokamak plasmas *Transworld Research Network Magazine* Recent Research Developments in Plasmas **1** 185–297
[97] Li M H *et al* 2019 *Plasma Phys. Control. Fusion* **61** 065005
[98] Smirnov A P, Harvey R W and Kupfer K 1994 *Bull. Am. Phys. Soc.* **39** 1626 Abstract 4R11
[99] Liu L *et al* 2023 *Fusion Eng. Des.* **189** 113444
[100] Song Y *et al* 2022 *Fusion Eng. Des.* **183** 113247
[101] Dougherty J P 1964 *Phys. Fluids* **7** 1788